A Comparison of Some Methods for Coherence Estimation for Application in the Analysis of EEG

by

Helena Kadlec

A thesis
presented to the University of Manitoba
in partial fulfillment of the
requirements for the degree of
Master of Arts
in
Department of Psychology

A COMPARISON OF SOME METHODS FOR COHERENCE

ESTIMATION FOR APPLICATION IN THE ANALYSIS OF EEG

BY

HELENA KADLEC

A thesis submitted to the Faculty of Graduate Studies of the University of Manitoba in partial fulfillment of the requirements of the degree of

MASTER OF ARTS

ABSTRACT

The frequency components of the electroencephalogram (EEG), as derived from spectral analysis, have been used by psychologists primarily as a descriptive statistic to characterize changes in brain activity. More recently, the coherence matrix, a cross-spectral estimate that measures the degree of association between pairs of EEG channels, is being used as input for further multivariate statistical analyses, such as principal components and factor analysis. The standard spectral analysis procedures are based on the assumptions that the observed data are (a) Gaussian and (b) stationary. It has however been shown that EEG data does not generally satisfy these assumptions, a situation which may be aggravated in the presence of neurological disorders or during the performance of a cognitive task. The statistical properties of coherence estimates obtained from EEG data that contain nonstationarities have not been extensively studied. This study compares the mean square error (MSE) and bias of coherence estimates obtained with three estimation methods; 1) the bivariate Fast Fourier transform (FFT), 2) bivariate autoregressive model estimation (AR), and 3) generalization of Burg's maximum entropy method (MEM). Simulated EEG data was employed to compare the estimates under stationary as well as various nonstationary con-

ditions such as may be encountered in practice. Three general types of nonstationary conditions were simulated, 1) by changing the magnitude of the variance of the Gaussian noise component at different locations in the interval, 2) by changing the distribution of the noise component from Gaussian to exponential, and 3) by adding a low frequency transient sine wave to one or both series. In addition, the estimates were compared for three different and relatively short interval length conditions, N=64, 128, and 256. As expected, the results in the stationary conditions indicate that as interval length increases, the MSE and bias of the coherence estimates obtained with all three estimation methods decrease. All three methods perform very similarly, with the MEM method giving the best estimates at the frequency where both spectra contain the most power. The FFT method is very comparable to the other two, except it lacks resolution due to its smoothing requirements. In the tested nonstationary conditions, again all three methods performed well. The FFT was more robust than the other two methods to exponentially distributed noise. Changing the magnitude of the Gaussian noise variance had small effects on all three types of coherence estimates, while the addition of a transient sine wave severely impaired the low frequency estimates only when both series contained the transient. Recommendations for coherence estimation in practice are discussed.

ACKNOWLEDGEMENTS

My first and biggest "thanks" must go to John Lind, my supervisor, who not only advised, helped and supported me over the last two years, but also rekindled my fondness for mathematics and introduced me to the field of quantitative psychology.

I would also like to thank my committee members, Dr. E. Schwedyk from Electrical Engineering, and Drs. L. Sandler and R. Tait from Psychology for all their helpful suggestions and the time they put into this thesis.

Last, but certainly not least, I want to thank my parents for their never-ending support and love, and also for their help with the graphs. And to my good friends who kept me sane, "thanks" for their good humor, patient ears, and shoulders.

CONTENTS

LIST OF TABLES

LIST OF FIGURES

A COMPARISON OF SOME METHODS FOR COHERENCE ESTIMATION FOR APPLICATION IN THE ANALYSIS OF EEG

The power spectrum of the electroencephalogram (EEG) represents the frequency composition of the general electrical activity emitted by the brain. In psychology, the EEG is important for studying normal and abnormal human brain functioning by searching for correlates between various types of behavioural, particularly cognitive, tasks and the anatomic distribution of this brain activity. The brain potentials measured from the scalp normally range from 10 to 200 uV, with epileptic seizures producing up to 1 mV (Gevins,1983). The intensity and pattern of the electrical activity are highly dependent on the overall excitation of the cerebral cortex, resulting mainly from activity in the reticular activating system (Guyton, 1981, pp. 676). Simultaneous recordings of the scalp and areas within the brain indicate that brain waves occur when large numbers of neurons partially discharge without emitting action potentials but give rise to periods of current flow that undulate with the changing degree of excitability of the neurons (Guyton, 1981, pp. 676).

The conventional frequency bands that are characteristic of the EEG are 0 to 3 Hertz (delta activity), 4-7 Hz (theta activity), 8-13 Hz (alpha activity), 14-19 Hz (beta I activity), and 20-32 Hz (beta II activity). Delta activity occurs in deep sleep, in infancy and in severe organic brain disorders. Delta waves can be produced in the cortex with all connections to the thalamus severed, implying that the cortical neurons are capable of some independent synchronizing to produce delta waves (Guyton, 1981, pp. 676). Theta waves occur primarily in the parietal and temporal regions in children, and during emotional stress in some adults.

Alpha activity is found to be most intense in the occipital region and sometimes in the parietal and frontal regions of the scalp in almost all normal adults in a quiet, resting, waking state. During sleep, alpha activity disappears completely, while during cognitive tasks it is replaced by asynchronous, higher frequency and lower voltage beta activity. Based on the results of brain stimulation and lesion studies, alpha activity is assumed to result from spontaneous activity in the generalized thalamocortical system (Guyton, 1981, pp. 676).

Beta waves occur most frequently in the parietal and frontal regions. Beta I activity is affected by cognitive functioning similarly to alpha waves (i.e., it is suppressed by higher frequency and lower voltage activity). Beta II waves are activated by arousal of the central nervous system or during tension (Guyton, 1981, pp. 675).

Traditionally, the frequency components contained in the power spectrum of the EEG have been primarily used as a descriptive statistic in a variety of studies investigating normal and neuropathological conditions affecting the brain. However, with more routinely available methods of signal analysis (e.g., the statistical package BMDP has two programs for analyzing time series) and the increased efficiency of modern laboratory computers, spectral estimates of the EEG are becoming more widely used. This facilitates further statistical analyses, such as discriminant analysis, principal components and factor analysis, and thus aids the interpretation of the vast amounts of data collected. Frequently, however, this may result in the analysis of EEG data in the absence of information about the statistical properties of the obtained spectral estimates. This study investigates some of the statistical properties of spectral and cross spectral estimates, particularly coherence, which is a measure of the linear relationship between EEG channels.

Areas of EEG Applications

This section illustrates some examples where the EEG has been used to study cognitive and physiological aspects of the brain. It is not intended to be an exhaustive review; however, it demonstrates the wide range of research areas which take advantage of the EEG as a quantitative measure of brain activity.

Clinical Psychology

In clinical psychology, differences in EEG characteristics may provide useful information for the functional understanding of, and differentiation between, various psychopathologies. For example, it was found that compared to normal matched subjects, schizophrenic patients show increased activity in the low frequency range in the frontal regions, while the post-central and the left anterior-temporal areas exhibit increased beta activity (Morstyn, Duffy, & McCarley, 1983; Selin & Gottschalk, 1983). Moreover, schizophrenic patients exhibit increased high-frequency activity in the left anterior-temporal region and in general possess less lateral brain organization than normal subjects, as measured by changes in alpha activity during visual imagery tasks (Shaw, Colter, & Resek, 1983). In addition, schizophrenia is differentiated from neurosis by a diminished orienting responsiveness of the EEG to repeated auditory stimuli (Bernstein, Taylor, Starkey, Lubowsky, Juni, & Paley, 1983). Patients with conduct disorders show a greater proportion of abnormal EEG frequencies than is seen in depressive disorders (Selin & Gottschalk, 1983).

Experimental Psychology

In experimental psychology, the EEG is used to gain insight into the underlying brain activity associated with different behavioural tasks. For example, studies have investigated EEG correlates of learning effects on visual-motor tasks, such as eye-hand tracking and the mirror star task (Busk & Galbraith, 1975; Gliner, Mihevic, & Horvath, 1983). These studies reported that these tasks produced only a few significant changes of small magnitude in the EEG. However, Gevins and his colleagues (Gevins, Zeitlin, Doyle, Schaffer, & Callaway, 1979; Gevins, Zeitlin, Yingling, Doyle, Dedon, Schaffer, Roumasset, & Yeager, 1979; Gevins, Zeitlin, Doyle, Yingling, Schaffer, Callaway, & Yeager, 1979; Gevins, Doyle, Schaffer, Callaway, & Yeager, 1980) did observe significantly different EEG patterns for various complex tasks, such as reading, writing, scribbling, Koh's block design, block manipulation and mental paper folding (but see below).

Lateralization differences. A large body of psychological research literature investigating cognitive functioning is concerned with lateralization differences. It has long been hypothesized that in right handed persons spacial tasks are mainly processed by the right hemisphere while verbal tasks are mediated primarily by the left hemisphere. Many studies have been conducted which seem to support this lateralization of function. For example, Shepherd and Gale (1982) found that the left hemisphere was more strongly activated in some frequency bands in a rapid calculation task where the subjects were required to respond only when all four of the digits presented sequentially in one trial were odd and summed to 20 or more. In clinical studies, lateralization differences were found in various psychopathological populations. For example, Shaw et al. (1983) found that schizophrenic patients possess less lateral organization than normal subjects when responding to a visual task, and Schaffer, Davidson, and Saron (1983) found that depressed subjects exhibited an elevated right hemisphere spontaneous activity in the frontal EEG as compared to normal controls.

Often, however, inconsistent lateralization results have been found. For example, in language and information processing research, some studies show enhanced amplitudes to linguistic stimuli in the left hemisphere, while others found no differences or some changes in the right hemisphere particularly with visual stimuli (see Boddy, 1981, for a review).

Due to the often inconsistent results reported, this area of research has recently been criticized on methodological grounds by Gevins (1983). Some of the methodological problems emphasized were: 1) failure to demonstrate that it was the cognitive aspects that distinguished between tasks and not the level of difficulty (or the number of cognitive processes involved) or other response related factors; 2) failure to validate that the tasks were actually, and correctly, performed; 3) failure to demonstrate that the obtained asymmetry of EEG was not due to a combination of irrelevant factors, such as handedness, improperly balanced electrodes, or asymmetric skull thickness; 4) using a between-subjects design to infer within-subject differences; and 5) relying on measures that are ambiguous with respect to the actual locus of right and left EEG activities (Gevins, 1983, pp. 349,352). In his own research, Gevins and his colleagues, in the studies previously cited (Gevins, Zeitlin, Doyle, et al., 1979; Gevins, Zeitlin, Yingling, et al., 1979; Gevins et al., 1980) have also found lateralization differences in the various cognitive tasks, but these differences disappeared when limb and eye movements, and performance related factors, such as task difficulty level, were controlled. A new 'dynamic' methodology, including a new set of tasks which seek to control the problems previously mentioned, has been developed (Gevins, 1983, pp. 369). In this method, the EEG recording obtained for each task is divided into smaller intervals and is analyzed separately. The studies reported have shown that the tasks were similar in the intervals immediately following the stimulus and preceding the response, but differed in the middle intervals. In these middle intervals, lateralization differences followed a complex and rapidly changing pattern. These studies thus support that lateralization may occur in 'truly' cognitive functioning, but also indicate that further investigation is required.

Physiological Research

Epilepsy. One of the major areas which uses the EEG extensively is in the study of epilepsy. The EEG recordings of epileptic patients are used in both applied and basic research as well as for diagnostic purposes. Some examples of research studies in this area include predicting spike-wave activity in patients with Absence epilepsy (Siegel, Grady, & Mirsky, 1982) and using estimates of time differences between EEG channels to assess the presence of an epileptic focus in wide-spread epileptic activity and to make inferences about the possible routes of propagation of seizure activity (Gotman, 1981, 1983).

Other areas. The spectral analysis of EEG has been applied in many other areas of research where changes in brain activity are of interest. For example, the effects of drugs such as interferon (Dafny, 1983), antidepressants (Reilly, 1976), alcohol (Pollock et al., 1983), and nicotine (Herning, Jones, & Bachman, 1983) on brain functioning have been researched. In clinical populations, different EEG patterns have been observed in juvenile diabetes mellitus (Keene et al., 1983) and in patients with renal disorders (Bowling & Bourne, 1978).

Often these types of studies use numerous features of the EEG and/or its spectrogram to discriminate and classify various groups of observations. For example, 'neurometrics'

(John, Karmel, Corning, Easton, Brown, Ahn, John, Harmony, Prichep, Toro, Gerson, Bartlett, Thatcher, Kaye, Valdes, & Schartz, 1977) involves extracting features such as 1) signal power, 2) signal variance, 3) signal-to-noise ratio, 4) mean squared first difference, 5) difference and normalized difference in signal energy between homologous pairs in power and waveshape asymmetry, and 6) the coherence. Multivariate statistics were used on these features to characterize and classify learning disabled children and old adults with cognitive deterioration (John et al., 1977). Gevins et al. (1979) used the frequency band components obtained from different areas of the brain in a nonlinear pattern recognition algorithm to classify various cognitive tasks. Finally, Bowling and Bourne (1978) used stepwise discriminant analysis on components of the EEG spectra to successfully classify patients with and without renal failure.

Standard Methods of Spectral Analysis of EEG Data

Four general classes of spectral estimation methods for scalar time series have been applied to the analysis of EEG recordings. These methods and their generalizations to vector valued series are described below.

Univariate Spectral Analysis

The Fast Fourier Transform. The frequency components of a series of data, $x(t)$, $t=0,\ldots,N-1$, sampled at regular time intervals, $\Delta t=1/N$, can be obtained by the Fourier transform

$$X(f) = 1/N \sum_{t=0}^{N-1} x(t) \exp(-i2\pi ft), \qquad f=0,\pm1,\pm2,\ldots,\pm N/2,$$

where $i=\sqrt{-1}$. Since the introduction of the Fast Fourier Transform (FFT) by Cooley and Tukey (1965), which substantially decreases the computational burden of the standard Fourier transform, the estimation of the power spectrum directly from the original data has become standard practice. Transforming a finite data record, however, requires the application of a window function prior to the transformation in order to reduce leakage from one frequency band to another (e.g., Brillinger, 1981, pp. 131-142; Otnes & Enochson, 1972, pp. 201-204, 281). Various tapering windows have been proposed, each requiring a compromise between the amount of allowable leakage, resolution loss, and the corresponding loss in degrees of freedom of the spectral estimates. The most commonly used tapering function in EEG analysis is the split-cosine window (Bloomfield, 1976). The windowed spectrogram thus obtained, however, still yields an inconsistent estimate, its variance being equal to the squared power which cannot be decreased by increasing the length of the series (e.g., Brillinger, 1981, pp. 125). The spectrogram, therefore, also requires smoothing, either by ensemble averaging or averaging over frequency. The smoothing procedures increase the degrees of freedom of each of the estimates and reduce their asymptotic variance. In averaging over frequency, however, there is a limit to the amount of smoothing allowed, since increasing the bandwidth decreases the variance but also increases the bias of the estimates.

The autocorrelation function. An alternative estimator for the spectrogram can be obtained from the Fourier transform of the autocorrelation function, which itself already emphasizes the regular activity of the data in the time domain. Again, to obtain consistent estimates, it is recommended that the autocorrelation function be windowed by one of the available windows, such as the Hanning, Hamming or Parzen's windows, prior to the transformation, and the resulting estimates smoothed over frequency (Otnes & Enochson, 1972, pp. 270; Walter, 1963). This method is based on the work of Blackman and Tukey (1958) and was first applied to the EEG by Walter in 1963.

These estimates are very comparable to, although not identical to, the estimates obtained by the FFT method (Bendat & Piersol, 1971), and it has been shown that mathematically the two methods are equivalent (Khinchine, 1934 and Wiener, 1930 cited in Otnes & Enochson 1972, pp.254-255). Currently, however, with the increase in speed of computation with the FFT, most researchers seem to prefer calculating the spectral estimates directly in the frequency domain by the FFT.

<u>The Box-Jenkins approach</u>. A time-series may be represented in the time domain by parametric regression models such as those described by Box and Jenkins (1976). The three models most commonly used are the moving average (MA), autoregressive (AR), and the autoregressive-moving average (ARMA) models. If $y(t)$, $t=1,\ldots,N$, is the observed series, then the finite MA(m) representation of $y(t)$ is

$$y(t) = e(t) + \sum_{j=1}^{m} b(j)e(t-j),$$

where m is the order of the model, $e(t)$ are independently normally distributed with mean 0 and variance 1, and $b(j)$, $j=1,\ldots,m$, are the coefficients to be estimated. The AR(p) model represents the observed data as

$$y(t) = e(t) + \sum_{k=1}^{p} a(k)\, y(t-k),$$

where p is the order of the model, $e(t)$ is again $N(0,1)$ white noise, and $a(k)$, $k=1,\ldots,p$, are the AR coefficients to be estimated. This model expresses the observed series as a linear combination of its own past values plus an uncorrelated random component. A more general representation combines the MA(m) and AR(p) models into the ARMA(m,p) model given by

$$y(t) + \sum_{k=1}^{p} a(k)y(t-k) = e(t) + \sum_{j=1}^{m} b(j)e(t-j).$$

One of the most important aspects of fitting these models to observed data is the determination of the model orders m and(or) p. For the MA(m) model, m can be found from the autocorrelation function since theoretically it will be zero for lags greater than m (Box & Jenkins, 1976, p.68). Similarly, the order p of an AR(p) process may be estimated from the partial autocorrelation function which will be insignificant for lags greater than p. These methods of determining the orders are considered somewhat subjective, since judgement is required to establish at which point the estimated autocorrelation functions become insignificant.

Akaike (1969a,1969b, 1971) has been foremost in developing objective methods for determining the order of the AR models. One method is based on minimizing the final prediction error (FPE) of the AR models of successively higher order. The order p and the corresponding coefficients yielding the smallest FPE are chosen to represent the series. In a simulation study, Gersch and Sharpe (1973) generated an ARMA process, whereby the series was equivalent to an infinitely long AR model, and using Akaike's FPE criterion, they found that finite AR models of average order of 18.6 provided close agreement with the theoretical results. Akaike (1973) later developed a maximum likelihood estimate of the order, called the information (AIC) criterion. The FPE and AIC have been shown to be approximately related by

$$AIC = N \log(FPE)$$

(Jones, 1978), and asymptotically the minimum FPE and minimum AIC are equivalent (Sawaragi, Soeda, & Nakamizo, 1981).

Least squares estimates of the AR coefficients can be obtained by solving the set of linear Yule-Walker equations. This classical method involves estimation of the autocorrelation function which assumes that data outside the sampled range are zero. This may result in estimates which are less than optimal, especially for short series. Alternatively, the AR coefficients may be estimated recursively by the Levinson-Durbin procedure (Durbin, 1960; Levinson & Wiener, 1949). This latter method does not require prior knowledge of the autocorrelation function and thereby has the advantage of using only the available data. Maximum likelihood estimates of the model parameters have been derived (Box & Jenkins, 1976, pp. 327), however, the numerical complexity of the resulting normal equations has deterred investigators from using these methods routinely.

The obtained estimates of the model parameters, the coefficients $\hat{a}(k)$, and the estimated one-step-ahead prediction error variance $\hat{v}(p)$, are then readily transformed to obtain the estimate of the spectrum by the equation

$$\hat{S}(f) = \frac{\hat{v}(p)\,\Delta t}{\left|\sum_{k=0}^{p} \hat{a}(k)\exp(i2\pi kf)\right|^2}, \quad \text{for } f=0,\ldots,N/2,$$

where $\hat{a}(0) = 1$.

Spectral analysis using the AR and ARMA representations were applied to the EEG by Gersch (1970), Gersch and Yonemoto (1977), Jones (1974), and Pfurtscheller and Haring (1972), among others. It was found that orders of less than ten were generally adequate for modeling the EEG of an epileptic patient (Gersch, 1970), and a bivariate AR model of order six was selected for the sleep EEG of a human infant (Jones, 1974). Gersch and Yonemoto (1977) found that AR model of order ten and an ARMA model of order seven fit sleep EEG data.

The AR models may be viewed as regression models in which the immediately past observations of the series serve as predictor variables for the current observation. An interesting development of these estimation methods has emerged, whereby rather than constraining the regression coefficients to be fixed, a stochastic component can be introduced to them. Linear dynamic estimation methods have thus been developed to estimate the time variable parameters of these regression models (Harrison & Stevens, 1976). Probably the most well known linear dynamic recursive estimation method is the Kalman filter.

Since its first introduction in the engineering literature by Kalman (1960; Kalman & Bucy, 1961), which involved the state-space representation of the linear filter, a number of reinterpretations of the Kalman filter appeared in the statistical literature in order for this dynamic estimation procedure to become more accessible to statisticians. In 1972, Duncan and Horn developed the Kalman results from regression analysis theory by viewing the regression weights as random variables rather than fixed. An alternate view was provided by Meinhold and Singpurwalla (1983) who have shown how the Kalman filter can be interpreted as a problem in Bayesian inference; the conditional probability of the state parameters at time t, given data up until time t, is proportional to the product of the likelihood of the state at time t and the prior conditional distribution of the state parameters given the data from time 0 to t-1.

Regardless of its statistical interpretation, the Kalman filter is a powerful recursive method for estimating time-variable parameters, and when applied to an autoregressive time series model, it is an adaptive AR model. The adaptive model is particularly useful since it is not restricted to stationary signals. By allowing the coefficients to vary over time, these models can be used to track the time-variable properties of the signal. This is especially relevant in the application of these models to the EEG, since changes in cognitive functioning may thus be observed and analyzed over time.

The Kalman filter method has been applied to track changes of the spectral characteristics of simulated nonstationary EEG (Wennberg & Isaksson, 1976) and real stationary, slow-changing and fast-changing EEG (Bohlin, 1977; Isaksson

& Wennberg, 1976). The Kalman filter was shown to follow well the fast and slow changes in all the studies, even when large low frequency disturbances and instantaneous major changes in the signal (eyes opening and closing) were present (Bohlin, 1977). Bohlin (1977), however, also indicates that this ability to track changes in the spectrogram may result in greater statistical uncertainty of the estimates.

Maximum entropy. In 1967, Burg introduced the maximum entropy method (MEM) of spectral estimation. MEM involves maximizing the entropy, H, of a process, defined as the integral

$$H = \int_{k} \ln S(f)$$

where S(f) is the power spectrum and K is the region over which S(f) is assumed to be nonzero. In the univariate case, the MEM estimates are readily computed by AR modeling, since the two methods are mathematically similar (McClellan, 1981). An efficient algorithm for univariate MEM coefficient estimation was developed by Andersen (1974) and was shown to work well in EEG spectral estimation (Jansen, Bourne, & Ward, 1981). This algorithm is analogous to the Levinson-Durbin recursive method of AR estimation whereby the model of successively increased order is estimated recursively until the residual error matrix is minimized. This method also has the advantage of using only the available data, without assuming that the data outside the sampling interval are zero. Clearly, the same problem of order selection as in AR modeling also occurs in the MEM method.

Multivariate Spectral Analysis and the Coherence

Generally, most of the methods of spectral analysis reviewed above generalize easily to the multivariate case. If x(t) and y(t) are two observed series, then the bivariate FFT spectral estimates are given by

$$S(f) = \frac{2}{N\Delta t} \left| X(f) * Y(f) \right|$$

where X(f) and Y(f) are the univariate FFTs of the series x(t) and y(t), respectively, and * denotes convolution.

The multivariate AR, MA, and ARMA models are given by

$$\underset{\sim}{y}(t) = \sum_{k=1}^{p} A(k)\ \underset{\sim}{y}(t-k) + \underset{\sim}{e}(t),$$

$$\underset{\sim}{y}(t) = \underset{\sim}{e}(t) + \sum_{j=1}^{m} B(j)\ \underset{\sim}{e}(t-j),$$

and

$$\underset{\sim}{y}(t) - \sum_{k=1}^{p} A(k)\ \underset{\sim}{y}(t-k) = \underset{\sim}{e}(t) + \sum_{j=1}^{m} B(j)\ \underset{\sim}{e}(t-j),$$

respectively. Here the uppercase letters indicate matrices which are scalar values in the univariate case. If the series is s-variate, matrices A(k), k=1,...p, and B(j), j=1,...,m are s x s matrices, and $\underset{\sim}{y}(t)$ and $\underset{\sim}{e}(t)$ are vectors of length s.

A multivariate method for estimating AR coefficients was developed by Whittle (1963). It is a generalization of the Levinson-Durbin algorithm, and fits a forward and backward AR model simultaneouly. As in the univariate case, the coefficients along with the corresponding residual error matrix are used to calculate the spectral matrix which contains the auto-spectral estimates on the diagonal and the cross-spectral estimates in off-diagonal positions.

Generalizing the MEM method from the univariate to multivariate case is not as straightforward. While in the univariate case, the MEM estimates are the same as the AR estimates, this is generally not true in the multivariate case. Thus Burg's algorithm, which in essence fits a forward and backward AR model to the observed data, does not generalize directly to the multivariate case since the coefficient and prediction error matrices are not the same for the forward and backward calculations. Jones (1978), however, reported an indirect MEM estimation procedure which estimates the coefficient matrix by fitting a forward and backward model to the residuals at each successive step.

To obtain the true multivariate MEM estimate seems to involve the optimization of a nonlinear system. McClellan (1981) discussed some of the conditions for the existence and uniqueness of the multivariate MEM estimate, as well as some of the algorithms that solve the nonlinear system by using an approximation, or a general optimization algorithm.

These are generally complex and are beyond the scope of this thesis.

Comparison of Methods in EEG Spectral Analysis

A number of studies have compared the spectral estimates from the AR model fitting method with those obtained by the transformation of a Parzen windowed autocorrelation function. Jones (1974) and Gersch and Yonemoto (1977) found that in most cases, similar spectral estimates were obtained, although the AR method always produced smoother looking plots of the spectrogram, coherence, and phase angle functions, which in turn look more interpretable. Underparameterized AR and ARMA models yielded smoother looking but excessively biased estimates comparable to those obtained using a Parzen window of smaller lag. On the other hand, overparameterized models resulted in less smooth spectrograms resembling those obtained with larger-lag windows that were relatively unbiased but excessively variable (Gersch & Yonemoto, 1977). Akaike (1969b) found similar results comparing the AR estimates with Hanning-windowed spectral estimates.

More recently, Jansen et al. (1981) investigated the performance of EEG power spectral estimates obtained directly by the FFT and three different methods of calculating AR model estimates. Correct classification rates obtained from discriminant analysis procedures were used for the comparisons. Two of the AR model estimates were obtained nonadaptively, 1) by the standard method of solving the Yule-Walker equations, and 2) by using Burg's recursive algorithm of Andersen's (1974) which is based on the Levinson-Durbin procedure. The third set of AR estimates were adaptive, calculated by the Kalman filtering method which updates the initial AR coefficients based on every new observation of the signal. It was found that of the spectra computed from the AR coefficients by the three methods, Burg's method had the best classification rates. However, they were not as high as those obtained by the FFT. When the EEG was cosine tapered prior to computing spectra with Burg's method, however, the classification rates of the two spectra became identical. The spectra obtained with the Kalman filter AR coefficients performed less well, while those estimated by the Yule-Walker equations produced rather poor results in all respects. In evaluating the spectra themselves, it was found that the Kalman filter method tended to estimate the frequency of artifact activity more correctly than the Burg and Yule-Walker methods, but the peak widths were wider with the Kalman filter than with Burg's method. In most cases, the spectra obtained by the FFT and Burg's method were very similar. Overall, Burg's method performed the best of the AR coefficient based estimates, while the use of the Yule-Walker equations is not recommended by Jansen et al.

The advantage of the AR method is that good spectral estimates can be obtained on shorter data records than are required by the FFT; however, unstable models may result if the estimation is based on the Yule-Walker equations (Jansen et al., 1981). Gersch (1970) points out that statistically, the AR estimates perform much better than the windowed Fourier estimates, since they yield a larger number of degrees of freedom and are asymptotically normal and consistent. The AR coefficients, however, are estimated by least square methods and therefore spectral estimates based on these may be more sensitive than FFT estimates to departures from an underlying Gaussian stationary model.

Coherence and its Applications in EEG Analysis

For multi-channel EEG recordings, a number of measures of association between pairs of channels are available. These can often be useful in relating EEG asymmetry to interhemispheric and/or intrahemispheric functions. The most commonly used measure is the coherence, which is analogous to the correlation coefficient in classical statistics, and indicates the degree of linear relationship between the two channels. The coherence, sometimes also called the coherency, is defined at each frequency value as the ratio of the cross spectrum between two channels, X and Y, to the square root of the product of the individual spectra; that is,

$$R_{xy}(f) = \frac{S_{xy}(f)}{|S_x(f)\ S_y(f)|^{1/2}}.$$

Brillinger (1981, pp.257) calls this ratio the coherency, and its modulus squared, $|R(f)|$, the coherence. The estimates used for comparisons in this study are the moduli, $|R(f)|$, of this ratio, and since they are required to be in this form, the $|R(f)|$ will be referred to as coherence. The values of the coherence range from 0, meaning no linear relationship, to 1 indicating a perfect linear relationship.

Since one coherence value is obtained for each frequency, this often results in large amounts of data for interpretation. To alleviate this potential problem, some summary statistics for the coherence have been proposed. The 'weighted average coherence' is computed across a number of frequencies and expresses the overall degree of relationship between pairs of EEG records (Busk & Galbraith, 1975). Bohdanecky, Lansky, and Radil (1982) have proposed a similar measure, a total 'integral measure of coherence', and a related relative measure which estimates the contribution of a particular frequency band to the total integral coherence. Although it is argued that such data reduction aids interpretation, this facility is obtained at the expense of loss of information. In some applications, however, these summary statistics are useful.

In EEG applications, the coherence has been used to measure the degree of EEG synchronization between the hemispheres in schizophrenic and neurotic patients during a visual imagery task (Shaw et al., 1983) and during bilateral spike-and-wave activity in epileptic patients (Gotman, 1981). Gotman (1983) has also used the coherence in calculating small time differences between two channels which appeared synchronous on visual inspection. Gotman concluded that this method may allow assessment of an epileptic focus when only widespread seizure activity can be recorded and may enable the inference of possible routes of seizure activity (Gotman, 1983).

Recently, coherence estimates have been used as input data for further multivariate statistical analyses, namely factor analysis and principal components, under the assumption that the activities across brain regions may be characterized by a few common factors. Douglas and Rogers (1983) developed a stability measure, based on the estimated coherence matrix, which was then used to determine the dimension of maximum likelihood factor analysis of the power spectra obtained from eight EEG leads. The stability measure, called the 'ambient matrix coherence (AC)', was found to be robust on various simulated data sets. The AC produced stable maximum likelihood factor loading matrices, but when it was applied to principal components inaccurate solutions resulted. When maximum likelihood factor analysis was applied to the EEG data from the eight leads, the authors found that three of these contained three factors; one with primarily high frequency components in the 21 to 30 Hz range, the frequencies of the second factor were in the 10 to 18 Hz range, and the third factor contained the low frequencies of 1 to 7 Hz. The remaining five EEG derivations appeared to be more stable with a fourth factor, a sharper vector centered at 9 Hz.

Swenson and Tucker (1983) used the coherence matrix obtained from eight EEG derivations, one matrix per frequency band, directly as input data for factor analysis. Results showed that the first two factors that accounted for most of the variance in the coherence matrix, one posterior and one anterior, were both 'right-lateralized', that is, the coherences were generally higher in the right hemisphere; a third residual factor described the left hemisphere variance. In addition, Swenson and Tucker (1983) compared the factor analytic results to an a priori de-structuring of the coherence matrix with partial multiple coherence methods. These results suggested that intra-hemispheric coherence is generally higher on the right side of the brain. Additionally, the a priori de-structuring revealed that the inter-hemispheric coherence of the right parietal region was higher than the left, while the left occipital area showed higher coherence values than the right.

While both of these studies used various arousal conditions -- resting, scribbling and solving mathematical problems in the Douglas and Rogers (1983) study, and resting, relaxing and a high arousal state where noise was continuously presented in the Swenson and Tucker (1983) study -- no attempt was made at distinguishing the experimental conditions in the factor analyses. However, factor analysis and other multivariate techniques could prove useful in interpreting psychological data, as the analysis of EEG is applied in behavioural studies in attempts to identify factors underlying brain functioning during cognitive tasks.

Many of the multivariate analyses are based on the correlation matrix, but it has been shown that the correlation coefficient is very sensitive to outliers and deviations from normality (Devlin, Gnanadesikan, & Kettenring, 1981). Since the coherence has the same asymptotic distribution as the Pearson moment correlation coefficient, it may also be affected by violations of assumptions underlying its estimation procedures.

Assumptions underlying spectral estimation

Spectral analysis of time series is based on the assumptions that the series is Gaussian and stationary, or at least weakly stationary, that is, where the first two moments are time-invariant. Although in the past, inconsistent findings could not resolve the question whether EEG data satisfied one or both of these assumptions, more recently it is generally recognized that nonstationary EEG data does occur, and quite frequently when longer epochs are analyzed. McEwen and Anderson (1975) have identified several factors contributing to the inconsistencies found in past literature, including 1) the small number of ensembles of EEG segments from too few subjects, 2) the use of only one nonstandardized channel, and 3) different digitization rates employed to sample the data.

In their study investigating the stationarity and normality of spontaneous EEG, McEwen and Anderson (1975) found that as the sampling (digitization) rate was increased, or as the length of the sample record increased, a greater proportion of the EEGs tended to be non-Gaussian and nonstationary, although stationarity was somewhat less sensitive to sample length. Now it seems generally accepted that in visually inspected artifact-free epochs of one second duration, although some studies use longer epochs, the occurrence of nonstationarity and nonnormality is sufficiently negligible to make standard spectral analysis techniques satisfactory. From the graphs presented in McEwen and Anderson (1975), it can be seen that for the frequently used sampling rate of 128 Hz, of the one second artifact-free, resting (eyes closed) EEG segments, almost 100% were Gaussian and stationary in the occipital regions, while 5% of the frontal EEGs in both hemispheres were nonstationary. For a five second epoch, frontal EEG was 75% Gaussian, about 83% stationary and about 62% were both Gaussian and stationary, whereas in the occipital region these values were 84%, 90%, and 70%, respectively.

A number of transformations for normality have been shown effective for broad band (i.e., delta, theta, alpha, etc.) spectral estimates (Gasser, Bacher, & Mocks, 1982). These authors found the transformation log(x/(1-x)) to be excellent in transforming the relative power to normality, while log(x) performed the best for absolute power but was not completely satisfactory for all bands. Here x is the absolute or relative band power.

Nonstatonarities and Artifacts in the EEG

Violations of the assumptions may be of lesser importance to investigators when the spectrum is used as a descriptive statistic, since it is generally believed that conventional methods of power spectrum estimation are inherently robust to all but extremely bad contamination. Kleiner, Martin, and Thomson (1979) point out that this may only be true for the general shape of spectra that consist mostly of narrow band components or when a low frequency component is of primary interest. Since EEG data are considered to contain mostly noise with only a few lower frequency bands of interest, that is, only some frequencies in the 0 to 30 Hz range, these considerations may apply to the shape of EEG power spectra. Kleiner et al. (1979), however, have also shown that even as few as two outliers that were relatively small compared to the observed series but large in comparison with the error, may result in large distortions in the shape of the spectrum.

Considerable attention has been paid to the removal of artifacts from EEG data. Several types of artifacts have been identified, including gross head and body movements, eye-movement potentials in frontal channels, perspiration, low frequency instrumental artifacts, depolarization of scalp and neck muscles overlying the brain, and electrochemical effects at the surface-metal junction (Gevins, Yeager Zeitlin, Ancoli, & Dedon, 1977; Johnson, Wright, & Segall, 1979). Since these are not generated by the brain, they are usually considered to lack useful information and efforts are made to identify and discard them prior to analysis. Woestenburg, Verbaten and Slanger (1983) showed that some potential exists for removing eye-movement artifacts statistically. They applied a complex linear regression analysis method in the frequency domain, which successfully removed artificially added artifacts from simulated EEG data. Automated methods, however, are more widely used to detect and remove the artifacts. Many have been developed and continue to be improved (e.g., Gevins, Yeager, Diamond, Spire, Zeitlin, & Gevins, 1975; Gevins et al., 1977; Johnson et al., 1979). Most computerized systems have some provisions for optionally removing artifacts from clinical EEG data (Barlow, 1979).

Often, nonstationarities do provide useful information about brain activity. Occassional transient activity, such as epileptic spikes or evoked potential responses, have been examined, and various features of these transients have been used for their detection and characterization (see Barlow, 1979 for a review). Briefly, some of these features include the analysis of 1) rise-time, fall-time, and peak angle to classify spikes as steep triangular waves, 2) peak-to-peak amplitude and separation (duration), 3) the second time derivative (curvature), 4) the angle at the peaks, 5) maximum slopes of the sides and their time of occurrence relative to the peak, 6) spike duration, 7) matched filtering, and 8) inverse filtering. John et al. (1977) include other characteristics in their 'neurometric taxonomy' scheme mentioned earlier. Some of these features are also used in the automatic removal of artifactual contamination.

The generally nonstationary character of longer epochs of spontaneous EEG has been investigated with the use of the Kalman filter. A number of studies have shown the Kalman filter to be excellent in tracking the changes of the spectral characteristics in EEG (Bohlin, 1977; Isaksson & Wennberg, 1976; Wennberg & Isaksson, 1976). This method may have potential in psychological studies where nonstationary EEG data may result from changes in cognitive functioning during various mental tasks.

Purpose of Proposed Study

The effects of nonstationarity on the coherence estimates has not been extensively studied. Since the EEG segments of interest may often be nonstationary, for example, during cognitive activity, it is important to find optimal or nearly optimal coherence estimates under various conditions, particularly if use of the coherence values is required in further statistical analyses, such as factor analysis or principal components.

This study investigates the effects of three kinds of nonstationarities on the bias and mean square error of coherence estimates obtained by three estimation methods: 1) the bivariate Fast Fourier Transform, 2) a bivariate autoregressive recursive model estimation, and 3) the indirect generalization of Burg's maximum entropy method proposed by Jones (1978). In addition, spectral estimates obtained by an adaptive method of the Kalman filter type are compared to those of the three methods. Coherence estimates derived from a bivariate Kalman filter are not investigated in this study because of the computational complexity of this method in the two dimensional case (Woods & Radewan, 1977).

In order to be able to compare estimates to the known values, the spectral analyses were obtained from simulated data. Thus three kinds of nonstationarities simulated were chosen to represent changes most likely to be observed in real EEG, and a stationary condition was included for comparisons of methods under optimal conditions.

METHOD

Two channels of simulated EEG data were obtained for 0.5, 1.0 and 2.0 second data segments. The sampling rate was set at 128 points per second, thereby giving a Nyquist frequency of 64 Hz. This rate was chosen to correspond to the sampling rates most frequently used in applied research, with consideration for the recommendations of McEwen and Anderson (1975). These authors suggested that the sampling rate be chosen as little above the Nyquist frequency as is practical in order to satisfy the assumption of statistical independence of successive samples of EEG while still allowing for accurate estimates to be made.

Stationary and three types of nonstationary data were simulated for each record length, that is, for 0.5, 1.0, and 2.0 seconds. The results of the spectral analyses using the four methods were obtained from 200 replications of each condition.

The entire experiment was run on the Amdahl 5850 computer at the University of Manitoba. The programs were all written in Pascal language and compiled by the Pascal/VS compiler. All random numbers were generated using routines from the International Mathematical and Statistical Library (IMSL).

Data Simulation

Stationary data

The bivariate stationary series was simulated by the AR(7) model

$$Y(t)=\sum_{k=1}^{7}A(k)\ Y(t-k)\ +\ E(t), \qquad t=1,\ldots,N \tag{1}$$

where E(t) is normally distributed white noise with zero mean and covariance matrix $\begin{bmatrix}1 & 0\\ 0 & 1\end{bmatrix}$. The bivariate series of random numbers were generated by the IMSL routine GGNSM. Furthermore, in equation (1), N is the total length of the series with N=64 in the 0.5 second conditions, N=128 in the 1.0 second conditions, and N=256 in the 2.0 second conditions; and A(k), k=1,...,7, are the bivariate AR coefficients,

$$A(1)=\begin{bmatrix}0.3023 & -0.0974\\ -0.1344 & 0.3614\end{bmatrix} \qquad A(2)=\begin{bmatrix}0.1351 & 0.0414\\ -0.0310 & 0.1249\end{bmatrix}$$

$$A(3)=\begin{bmatrix}-0.0703 & 0.3670\\ 0.0893 & -0.1078\end{bmatrix} \qquad A(4)=\begin{bmatrix}-0.1279 & 0.0383\\ 0.0466 & -0.2356\end{bmatrix}$$

$$A(5)=\begin{bmatrix}-0.1438 & -0.0793\\ -0.0230 & -0.2505\end{bmatrix} \qquad A(6)=\begin{bmatrix}-0.1887 & -0.0229\\ -0.0941 & -0.1353\end{bmatrix}$$

$$A(7)=\begin{bmatrix}-0.1942 & -0.0225\\ -0.0464 & -0.1005\end{bmatrix}$$

This model was found to be stable. All 14 zeros of the characteristic polynomial

$$\det\left(\sum_{k=0}^{7} A(K)\ z^{k}\right)=0, \qquad \text{with } A(0)=\begin{bmatrix} -1 & 0 \\ 0 & -1 \end{bmatrix}$$

fall outside the unit circle (see Figure 1). In a test simulation using this model to generate a bivariate series of 1000 points with E(t) distributed N(0,I), where I is the identity matrix, the means of the series for channel 1 and channel 2 were 0.00430 and 0.02206, respectively, with an obtained covariance matrix at zero lag,

$$C(0)=\begin{bmatrix} 8.9004 & -3.8767 \\ -3.8767 & 5.1493 \end{bmatrix}.$$

To ensure immediate stability of the simulated data in each experimental condition, the last 7 generated data points of the test simulation, that is, Y(994) to Y(1000), were used as the initial seven values for simulating data in the experiment. The data was simulated by first generating the random numbers, storing them in a 2 x N dimensional array, and passing these through the linear system given by equation (1). A sample of approximately one second duration of the generated stationary series for the two channels is shown in Figures 2 and 3.

The theoretical values for spectral and coherence estimates were calculated by

$$S(f)=\Delta t[D(f)]^{-1}\, V\ [D(f)^{\ddagger}]^{-1}, \qquad f=1,\ldots,64,$$

where Δt is the sampling interval (1/128), V is the one-step-ahead prediction error matrix, that is, the covariance

Figure 1. Zeros of the characteristic polynomial, $\det(\sum_{k=0}^{7} A(k)z^{k})=0$, where $A(k)$ are the coefficients of the AR(7) model used in data simulation.

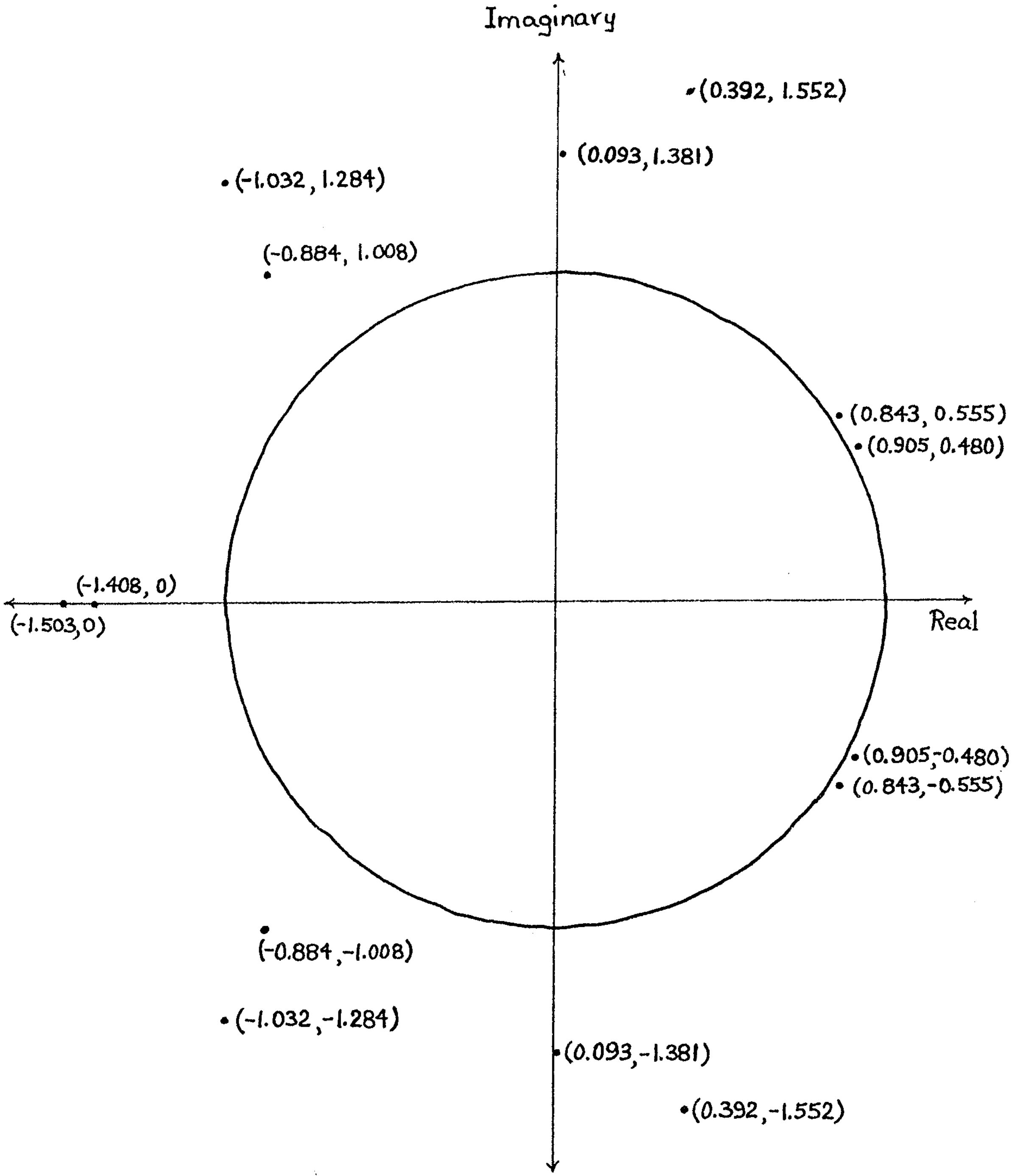

Imaginary
(0.392, 1.552)
(0.093, 1.381)
(-1.032, 1.284)
(-0.884, 1.008)
(0.843, 0.555)
(0.905, 0.480)
(-1.408, 0)
(-1.503, 0)
Real
(0.905, -0.480)
(0.843, -0.555)
(-0.884, -1.008)
(-1.032, -1.284)
(0.093, -1.381)
(0.392, -1.552)

Figure 2. A sample of an approximately one second segment of series 1 data generated by the AR(7) bivariate model.

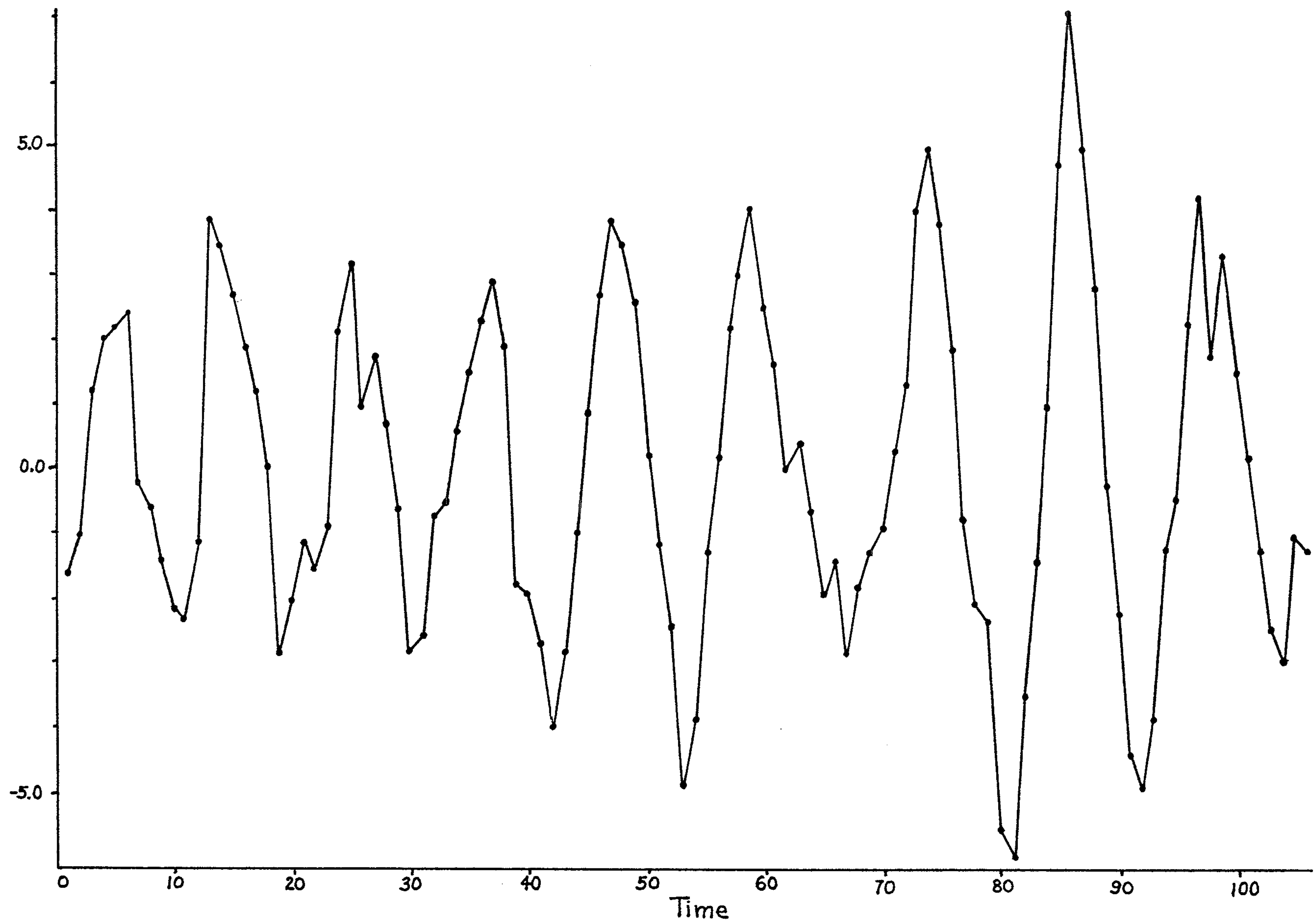
5.0
0.0
-5.0
0
10
20
30
40
50
60
70
80
90
100
Time

Figure 3. A sample of an approximately one second segment of series 2 data generated by the AR(7) bivariate model.

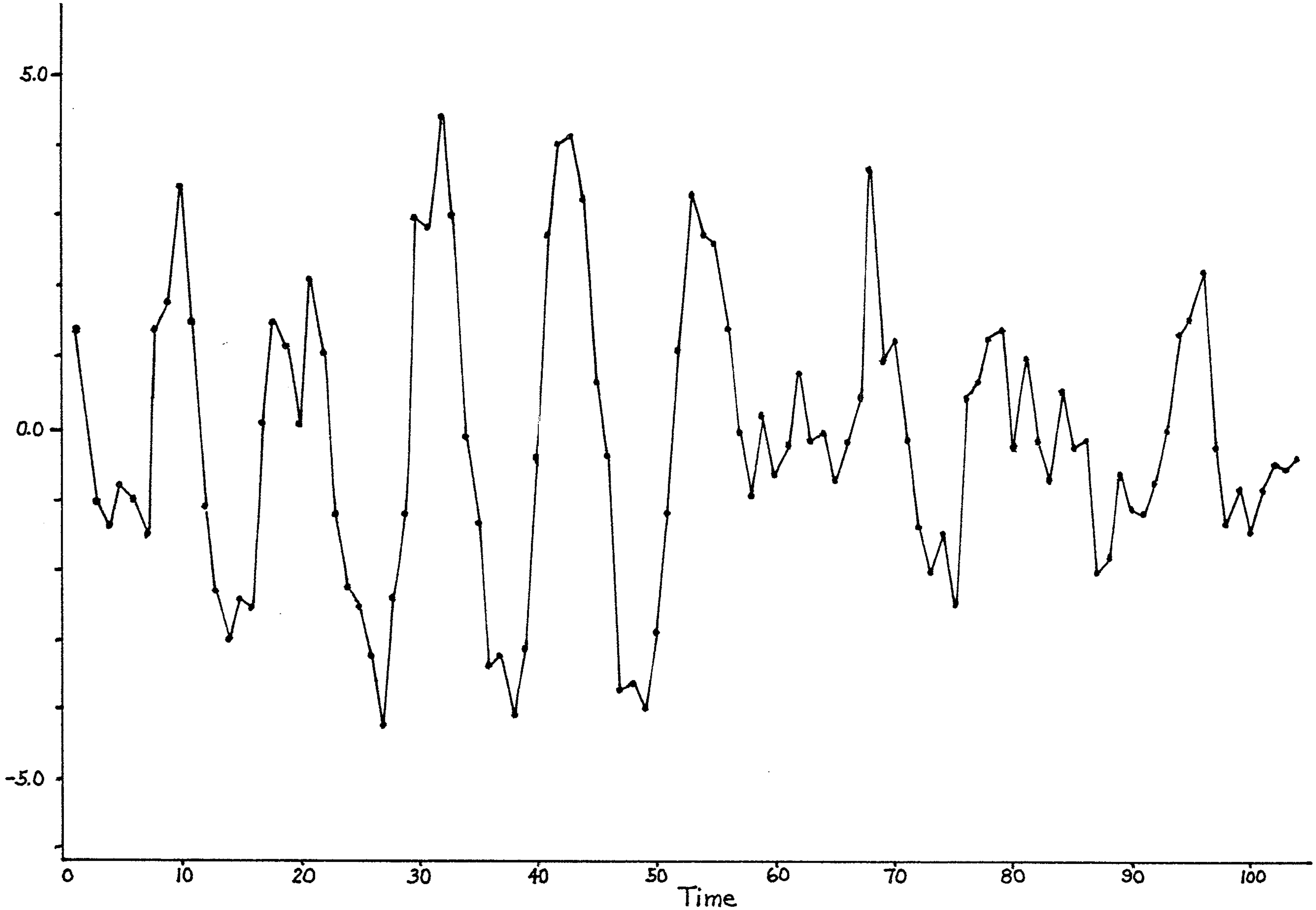
5.0
0.0
-5.0
0
10
20
30
40
50
60
70
80
90
100
Time

matrix of the error left over after the model is fitted, and theoretically equals the identity matrix since the covariance of E(t) in equation (1) was set to $\begin{bmatrix} 1 & 0 \\ 0 & 1 \end{bmatrix}$. The complex conjugate transpose is denoted by ‡, and

$$D(f) = \sum_{k=0}^{7} A(k)\ \exp(-i2\pi kf\Delta t)$$

where A(k) are the given AR coefficients with $A(0) = \begin{bmatrix} -1 & 0 \\ 0 & -1 \end{bmatrix}$. The theoretical spectra and coherence functions are shown in Figures 4 and 5, respectively.

Figure 4. Theoretical spectral curves for series 1 (top) and series 2 (bottom).

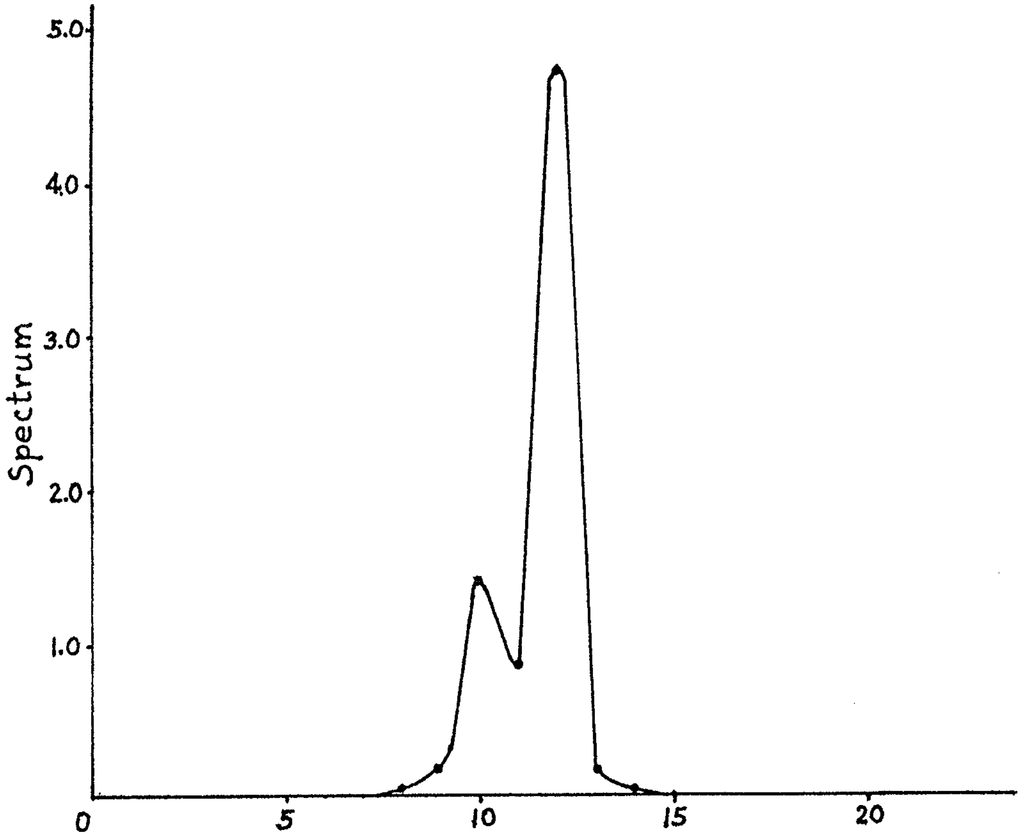

5.0
4.0
3.0
2.0
1.0
Spectrum
0
5
10
15
20

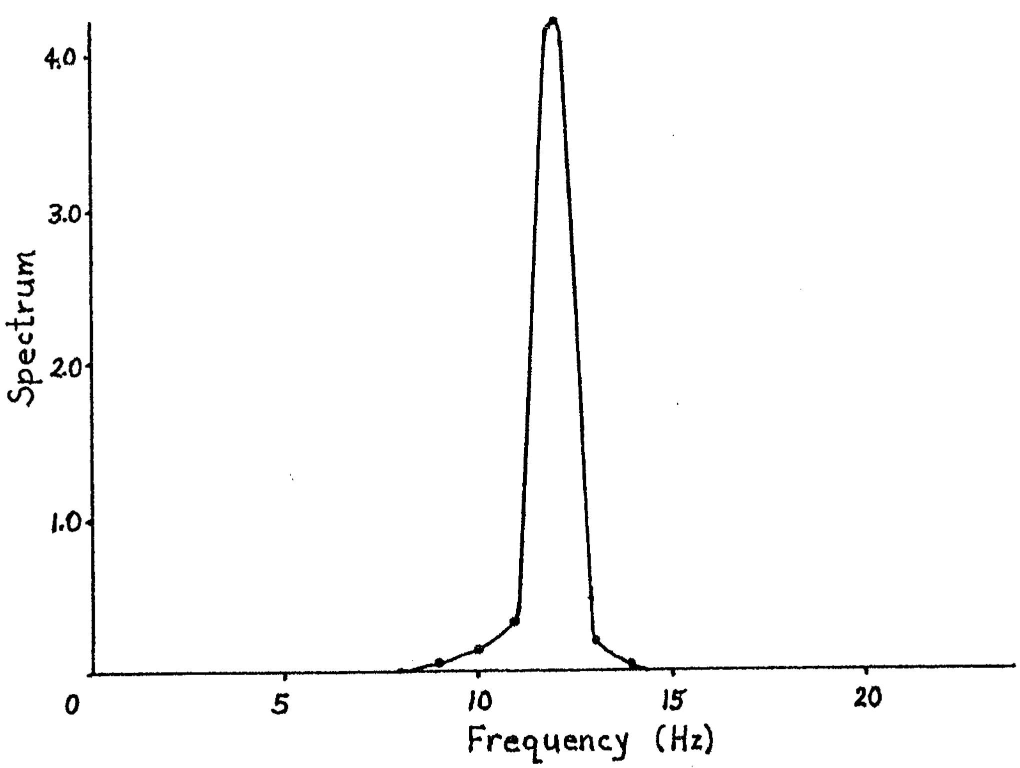

4.0
3.0
2.0
1.0
Spectrum
0
5
10
15
20
Frequency (Hz)

Figure 5. Theoretical coherence curve.

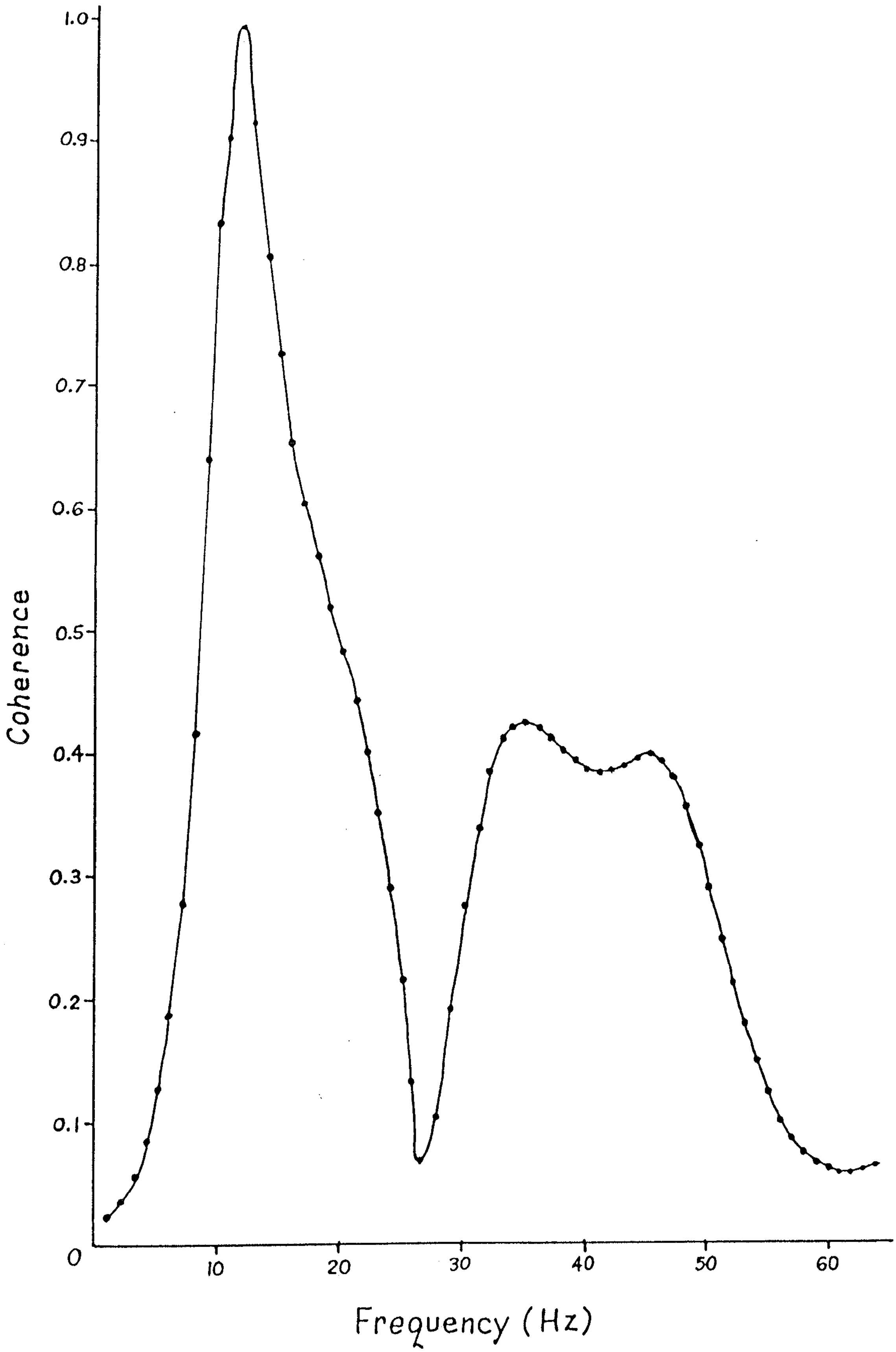

1.0
0.9
0.8
0.7
0.6
0.5
0.4
0.3
0.2
0.1
0
Coherence
10
20
30
40
50
60
Frequency (Hz)

Nonstationary Series

Three types of nonstationary data were simulated; 1) the variance of the normally distributed error in equation (1) was changed at various times in the data segment, 2) the distribution of the noise was changed from normal to exponential and 3) a transient sine wave was added to the stationary series.

Change of noise. In one set of experimental conditions, the N(0,I) error of the stationary series simulated by equation (1) was changed to N(0,S) with $S=\begin{bmatrix} 9 & 0 \\ 0 & 9 \end{bmatrix}$, such that

$$
\begin{aligned}
Y(t) &= \sum_k A(k)\; Y(t-k)+E_1(t), \qquad t=1,\ldots,N_1 \\
Y(t) &= \sum_k A(k)\; Y(t-k)+E_2(t), \qquad t=N_1+1,\ldots,N.
\end{aligned}
\tag{2}
$$

For the 2.0 second segments, this change was made for a) the second half of the segment at $N_1=128$, b) the last fourth of the data, $N_1=192$, and c) the last eighth of the data, $N_1=224$. Similarly, for the 1.0 second segment simulations, the variance was changed a) halfway through the interval ($N_1=64$), or b) for the last quarter of the data ($N_1=96$). Finally, for the 0.5 second conditions, the change was made halfway through the segment at $N_1=32$. Thus comparisons of record length and the amount (ratio) of added data could be made.

The second set of experimental conditions was created similarly, but rather than changing the variance of the normally distributed noise, the distribution of the noise was changed to exponentially distributed, $\exp(\mu)$, with the mean $\mu=2.0$. The exponential probability density is given by the equation

$$f(x) = \mu \exp\{-\mu x\}, \quad x \geq 0.$$

The exponentially distributed random numbers were generated by the IMSL routine GGEXN. The data was simulated by equations (2) as above with $E_2(t)$ in this condition distributed exponentially with $\mu=2.0$. For the three different record length conditions, this change was made halfway through the segment ($N_1=N/2$) in either one or both series, simply by replacing the normal random numbers by the exponential random numbers in the series prior to data simulation.

Transient sine wave. The third set of nonstationary conditions was simulated by adding a simulated transient sine wave of approximately 300 msec duration (40 data points) to data generated by equation (1); that is,

$$Y_T(t)=Y(t) + 8.0 \sin(2\pi k/40),$$

where k=1 for t=19, k=2 for t=20,..., and k=40 for t=58. This transient was added either to one or both series, and always at the same time points for all record length conditions.

Spectral Analysis

FFT estimates

The raw simulated data of each series was first tapered by a split-cosine window over 10% at each end of the series by the function

$$u(t)=\begin{cases}\frac{1}{2}\left[1-\cos\left(\pi\frac{(t-\frac{1}{2})}{m}\right)\right], & t=1,\ldots,m\\ 1, & t=m+1,\ldots,N-m\\ \frac{1}{2}\left[1-\cos\left(\pi\frac{(t-\frac{1}{2})}{m}\right)\right], & t=N-m+1,\ldots,N\end{cases}$$

where m is the proportion at each end (0.10). The tapered data was Fast Fourier transformed using the 'successive doubling' algorithm (Cooley, Lewis, & Welch, 1969), based on the Cooley-Tukey FFT method, and adjusted for tapering by multiplying each transformed value by 1/0.875 (Bendat & Piersol, 1975, pp. 327); that is,

$$\hat{S}(f)=(2\Delta t/0.875\ N)\ \left|\sum_{t=1}^{N} Y(t)\ \exp(-i\frac{2\pi t f}{N})\right|^2, \qquad f=0,\ldots,N/2,$$

where Y(t) is the tapered data series and the vertical bars denote the modulus.

Because smoothing of the resulting spectrogram is required, FFT spectral estimates were obtained for frequency bands at f=5, 10, ..., 60 Hz, and these were compared to theoretical values that were also averaged for these frequency bands. Thus the 0.5 second segments were smoothed by averaging S(f) for f=2-4, 4-6, 7-9, ..., 29-31; for the 1.0 second series the averaged frequency bands consisted of f=3-7, 8-12, ..., 58-62; and for the 2.0 second conditions, FFT values at f=5-14, 15-24, ..., 115-124 were averaged to correspond to the frequency bands at 5, 10, ..., 60 Hz.

The cross spectra between the two series, 1 and 2, were calculated by

$$\hat{S}_{12}(f)=(2\Delta t/0.875\ N)\ [\bar{S}1(f)\ S2(f)], \qquad f=0,\ldots,N/2,$$

where $\bar{S}(f)$ denotes the complex conjugate of $S(f)$. The coherence function was then calculated by

$$\hat{R}(f)=\left(\frac{|\hat{S}_{12}(f)|^2}{\hat{S}_1(f)\ \hat{S}_2(f)}\right)^{1/2}.$$

The cross spectra were smoothed analogously to the power spectra prior to the calculation of the coherence function, thus coherence estimates were also produced for the frequency bands at 5, 10, ..., 60 Hz.

AR Estimates (Whittle's Method)

The AR coefficients of the model were estimated using Whittle's (1963) recursive algorithm. This method estimates the coefficients and the one-step-ahead prediction error matrix for each successive order. The order p of the model was chosen such that Akaike's (1969a) final prediction error (FPE) criterion, defined as

$$FPE(p)=\frac{N+p+1}{N-p-1}\ |\hat{V}(p)|$$

is minimized. Here $\hat{V}(p)$ is the one-step-ahead prediction error matrix for the p-th order fitted. Models up to a maximum order of 15 were tested, but testing was stopped once a local minimum was found, since Ulrych and Bishop (1975) found that the first minimum, rather than the overall minimum, gives a good estimate of the order. The maximum order of 15 was chosen since Gersch and Sharpe (1973) found that for infinite order AR models, the mean value of the order that fit the theoretical results was 18.6.

Once the order $\hat{p}$ and the corresponding AR(p) coefficients and error matrix $\hat{V}(\hat{p})$ were found, the power spectrum at each frequency was estimated by

$$\hat{S}(f)=\Delta t\,[\hat{D}(f)]^{-1}\ \hat{V}(\hat{p})\ [\hat{D}(f)\ddagger]^{-1}\ ,\qquad f=1,\ldots,64 \tag{3A}$$

where Δt is the sampling interval (1/128) and

$$\hat{D}(f)=\sum_{k=0}^{\hat{p}}\hat{A}(k)\ \exp(-i2\pi kf\Delta t). \tag{3B}$$

The matrices $\hat{A}(k)$, $k=1,\ldots,\hat{p}$ are estimates of the AR coefficients with $\hat{A}(0)=\begin{bmatrix}-1 & 0\\ 0 & -1\end{bmatrix}$.

Since the theoretical order of the AR model is known, the same calculations were performed for the known order of seven, except the coefficients $\hat{A}(7)$ and the error matrix $\hat{V}(7)$ were used in equations (3A) and (3B). This permits a comparison of the results for the true and obtained orders, that is, the effect of incorrect order on spectral estimates.

The coherence estimates were then calculated by

$$\hat{R}(f)=\left(\frac{|\hat{S}_{12}(f)|^2}{\hat{S}_{11}(f)\,\hat{S}_{22}(f)}\right)^{1/2} \quad f=1,\ldots,64, \tag{4}$$

where $\hat{S}_{12}(f)$ is the off-diagonal entry of the matrix $\hat{S}(f)$ and represents the cross spectrum between series 1 and 2, and $\hat{S}_{11}(f)$ and $\hat{S}_{22}(f)$ are the diagonal values in matrix $\hat{S}(f)$ and correspond to the autospectra for series 1 and 2, respectively.

MEM Estimates

The MEM estimates were obtained by the indirect generalization of Burg's algorithm.[1] Essentially the same routine as that given in the Appendix of Jones (1978) was used, with some slight modifications to simplify computation. The routines were translated from a Fortran listing and simplified for a bivariate, rather than a general, system. Akaike's FPE criterion was used instead of the AIC criterion used by Jones (1978) to estimate the order so that the MEM procedure would be more comparable with the order selection procedure used with AR method. As was mentioned in the introduction, the FPE and AIC criteria are asymptotically equivalent, and in a preliminary trial I found that both criteria selected the same orders on the simulated data.

The MEM method estimates the coefficients and the prediction error matrix similarly to the AR method. Thus spectral estimates were calculated using equations (3A) and (3B) with the MEM estimated coefficients and the forward prediction matrix, for selected and known orders, replacing $\hat{A}(k)$ and $\hat{V}(p)$, respectively. Similarly, coherence estimates were calculated by equation (4).

Estimates of an Adaptive Method of the Kalman Type

The Kalman filter spectral estimates can be obtained from the univariate analogue of equations (3); that is,

$$\hat{S}(f,t) = \frac{\hat{e}_p(t)}{\left|\sum_{k=0}^{p} \hat{a}_k(t)\ \exp(-i2\pi k \Delta t)\right|^2}$$

where $\hat{a}_k(t)$ represent the coefficients which may now be time-variable, and $\hat{e}_p(t)$ is the residual error of the model at time t. Again, p is the number of coefficients required by the model and is analogous to the order in AR modeling, and must be specified.

The method of estimating adaptive time-variable parameters used in this study was based on the UD method proposed by Bierman (1977). This method involves factoring the covariance matrix of the coefficients M, into an upper triangular (U) and a diagonal (D) matrices, such that M=UDU'. The routine for this recursive least squares method was translated from the Fortran listing given in Table 2 in Clarke (1980), with the forgetting factor set to 0.98 for all conditions and the order, p, set to 7. Clarke's algorithm of estimating the model coefficients was chosen for its computational efficiency and numerical stability, and also because it has been widely used in practice.

RESULTS

The average bias and mean square error (MSE) of the spectral and coherence estimates were calculated from 200 replications of each condition. The coherence estimates were first transformed to obtain normally distributed variables using Fisher's r to z transform (Brillinger, 1981, pp. 314). The MSEs were then calculated for the transformed coherence estimates. The bias values reported correspond to the actual bias of the original coherence estimates.

Order Selection

The orders estimated by Akaike's (1969a) FPE criterion, which was used by both the AR and MEM methods in the various conditions, are presented in Table 1. In every condition, stationary and nonstationary of all interval lengths, the MEM method selected higher orders, on the average, than the AR method.

For the AR method in the stationary conditions, the estimated order was quite low (5.065) for the shortest data segments, but as the sampling interval was lengthened the average order selected became successively closer to the theoretical value of 7. The estimated orders of the MEM method were much closer to the underlying model order in all

Table 1

Order Estimation of the AR(7) Model by the FPE Criterion by the AR and MEM Methods in All Experimental Conditions

	AR Method			MEM Method		
Condition	0.5 s	1.0 s	2.0 s	0.5 s	1.0 s	2.0 s
Stationary	5.065	6.445	7.035	6.875	7.045	7.220
Change in Noise Variance at						
N/2	5.560	7.475	8.515	9.490	9.375	9.270
N/4		8.380	10.175		11.120	11.675
N/8			10.025			11.585
Transient Sine Wave Added to						
Series 1	4.815	6.360	10.250	7.165	8.710	12.570
Both series	4.600	6.040	11.195	6.630	7.980	12.615
Exponentially (mean=2) Distributed Noise Halfway in						
Series 1	4.525	6.475	9.175	7.090	8.320	10.785
Both series	4.230	7.160	10.885	7.210	9.650	12.000

Note. Values represent the average orders from 200 replications of each condition.

record length conditions, although a slight tendency of the order estimates to increase as intervals lengthened was present. In the 2.0 second stationary condition, the MEM method overestimated the order slightly more (7.220) than the AR method (7.035).

For the nonstationary series of all tested interval lengths, the MEM method always overestimated the order, except when a transient sine wave was added to both series in the shortest segments. The AR method in all 0.5 second record length conditions produced underestimated orders, while overestimated orders were obtained in all 2.0 second nonstationary conditions. In the 0.5 second interval lengths, the MEM method was generally less sensitive to nonstationarities than the AR method, except when the normal error variance was changed; in these conditions, the average orders of the MEM models were more overestimated than those of the AR models, regardless of record length. In the 2.0 second conditions, for both methods, the average order selected for all types of nonstationary series was always greater than 7.

Model Coefficient Estimation

Tables 2, 3, and 4 show the mean coefficient estimates, their bias, and mean square error, respectively, in the stationary conditions. These values were obtained from estimation by the AR and MEM methods with the order set to the theoretical value of 7.0, rather than using the optimal or-

Table 2

Mean Estimates (x 100) of Model Coefficients

in the Stationary Conditions

	Theoretical Values (x 100)	AR Method			MEM Method		
		0.5 s	1.0 s	2.0 s	0.5 s	1.0 s	2.0 s
A(1)	30.23	44.01	39.74	36.10	29.21	29.14	29.20
	-9.74	-12.17	-12.20	-11.62	-9.40	-9.08	-9.55
	-13.44	-20.49	-17.65	-16.37	-15.63	-13.57	-13.42
	36.14	38.51	39.30	37.60	35.93	35.77	35.36
A(2)	13.51	6.04	9.63	12.60	11.95	12.78	13.85
	4.14	9.23	6.81	5.63	1.73	2.98	3.73
	-3.10	3.72	0.01	-1.94	-0.58	-2.98	-3.49
	12.49	0.90	6.21	9.19	5.02	8.92	10.86
A(3)	-7.03	-3.89	-6.34	-7.68	-5.04	-6.09	-7.13
	36.70	32.97	35.02	35.88	37.26	36.51	36.75
	8.93	5.70	7.95	8.44	7.14	7.86	8.14
	-10.78	-7.45	-9.96	-9.88	-9.19	-9.91	-9.73
A(4)	-12.79	-16.28	-14.44	-14.22	-16.97	-14.43	-13.83
	3.83	3.24	2.44	2.52	8.01	6.02	4.90
	4.66	0.77	1.56	3.30	4.02	4.27	4.70
	-23.56	-14.33	-18.53	-20.87	-18.13	-21.86	-22.97
A(5)	-14.38	-7.78	-11.21	-12.39	-7.34	-11.32	-12.47
	-7.93	-3.84	-6.42	-7.59	-6.44	-6.84	-7.28
	-2.30	-0.21	-1.85	-1.78	-0.33	-1.61	-1.65
	-25.05	-20.89	-22.77	-23.21	-21.13	-23.20	-23.87
A(6)	-18.87	-9.23	-13.11	-15.43	-17.36	-18.32	-18.51
	-2.29	-8.41	-4.86	-4.67	-4.32	-2.65	-3.38
	-9.41	-4.19	-6.63	-8.46	-6.45	-7.97	-8.99
	-13.53	-14.71	-13.81	-13.61	-14.26	-13.53	-13.41
A(7)	-19.42	-14.49	-16.25	-17.54	-17.33	-18.64	-19.50
	-2.25	4.01	-0.26	-0.39	-0.65	-2.13	-1.00
	-4.64	-8.07	-7.11	-6.43	-5.10	-5.34	-5.28
	-10.05	-4.66	-7.09	-8.67	-6.80	-9.16	-9.79

Table 3

Average Bias (x 1000) of Model Coefficient Estimates

in the Stationary Conditions

	AR Method			MEM Method		
	0.5 s	1.0 s	2.0 s	0.5 s	1.0 s	2.0 s
A(1)	137.8	95.1	58.7	-10.2	-10.9	-10.3
	-24.3	-23.6	-18.8	3.4	6.6	1.9
	-70.5	-42.1	-29.3	-21.9	-1.3	0.2
	23.7	31.6	14.6	-2.1	-3.7	-7.8
A(2)	-74.7	-38.8	-9.1	-15.6	-7.3	3.4
	50.9	26.7	14.9	-24.1	-11.6	-4.1
	68.2	31.1	11.6	25.2	1.2	-3.9
	-115.9	-62.8	-33.0	-74.7	-35.7	-16.3
A(3)	31.4	6.9	-6.5	19.9	9.4	-1.0
	-37.3	-16.8	-8.2	5.6	-1.9	0.5
	-32.3	-9.8	-4.9	-17.9	-10.7	-7.9
	33.3	8.2	9.0	15.9	8.7	10.5
A(4)	-34.9	-16.5	-14.3	-41.8	-16.4	-10.4
	-5.9	-13.9	-13.1	41.8	21.9	10.7
	-38.9	-31.0	-13.6	-6.4	-3.9	0.4
	92.3	50.3	26.9	54.3	17.0	5.9
A(5)	66.0	31.7	19.9	70.4	30.6	19.1
	40.9	15.1	3.4	14.9	10.9	6.6
	20.9	4.5	5.2	19.7	6.9	6.5
	41.6	22.8	18.4	39.2	18.5	11.8
A(6)	96.4	57.6	34.4	15.1	5.5	3.6
	-61.2	-25.7	-23.8	-20.3	-3.6	-9.9
	52.2	27.8	9.5	29.6	14.4	4.2
	-11.8	-2.8	-0.8	-7.3	-0.0	1.2
A(7)	49.3	31.7	18.8	20.9	7.8	-0.8
	62.6	19.9	18.6	16.0	1.2	12.5
	-34.3	-24.7	-17.9	-4.6	-7.0	-6.4
	53.9	29.6	13.8	32.5	8.9	2.6

Table 4

Average Mean Square Error (x 1000) of Model Coefficients

in the Stationary Conditions

	AR Method			MEM Method		
	0.5 s	1.0 s	2.0 s	0.5 s	1.0 s	2.0 s
A(1)	39.8	19.1	8.0	18.5	8.1	3.6
	21.9	9.9	4.8	22.3	9.2	4.1
	22.5	9.5	5.8	18.7	7.6	4.3
	21.6	11.7	5.1	23.2	9.2	4.3
A(2)	25.3	11.3	4.1	21.6	9.6	3.7
	26.8	10.7	4.3	26.8	10.0	4.2
	23.3	9.6	4.9	24.1	9.8	4.9
	32.3	12.0	5.3	26.6	10.3	4.6
A(3)	17.7	8.5	4.5	18.7	8.3	4.5
	29.1	10.2	4.2	27.0	9.5	3.9
	16.4	6.6	4.0	22.0	8.0	4.1
	16.9	7.7	3.8	18.7	8.8	4.3
A(4)	17.4	8.1	4.8	19.3	7.6	4.6
	21.6	10.0	4.9	23.6	9.4	4.6
	18.0	8.2	4.1	22.1	8.1	4.2
	28.0	11.8	5.5	26.4	10.2	5.0
A(5)	20.6	8.9	4.7	23.0	9.7	4.5
	26.3	11.1	4.3	26.8	10.0	4.4
	17.6	8.0	4.1	24.2	9.8	4.3
	20.3	8.5	5.0	24.6	9.1	5.0
A(6)	24.4	11.2	5.4	19.5	7.7	4.0
	27.9	9.8	5.3	24.7	9.5	5.0
	21.4	7.9	3.7	23.3	8.1	3.8
	20.1	9.0	4.6	24.4	9.8	4.8
A(7)	17.4	7.7	3.8	17.5	7.1	3.5
	21.2	9.4	4.3	23.6	10.8	4.0
	14.4	5.9	3.4	17.0	6.9	3.3
	18.7	8.7	4.1	22.4	9.2	4.3

der selected by the FPE criterion, so that the average of each of the 28 (i.e., 2 x 2 x 7) coefficients can be directly compared to its theoretical counterpart.

The results show that as the record length was increased, both the bias and the MSE of each of the coefficient estimates decreased. Almost all of the MEM coefficient estimates were much less biased than those of the AR model, although the MSEs of the two methods' estimates were quite similar. For each method and within each data segment length condition, the MSEs (Table 4) were notably constant across all coefficient estimates. The variability, MSE and bias of the 28 coefficient estimates in each stationary condition were averaged together and compared for the two methods as a function of interval length in Figure 6.

Tables 5, 6, and 7 contain the variability, MSE and bias, respectively, averaged over the 28 model coefficients estimated in each of the nonstationary conditions. As in the stationary case, in all nonstationary conditions as the sampling interval lengthened, the variability, MSE and the bias decreased.

Both methods estimated the coefficients very similarly in the nonstationary conditions. In each experimental condition, the variability and MSE (Tables 5 and 6, respectively) were almost identical for the two methods; the average biases (Table 7) of the MEM coefficients were about half the

Figure 6. Comparison of the properties of model coefficient estimates obtained by the AR (△) and MEM (○) methods from stationary series as a function of interval length, averaged over all 7 x 2 x 2 coefficients. The mean (S.E.) variability is shown in part (a), MSE in (b), and bias in (c).

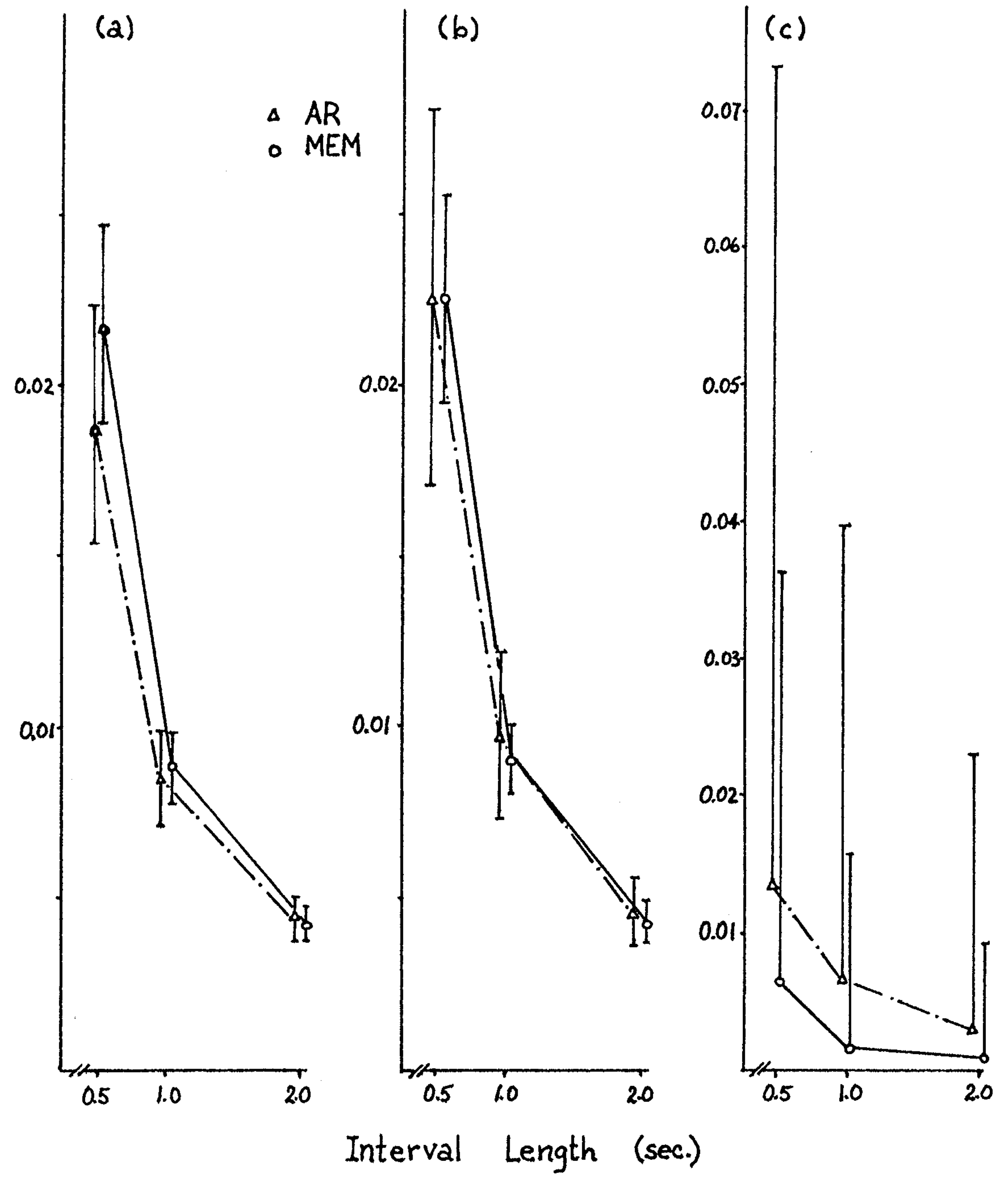

(a)
(b)
(c)
AR
MEM
0.02
0.01
0.07
0.06
0.05
0.04
0.03
0.5
1.0
2.0
Interval Length (sec.)

Table 5

Averaged Variability (x 1000) of Model Coefficients

in All Experimental Conditions

	AR Method			MEM Method		
Condition	0.5 s	1.0 s	2.0 s	0.5 s	1.0 s	2.0 s
Stationary	18.9 (3.4)	8.5 (1.3)	4.3 (0.5)	21.7 (2.9)	8.8 (1.0)	4.2 (0.4)
Change in Noise Variance at						
N/2	32.1 (7.5)	15.2 (2.7)	7.2 (1.1)	35.2 (6.7)	15.0 (2.1)	6.9 (1.0)
N/4		20.3 (4.4)	10.6 (2.4)		20.5 (2.9)	10.1 (1.5)
N/8			11.3 (2.5)			10.1 (1.4)
Transient Sine Wave Added to						
Series 1	23.8 (10.5)	11.4 (4.9)	5.6 (2.1)	29.4 (13.1)	12.5 (5.5)	5.8 (2.3)
Both series	23.9 (6.5)	11.1 (2.6)	5.6 (1.2)	29.8 (7.5)	12.5 (2.8)	5.9 (1.3)
Exponentially (mean=2) Distributed Noise Halfway in						
Series 1	26.2 (18.2)	12.9 (9.3)	6.5 (4.7)	32.8 (23.8)	14.3 (10.7)	6.8 (5.0)
Both series	27.1 (7.7)	13.4 (2.9)	6.6 (1.2)	31.4 (7.0)	14.4 (3.0)	6.6 (1.2)

Note. The numbers in brackets indicate the standard error (x 1000) in averaging all 28 coefficients in each condition.

Table 6

Average Mean Square Error (x 1000) of Model Coefficient Estimates in All Experimental Conditions

Condition	AR Method 0.5 s	AR Method 1.0 s	AR Method 2.0 s	MEM Method 0.5 s	MEM Method 1.0 s	MEM Method 2.0 s
Stationary	22.5 (5.5)	9.7 (2.4)	4.7 (0.9)	22.5 (3.0)	9.0 (1.0)	4.3 (0.5)
Change in Noise Variance at						
N/2	34.8 (7.5)	16.3 (3.5)	7.7 (1.8)	36.1 (6.4)	15.2 (2.0)	7.0 (1.0)
N/4		22.0 (5.0)	11.3 (3.1)		20.9 (2.8)	10.2 (1.5)
N/8			12.5 (3.9)			10.3 (1.4)
Transient Sine Wave Added to						
Series 1	48.0 (88.7)	33.3 (78.9)	25.4 (65.8)	52.4 (82.8)	31.0 (74.2)	25.6 (63.9)
Both series	49.3 (59.1)	33.3 (46.7)	25.1 (34.7)	52.7 (51.2)	34.0 (40.7)	25.3 (31.7)
Exponentially (mean=2) Distributed Noise Halfway in						
Series 1	31.6 (19.7)	16.6 (12.9)	10.1 (10.9)	36.6 (24.3)	17.6 (13.5)	10.4 (10.9)
Both series	34.8 (10.5)	20.7 (9.7)	14.0 (9.4)	38.3 (8.5)	20.9 (6.5)	13.6 (7.4)

Note. The numbers in brackets indicate the standard error (x 1000) in averaging the MSE of all 28 coefficients in each condition.

Table 7

Averaged Bias (x 1000) of Model Coefficient Estimates

in All Experimental Conditions

	AR Method			MEM Method		
Condition	0.5 s	1.0 s	2.0 s	0.5 s	1.0 s	2.0 s
Stationary	13.6 (59.8)	6.5 (34.5)	3.0 (20.6)	6.3 (30.1)	2.0 (13.3)	0.8 (8.2)
Change in Noise Variance at						
N/2	22.53 (49.5)	10.7 (33.4)	5.8 (24.3)	15.7 (30.0)	5.0 (15.8)	2.7 (8.9)
N/4		13.8 (40.9)	8.8 (26.8)		7.7 (20.5)	3.7 (10.8)
N/8			11.43 (34.6)			5.1 (12.1)
Transient Sine Wave Added to						
Series 1	52.4 (149.8)	48.1 (142.4)	46.9 (135.3)	34.1 (151.1)	36.4 (145.1)	40.5 (137.2)
Both series	88.8 (135.4)	87.9 (122.7)	86.9 (111.6)	88.7 (125.6)	87.9 (119.8)	86.9 (110.8)
Exponentially (mean=2) Distributed Noise Halfway in						
Series 1	28.6 (69.7)	20.0 (59.0)	15.6 (59.1)	22.8 (59.9)	15.1 (57.0)	12.6 (60.4)
Both series	66.6 (59.7)	58.9 (63.9)	57.7 (65.3)	68.0 (49.4)	59.2 (56.5)	57.9 (61.7)

Note. The numbers in brackets indicate the standard error (x 1000) in averaging the bias of all 28 coefficients obtained in each condition.

size of the biases of the AR estimates in the stationary and change of normal variance conditions. When a half of one or both series contained exponentially distributed noise and when one of both series contained a transient sine wave, the biases of the two methods' estimates were much larger but more similar for the two methods.

For both methods, the stationary estimates were the least variable and had the smallest MSEs and biases. The change-in-variance nonstationary conditions resulted in the most variable coefficients, although the variabilities were similar across all conditions for the same interval length (Table 5). The addition of a transient sine wave to either one or both series resulted in the highest MSE in the averaged coefficient; however, for both methods, the largest bias was observed when both series contained the transient. Similarly, when the series contained exponentially distributed error, although the MSEs were similar whether one or both series were nonstationary, the bias was much higher when both series were nonstationary.

When a transient sine wave was added to series 1, the greatest increase in MSE occurred in the first order $A(1)_{11}$ coefficient; adding a sine wave to both series increased the MSE primarily in the first order $A(1)_{11}$ and $A(1)_{22}$ coefficients.

Spectral and Coherence Estimates

Stationary Series

The theoretical spectral values for frequencies greater than 20 Hz indicate only noise present (see Figure 4 on page 40). Thus results in the Tables are reported for frequencies 1 to 20 Hz since these are of primary interest. Although the AR and MEM estimates were obtained from models where the optimal order was selected by the FPE criterion as well as from models of the known order of 7, the results show that the estimates from both sets of models and their properties were very similar. Tables 8 and 9 show the bias and MSE, respectively, of the AR estimates obtained from the 0.5 second stationary series as an example. Results for the spectra and coherence estimates of the other methods were very similar. Increasing the record length makes these differences generally even smaller, therefore only results with the optimal order estimated will be reported, since those would be the estimates obtained in practice.

The adaptive method of the Kalman type performed relatively poorly in comparison with the AR and MEM, and FFT methods in all conditions. Thus, since the performance of these estimates was similar across all conditions, the spectral estimates of the adaptive method will only be briefly reported for the stationary series.

Table 8

Bias (x 10) of AR Spectral and Coherence Estimates

from 0.5 sec Segments Obtained from Models

with Estimated Orders ($\hat{p}$) and from

Models Using p=7

	Series 1		Series 2		Coherence	
freq	$\hat{p}$	p=7	$\hat{p}$	p=7	$\hat{p}$	p=7
1	0.152	0.081	0.072	0.044	2.683	3.058
2	0.158	0.086	0.075	0.046	2.722	3.044
3	0.171	0.096	0.080	0.050	2.737	2.982
4	0.191	0.112	0.087	0.056	2.705	2.852
5	0.222	0.140	0.098	0.065	2.604	2.639
6	0.271	0.189	0.117	0.082	2.411	2.325
7	0.349	0.285	0.148	0.113	2.076	1.871
8	0.465	0.499	0.209	0.189	1.502	1.248
9	0.084	0.600	0.316	0.407	0.352	0.222
10	-9.003	-7.681	0.281	0.517	-0.700	-0.730
11	-1.292	-0.304	1.055	1.651	-0.522	-0.532
12	-36.660	-35.633	-34.181	-32.569	-0.809	-0.758
13	2.262	1.934	1.675	1.620	-0.148	-0.065
14	0.957	0.798	0.707	0.645	0.361	0.531
15	0.502	0.415	0.361	0.307	0.602	0.897
16	0.304	0.258	0.213	0.175	0.685	1.129
17	0.204	0.182	0.141	0.114	0.698	1.287
18	0.147	0.140	0.100	0.081	0.691	1.402
19	0.111	0.114	0.175	0.061	0.690	1.488
20	0.087	0.097	0.058	0.049	0.714	1.555

Table 9

MSE of Stationary AR Spectral and Transformed Coherence Estimates (of 0.5 sec segments) Obtained from Models with Estimated Orders ($\hat{p}$) and from Model of Order 7 (p=7)

	Series 1		Series 2		Coherence	
freq	$\hat{p}$ (x 1000)	p=7	$\hat{p}$ (x 1000)	p=7	$\hat{p}$ (x 10)	p=7
1	0.4	0.2	0.1	0.1	1.38	2.03
2	0.4	0.2	0.1	0.1	1.39	1.96
3	0.5	0.2	0.2	0.1	1.42	1.86
4	0.6	0.3	0.2	0.1	1.47	1.74
5	0.9	0.5	0.2	0.1	1.55	1.61
6	1.3	0.8	0.3	0.2	1.68	1.50
7	2.5	2.0	0.6	0.4	1.87	1.49
8	7.0	8.4	1.3	1.3	2.12	1.69
9	36.0	66.8	5.5	9.9	2.18	1.98
10	1072.3	990.9	27.9	37.9	2.88	2.68
11	670.4	897.0	196.0	288.1	3.97	3.98
12	14649.3	14304.4	12708.3	12076.9	15.15	14.23
13	144.6	111.9	124.4	103.8	2.90	2.79
14	15.8	13.1	11.6	10.2	2.35	2.48
15	4.1	3.2	2.6	2.0	1.98	2.26
16	1.5	1.2	0.9	0.6	1.67	2.06
17	0.7	0.6	0.4	0.3	1.45	1.91
18	0.4	0.3	0.2	0.1	1.30	1.79
19	0.2	0.2	0.1	0.1	1.18	1.70
20	0.1	0.2	0.1	0.1	1.09	1.63

Comparison of spectra. The estimates of the spectra of series 1 and 2 in the three segment length conditions are presented in Figure 7 for those estimates obtained by the AR method, and in Figure 8 for those estimated by MEM. The two methods produced very similar estimates, although in all record length conditions the MEM estimates of both series were very slightly less biased than the AR spectral estimates. As the interval length increased, both sets of estimates became less biased. In the 0.5 second intervals, both methods failed to detect the smaller peak at 10 Hz in series 1; with each record length increase, this smaller peak was estimated with successively less bias.

The spectral estimates of the stationary series obtained by the adaptive method are shown in Figure 9. This method consistently estimated the 12 Hz major peak of series 1 at 11 Hz, and with an equal bias regardless of record length. Results for series 2 were less satisfactory; although the position of the peak of series 2 was estimated accurately at 12 Hz in all three length conditions, the bias of these estimates was very large, particularly as the intervals lengthened to 1.0 and 2.0 seconds. The average bias was -0.517 for 0.5 second intervals, 7.967 for 1.0 second intervals, and 13.758 for 2.0 second intervals at the 12 Hz frequency.

The mean spectral estimates for both series and their average bias obtained by the FFT method are presented in Table

Figure 7. Spectral estimates obtained by the AR method from stationary 0.5 second (▲), 1.0 second (■), and 2.0 second (●) segments for series 1 (top) and for series 2 (bottom).

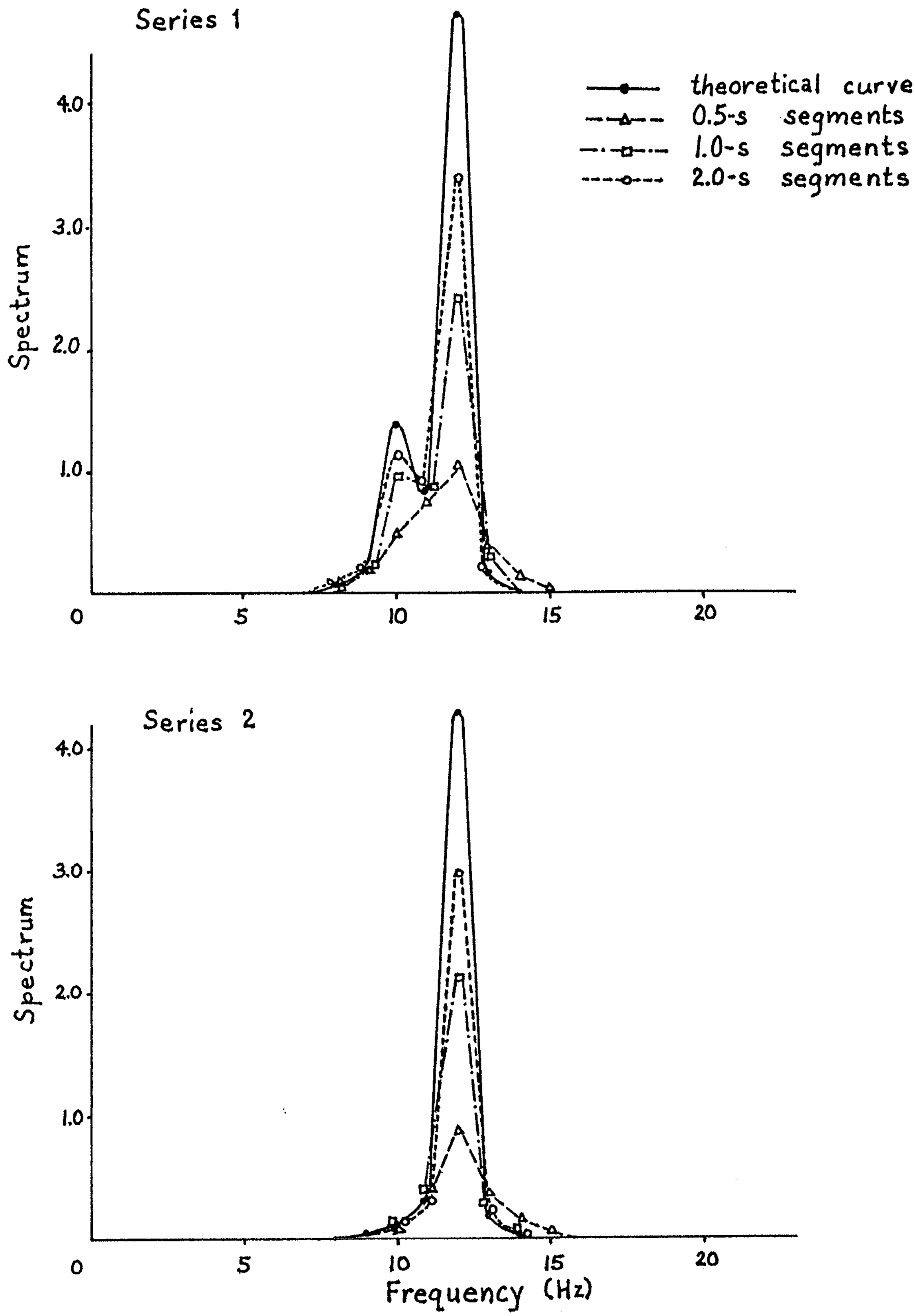

Series 1
theoretical curve
0.5-s segments
1.0-s segments
2.0-s segments
Spectrum
4.0
3.0
2.0
1.0
0
5
10
15
20
Series 2
Spectrum
4.0
3.0
2.0
1.0
0
5
10
15
20
Frequency (Hz)

Figure 8. Spectral estimates obtained by the MEM method from stationary 0.5 second (▲), 1.0 second (■), and 2.0 second (●) segments for series 1 (top) and for series 2 (bottom).

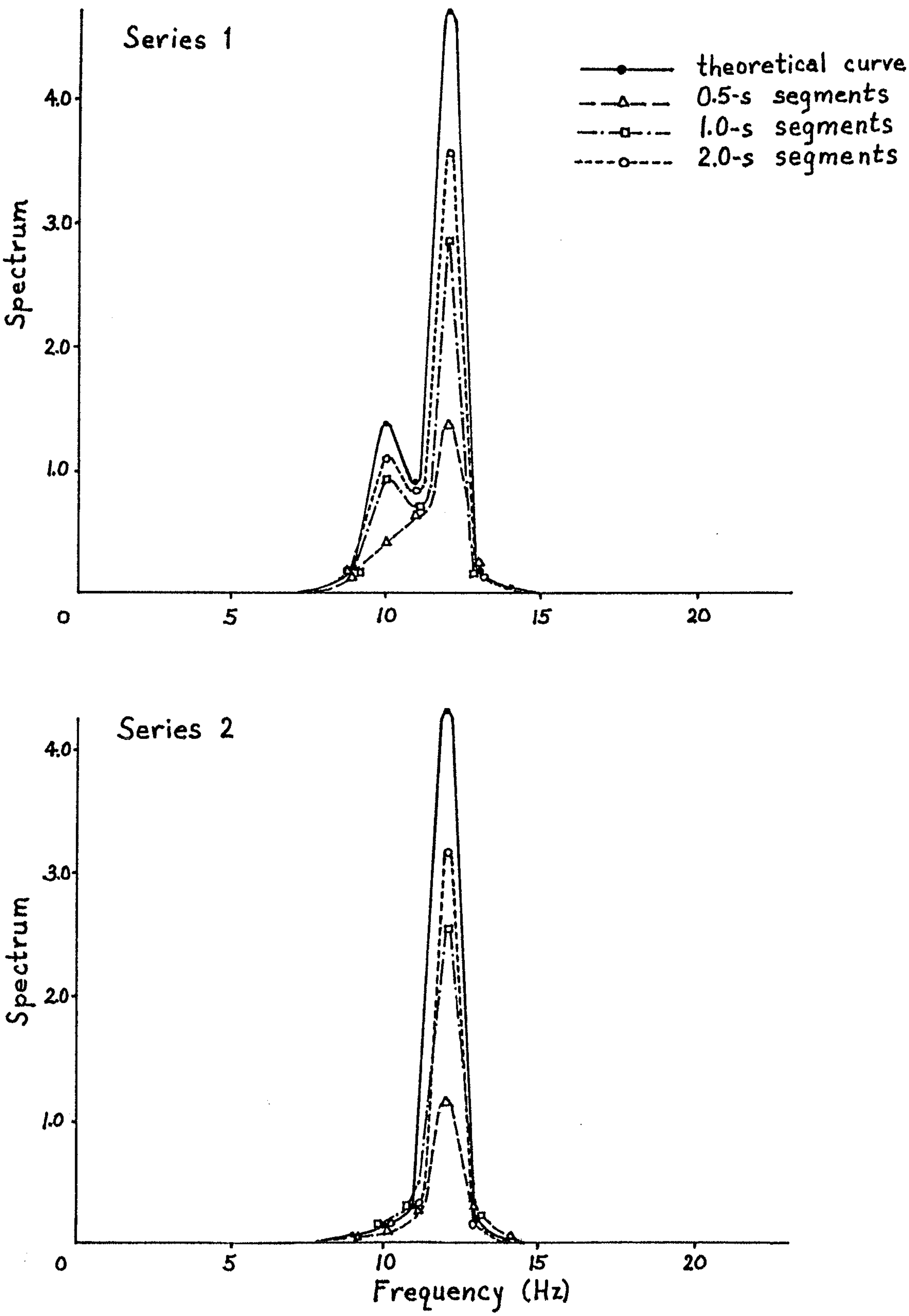

Series 1
theoretical curve
0.5-s segments
1.0-s segments
2.0-s segments
Spectrum
4.0
3.0
2.0
1.0
0
5
10
15
20
Series 2
Spectrum
4.0
3.0
2.0
1.0
0
5
10
15
20
Frequency (Hz)

Figure 9. Spectral estimates obtained by the adaptive method of the Kalman type from stationary 0.5 second (▲), 1.0 second (◘), and 2.0 second (●) segments for series 1 (left panel) and for series 2 (right panel).

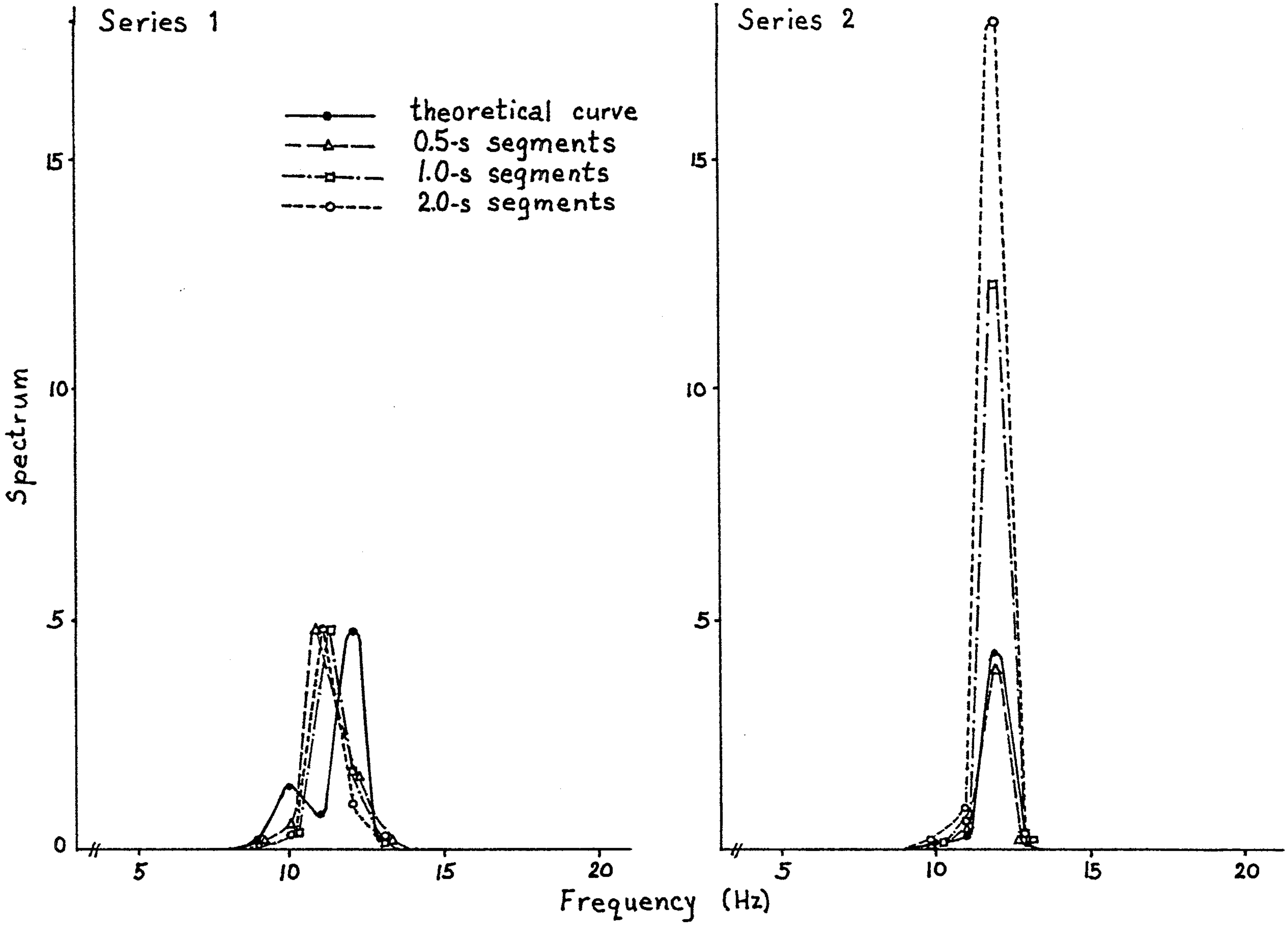
Series 1
Series 2
theoretical curve
0.5-s segments
1.0-s segments
2.0-s segments
Spectrum
0
5
10
15
20
Frequency (Hz)

Table 10

Mean Estimates and Bias of Spectra and Coherences from Stationary Data Obtained by the FFT Method

freq band	Theoretical value	Mean 0.5 s	Mean 1.0 s	Mean 2.0 s	Bias 0.5 s	Bias 1.0 s	Bias 2.0 s
			Series 1				
5	1.16	7.38	2.80	1.78	6.22	1.64	0.62
10	143.98	21.99	59.44	77.52	-121.99	-84.54	-66.47
15	4.77	3.37	6.41	10.32	-1.41	1.63	5.54
20	0.66	2.98	1.92	1.55	2.31	1.26	0.39
25	0.62	1.16	0.69	0.62	0.54	0.07	0.01
			Series 2				
5	0.81	3.62	1.76	1.03	2.80	0.94	0.22
10	96.17	15.75	40.67	49.18	-80.42	-55.50	-46.99
15	5.99	3.30	5.04	8.66	-2.69	-0.95	2.67
20	0.67	2.48	1.70	0.95	1.81	1.02	0.27
25	0.42	0.90	0.46	0.40	0.48	0.04	-0.03
			Coherence				
5	14.48	64.54	61.37	45.16	50.06	46.90	30.68
10	75.75	74.64	76.19	75.11	-1.10	0.44	-0.64
15	74.13	79.94	80.22	86.79	5.81	6.09	12.66
20	48.16	84.24	76.88	64.53	36.08	28.73	16.37
25	21.30	67.02	52.59	45.38	45.73	31.29	24.08

Note. Tabled values are obtained values x 100.

10. For both series, the greatest bias occurred in the 10 Hz frequency band in the shortest (0.5 second) intervals. As the record length was increased, the bias of these estimates generally decreased in all frequency bands, except in the 15 Hz band where the bias of both series increased with record length.

The MSE of the spectral estimates obtained by all four estimation methods are presented in Table 11. The spectral estimates of all four methods had the greatest MSE in the 12 Hz peak regions of both series. Although the MSEs of the MEM estimates were slightly smaller than those of the AR estimates in the frequencies with low or no power, the AR estimates had marginally smaller MSEs where power was present, that is, at 10 and 12 Hz in series 1, and at 12 Hz in series 2. The MSEs of the FFT spectral estimates were quite comparable to the MSEs of the AR and MEM estimates. The adaptive method's estimates had MSEs that were orders of magnitude larger than the estimates of the other methods in the 10 to 13 Hz frequency region, and particularly in the estimates of series 2 from the longer, 1.0 and 2.0 second, record length conditions.

Comparing the results of the spectral estimates for the different interval lengths, the MSEs of all four methods generally decreased with each increase in interval length. The most notable exceptions occurred in the frequencies where the series contained the most power. The MSE of AR

Table 11

Mean Square Error (x 10) of Spectral Estimates Obtained by

the Four Methods of Estimation from Stationary Data

	AR Method			MEM Method		
freq	0.5 s	1.0 s	2.0 s	0.5 s	1.0 s	2.0 s
			Series 1			
5	0.01	0.0	0.0	0.01	0.0	0.0
6	0.01	0.0	0.0	0.0	0.0	0.0
7	0.03	0.01	0.0	0.0	0.0	0.0
8	0.07	0.02	0.01	0.02	0.0	0.0
9	0.36	0.15	0.10	0.44	0.13	0.08
10	10.72	12.91	8.97	12.36	13.75	10.81
11	6.70	4.08	2.48	10.53	2.73	1.99
12	146.49	127.69	158.25	145.52	211.08	179.48
13	1.45	0.39	0.10	1.07	0.09	0.03
14	0.16	0.03	0.01	0.03	0.0	0.0
15	0.04	0.01	0.0	0.0	0.0	0.0
			Series 2			
5	0.0	0.0	0.0	0.0	0.0	0.0
6	0.0	0.0	0.0	0.0	0.0	0.0
7	0.01	0.0	0.0	0.0	0.0	0.0
8	0.01	0.0	0.0	0.0	0.0	0.0
9	0.06	0.02	0.01	0.04	0.01	0.0
10	0.28	0.23	0.11	0.21	0.19	0.11
11	1.96	0.85	0.40	1.61	0.35	0.23
12	127.08	108.16	130.75	125.65	171.23	151.53
13	1.24	0.38	0.09	1.21	0.13	0.04
14	0.12	0.03	0.01	0.03	0.01	0.0
15	0.03	0.01	0.0	0.01	0.0	0.0

(con't.)

Table 11 (con't.)

freq	FFT Method 0.5 s	FFT Method 1.0 s	FFT Method 2.0 s	Adaptive Method 0.5 s	Adaptive Method 1.0 s	Adaptive Method 2.0 s
			Series 1			
5	0.07	0.01	0.0	0.01	0.01	0.0
6				0.01	0.01	0.01
7				0.02	0.03	0.02
8				0.05	0.09	0.04
9				0.34	0.74	0.35
10	15.10	9.49	7.52	14.41	45.19	16.43
11				7282.47	4806.88	5960.06
12				196.65	343.65	392.47
13				41.74	3.32	0.84
14				0.35	0.11	0.09
15	0.01	0.02	0.08	0.05	0.03	0.03
16				0.02	0.01	0.01
17				0.01	0.01	0.01
18				0.01	0.0	0.0
19				0.0	0.0	0.0
20	0.01	0.0	0.0	0.0	0.0	0.0
			Series 2			
5	0.01	0.0	0.0	0.0	0.0	0.0
6				0.01	0.0	0.0
7				0.01	0.0	0.01
8				0.02	0.01	0.01
9				0.06	0.04	0.04
10	6.63	4.62	4.35	0.57	0.27	0.27
11				81.08	16.00	11.59
12				1625.52	103416.63	189131.67
13				6.96	4.69	0.82
14				0.14	0.12	0.08
15	0.01	0.01	0.04	0.03	0.02	0.02
16				0.01	0.01	0.01
17				0.0	0.0	0.01
18				0.0	0.0	0.0
19				0.0	0.0	0.0
20	0.01	0.0	0.0	0.0	0.0	0.0

estimates at 12 Hz were largest in the 2.0 second conditions and smallest in the estimates from 1.0 second intervals, in both series. For the MEM estimates of both series in the 12 Hz frequency, the largest MSEs were obtained from the 1.0 second intervals and the smallest MSEs were obtained from 0.5 second intervals. For the FFT estimates, the MSE increased with each increase in record length in the 15 Hz frequency band in both series; this increase in the MSE seems to reflect the increasing bias of the FFT estimates in this frequency band.

For the FFT spectral estimates, over 50 percent of the MSE in the 10 Hz band estimates of all length conditions was accounted for by squared bias. In the 0.5 second conditions, the squared bias accounted for about 98 percent of the MSE of the 10 Hz estimate in series 1, and for about 97 percent in series 2. The percentage decreased with increasing lengths, and in the 2.0 second condition the MSE of the 10 Hz estimates consisted of 59 and 51 percent of squared bias in series 1 and series 2 estimates, respectively. In the 15 Hz band the behaviour was less regular; in the series 1 estimate, about 28, 12 and 38 percent of the MSE was due to squared bias as the records lengthened from 0.5 to 1.0 to 2.0 seconds, respectively, and in the series 2 estimate these percentages were 60, 8, and 17, respectively. In the other frequency bands, where only noise was present in the spectra the percentages of the MSEs accounted for by the squared bias ranged from less than one to about 64 percent.

The MSEs of the AR and MEM spectral estimates at the 12 Hz frequency also contained a large percentage of squared bias in the shortest interval condition. For both methods, this percentage dropped off dramatically with increasing interval length. The MSEs of the AR estimates of both series' 12 Hz peak consisted of 92 percent in the 0.5 second intervals which decreased to 12 percent in the series 1 estimate and to 14 percent in the series 2 estimate from the 2.0 second segments. The squared bias accounted for slightly less of the MSE of the MEM 12 Hz estimates compared to the AR and FFT estimates, decreasing from about 78 percent in the shortest segments to about 8 percent in the 2.0 second segments.

For the AR and MEM estimates in the other frequencies, the percentages of MSE due to squared bias again ranged from less than one to about 62 percent.

Comparison of coherence estimates. The mean coherence estimates of stationary data obtained by the FFT method are presented at the bottom of Table 10 along with the average bias of these estimates. Although the spectral estimates of both series had the greatest bias in the 10 Hz frequency band of the shortest segments, the coherence estimates in this band were the least biased. As with the spectral estimates, bias of the FFT coherence estimates decreased with increasing record length, except in the 15 Hz frequency band estimates.

Figures 10 and 11 show the stationary coherence estimates obtained by the AR and MEM methods, respectively. Again, as the record length was increased, the AR and MEM coherence estimates generally became less biased over the whole curve. The MEM method approximated the peak of the coherence curve slightly more accurately than the AR method for the shorter (0.5 and 1.0 second) segments, although by the 2.0 second condition, the two methods produced very similar estimates.

Table 12 presents the MSEs of the transformed coherence estimates of the stationary data obtained by the three estimation methods. These results show that for all methods the MSE of the transformed coherence estimates decreased with each increase in series length. The MSEs of the AR and MEM estimates were largest around the 12 Hz frequency in all three length conditions. Similarly, the MSEs of the FFT estimates from 2.0 second segments were the largest in the 10 and 15 Hz bands, but in the shorter, 0.5 and 1.0 second, conditions these MSEs were the smallest. In the 0.5 second stationary conditions, the MEM transformed coherence estimates had greater MSEs than the AR transformed coherence estimates at all frequency values, except at the 12 Hz peak where the MSE of the MEM estimate (1.062) was not as large as that of the AR estimate (1.515).

As an indication of how the tabled MSEs for the transformed coherences translate to the actual MSE of the original coherence estimates, the tabled value of 1.062 corre-

Figure 10. Coherence estimates obtained by the AR method from stationary 0.5 second (▵), 1.0 second (□), and 2.0 second (○) segments.

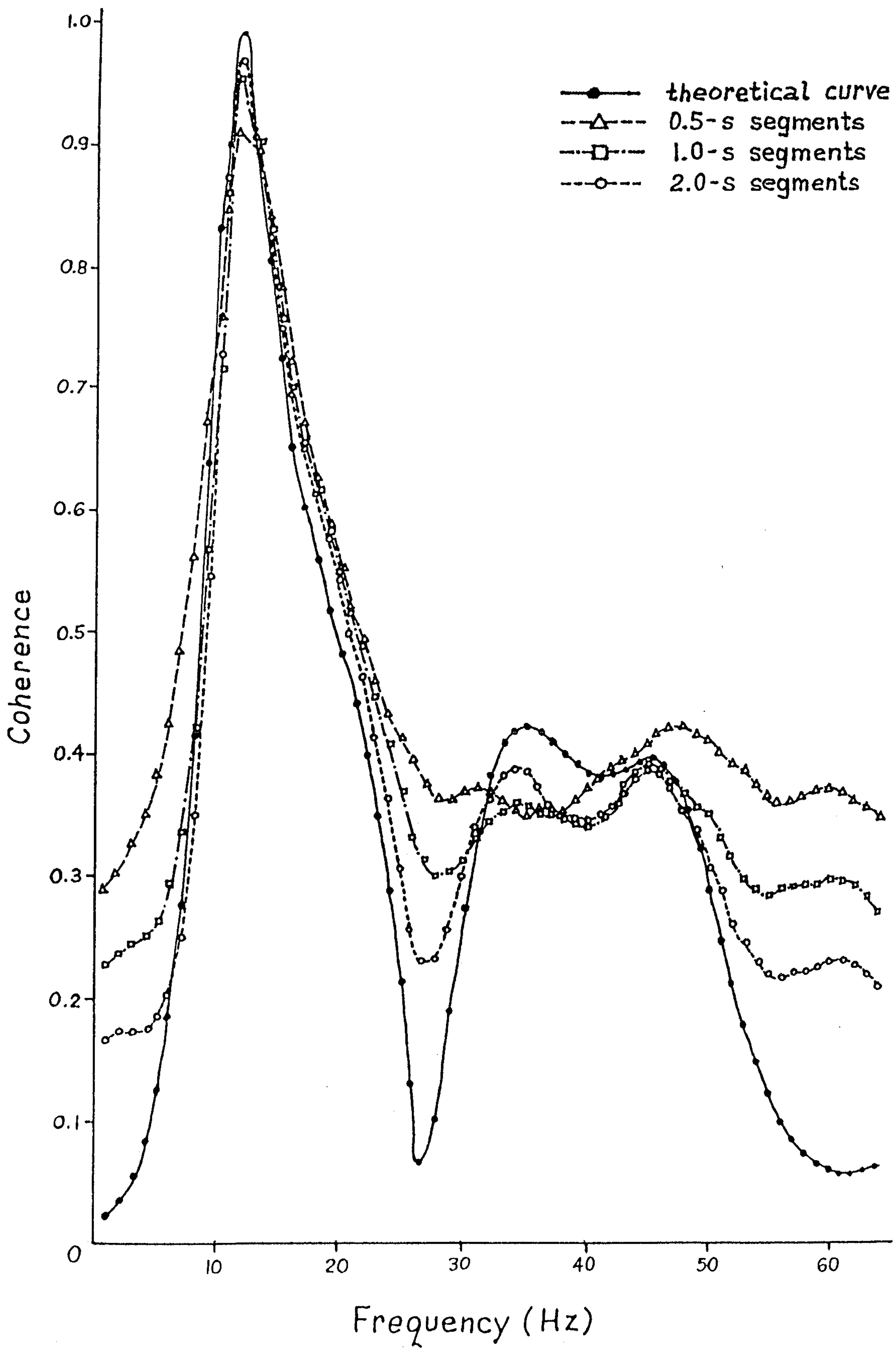

theoretical curve
0.5-s segments
1.0-s segments
2.0-s segments
Coherence
Frequency (Hz)
1.0
0.9
0.8
0.7
0.6
0.5
0.4
0.3
0.2
0.1
0
10
20
30
40
50
60

Figure 11. Coherence estimates obtained by the MEM method from stationary 0.5 second (▲), 1.0 second (◘), and 2.0 second (○) segments.

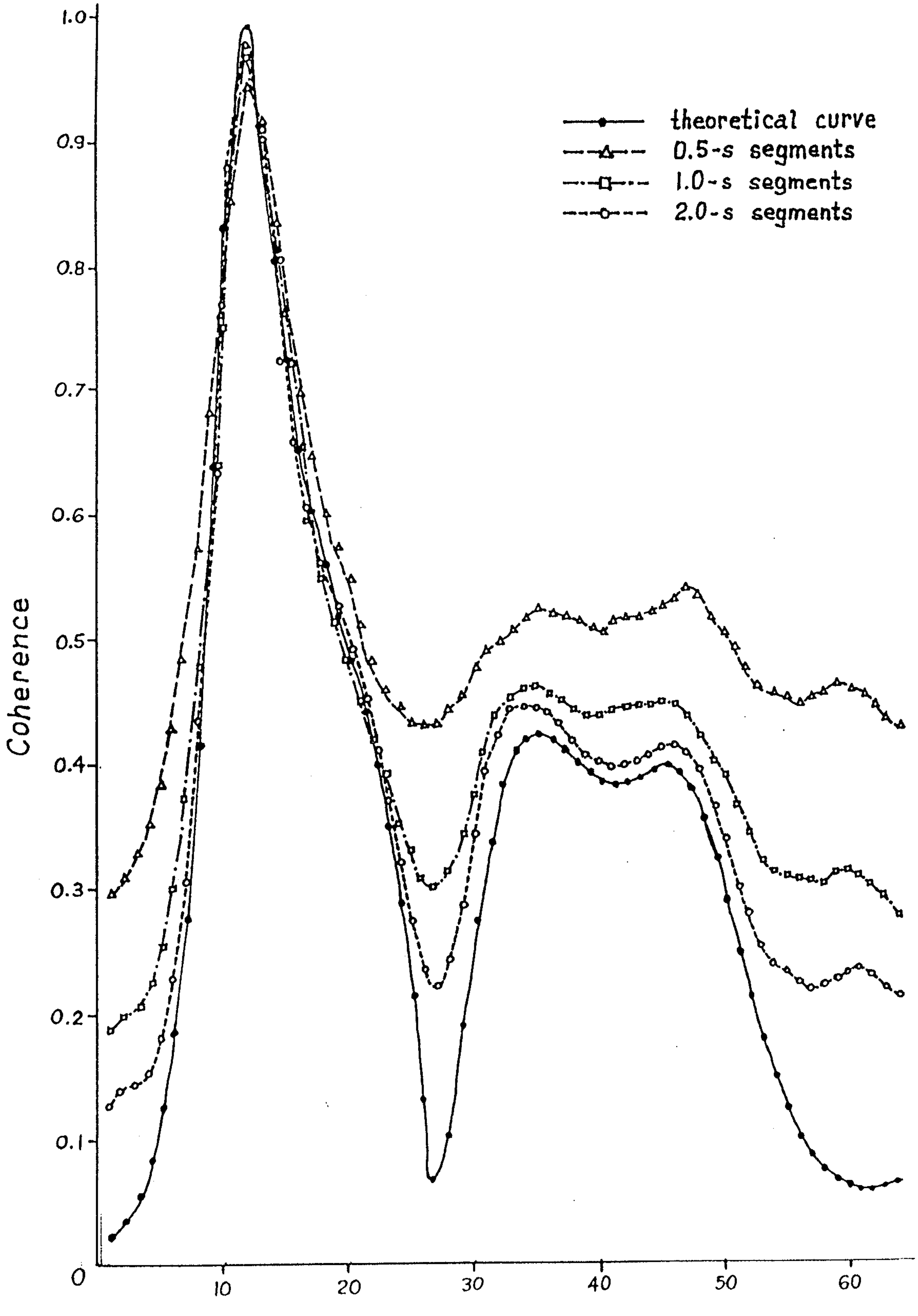
theoretical curve
0.5-s segments
1.0-s segments
2.0-s segments
Coherence
1.0
0.9
0.8
0.7
0.6
0.5
0.4
0.3
0.2
0.1
0
10
20
30
40
50
60
Frequency (Hz)

Table 12

MSE (x 10) of Transformed Coherence Estimates Obtained from Stationary Data

	0.5 s Segments			1.0 s Segments			2.0 s Segments		
freq	FFT	AR	MEM	FFT	AR	MEM	FFT	AR	MEM
1		1.381	1.902		0.904	0.557		0.446	0.221
2		1.389	1.884		0.846	0.521		0.391	0.190
3		1.416	1.950		0.763	0.484		0.315	0.159
4		1.468	2.072		0.659	0.452		0.227	0.140
5	7.790	1.553	2.130	5.520	0.546	0.427	2.085	0.149	0.141
6		1.681	2.212		0.449	0.421		0.111	0.163
7		1.869	2.472		0.417	0.472		0.156	0.212
8		2.119	2.859		0.540	0.638		0.314	0.316
9		2.175	3.354		1.076	1.176		0.720	0.639
10	3.642	2.875	3.601	2.542	2.169	2.395	2.420	1.638	1.569
11		3.968	4.565		1.582	1.795		0.927	0.962
12		15.150	10.619		8.826	6.088		5.103	3.782
13		2.904	3.300		1.106	1.090		0.484	0.383
14		2.354	2.542		0.870	0.819		0.391	0.253
15	3.535	1.977	2.104	2.359	0.779	0.666	3.188	0.363	0.205
16		1.673	1.729		0.728	0.584		0.346	0.183
17		1.454	1.557		0.693	0.515		0.335	0.175
18		1.298	1.487		0.666	0.476		0.327	0.176
19		1.183	1.411		0.645	0.459		0.321	0.180
20	13.052	1.091	1.285	5.390	0.628	0.442	2.069	0.318	0.187
21		1.018	1.242		0.616	0.426		0.317	0.194
22		0.978	1.117		0.609	0.418		0.319	0.200
23		0.974	1.168		0.618	0.427		0.325	0.208
24		1.024	1.328		0.645	0.452		0.329	0.218
25	7.379	1.158	1.700	2.889	0.697	0.518	1.562	0.342	0.230

sponds to an actual MSE of 0.786 for the 0.5 second 12 Hz MEM estimate, and 1.515 corresponds to an actual MSE of 0.908 for this AR estimate. In the noise regions, where the MSEs are usually much smaller, the tabled values for the transformed coherence estimates correspond very closely to the actual MSEs of the original coherence estimates.

As the record length increased to 1.0 and 2.0 seconds, the MSE of the MEM estimates became smaller than those of the AR transformed coherences at almost all frequencies. In the 2.0 second intervals, the actual MSE corresponding to the tabled value of 0.5103 for the AR estimate is 0.4702, and the actual MSE of the 12 Hz MEM estimate is 0.3611. Thus with longer epoch lengths, the MEM estimates seem to become better than the AR estimates, in terms of their MSE.

The MSE of the FFT transformed estimates was similar to the MSE of the AR and MEM estimates only in the 10 Hz region; elsewhere the MSEs of the transformed FFT estimates were about an order of magnitude larger. The actual MSE of the 10 Hz FFT coherence estimate from 2.0 second intervals, corresponding to the tabled value of 0.242, is 0.2374. The FFT method failed to produce the major coherence peak at 12 Hz, which should have appeared in the 10 and 15 Hz band (see theoretical FFT coherences in Table 10), and overestimated the coherences in the higher frequency bands, which resulted in comparatively large MSEs, particularly in the shortest segment lengths.

As with the bias of the FFT estimates, the MSE of the FFT spectra was highest in the 10 Hz band, even though the MSE of the FFT coherence estimates in the 10 Hz band were among the smallest. In contrast, the AR and MEM methods generated spectral as well as coherence estimates with the largest MSE at 12 Hz, relative to the MSE of the estimates in the other frequencies.

In the power peak region, squared bias accounted for less than 10 percent of the MSE of the transformed coherence estimates obtained with all three estimation methods in all segment length conditions. For the FFT 10 Hz coherence estimates, and for the AR and MEM coherences in the 11 to 14 Hz inclusive range, less than one percent of the MSE was due to squared bias. In the other noise frequency ranges, the percentage of squared bias in the MSE ranged from zero to about 60 percent, for all three methods in all segment length conditions.

<u>Coherence Estimates from Nonstationary Series</u>

<u>Changes in the variance of normally distributed error</u>. Estimates of the coherence function obtained in the nonstationary conditions where the variance of the noise used to generate the data was changed from $\begin{bmatrix}1 & 0\\0 & 1\end{bmatrix}$ to $\begin{bmatrix}9 & 0\\0 & 9\end{bmatrix}$ halfway in the sampling epoch are shown in Figure 12 for the AR method and in Figure 13 for the MEM method. While the MEM method can estimate the peak value of the coherence function at 12 Hz slightly better than the AR method for each segment

Figure 12. Coherence estimates of the AR method obtained from data with the noise variance changed halfway in the 0.5 second (▲), 1.0 second (◘), and 2.0 second (○) intervals.

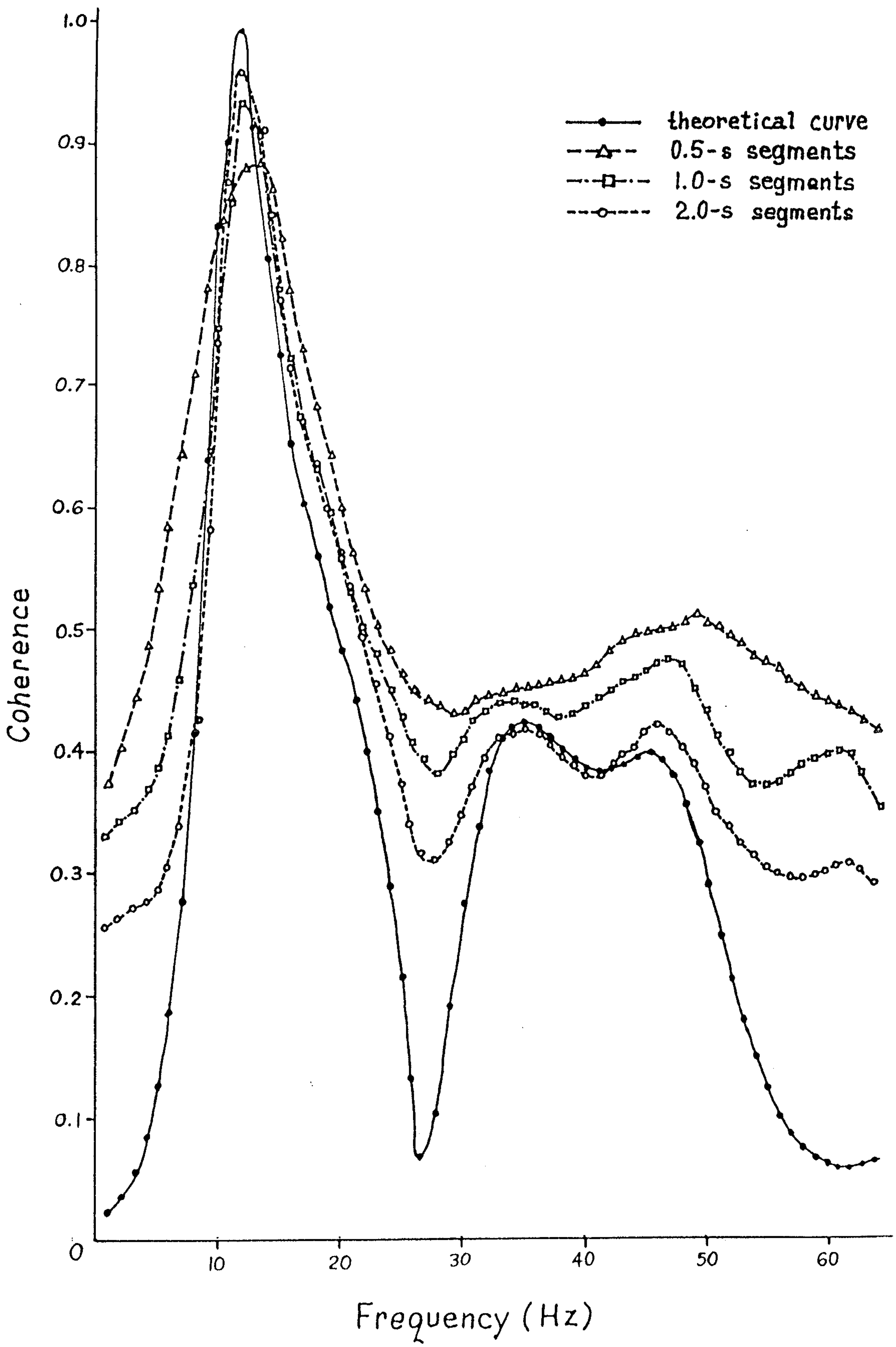
theoretical curve
0.5-s segments
1.0-s segments
2.0-s segments
Coherence
Frequency (Hz)
1.0
0.9
0.8
0.7
0.6
0.5
0.4
0.3
0.2
0.1
0
10
20
30
40
50
60

Figure 13. Coherence estimates of the MEM method obtained from data with the noise variance changed halfway in the 0.5 second (▲), 1.0 second (■), and 2.0 second (●) intervals.

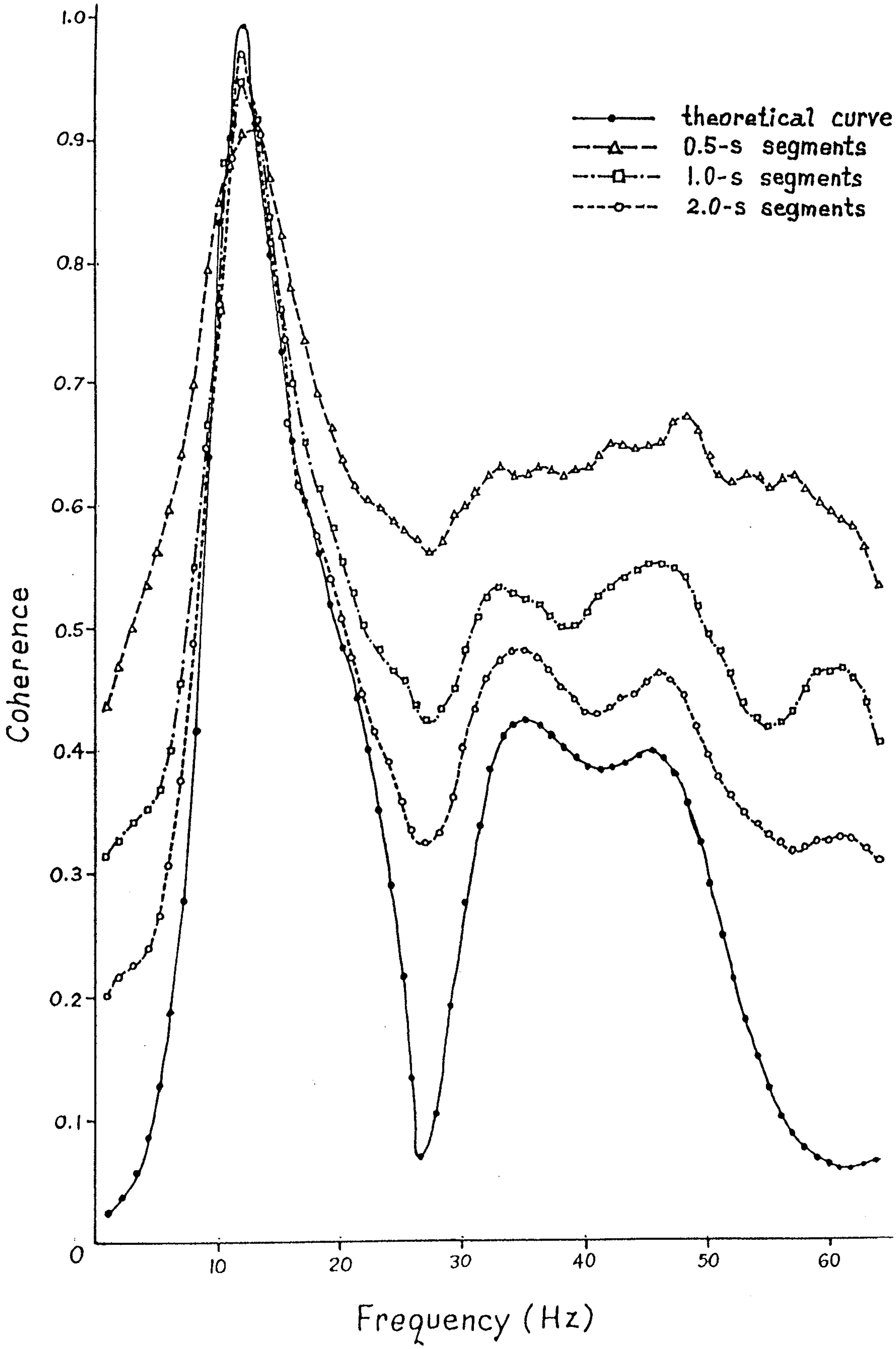

theoretical curve
0.5-s segments
1.0-s segments
2.0-s segments
Coherence
Frequency (Hz)
0
10
20
30
40
50
60
0.1
0.2
0.3
0.4
0.5
0.6
0.7
0.8
0.9
1.0

length, it overestimates more the values at frequencies where the coherences are small, particularly in the shortest intervals.

The FFT coherence estimates and their average bias obtained in all of the change of variance nonstationary conditions are presented in Table 13. Comparing the FFT estimates across record length for the first condition where the variance was changed halfway through the interval, at N/2, the estimates in the 10 and 15 Hz frequency bands became more biased with increasing record length; in the 10 Hz band the estimates tended to be progressively more underestimated as indicated by the increased negative bias, while the estimates in the 15 Hz band were increasingly overestimated. Compared to the stationary FFT coherence estimates (see bottom of Table 10), the biases of these nonstationary estimates were generally very similar.

The MSEs for the transformed coherence estimates of the three methods in these nonstationary conditions are presented in Table 14. The MSEs of the nonstationary FFT coherences were generally quite comparable to the MSEs obtained for the stationary series, particularly in the region of the coherence peak in all interval length conditions (compare with Table 12). The differences between stationary and nonstationary estimates in the noise region were not always in the same direction; for example, in the 5 Hz frequency band of 0.5 second segments, the stationary transformed FFT esti-

Table 13

Mean FFT Coherence Estimates x 100 (and Bias x 100) When the Noise Variance was Changed from $\begin{bmatrix}1 & 0\\0 & 1\end{bmatrix}$ to $\begin{bmatrix}9 & 0\\0 & 9\end{bmatrix}$

Condition	freq band	Segment Length		
		0.5 s	1.0 s	2.0 s
Noise Variance Changed at N/2	5	75.30 (60.82)	57.60 (43.13)	45.01 (30.53)
	10	75.21 (-0.54)	73.37 (-2.38)	73.05 (-2.70)
	15	78.15 (4.01)	80.12 (5.98)	86.56 (12.42)
	20	79.25 (31.10)	72.74 (24.58)	61.67 (13.51)
	25	66.42 (45.12)	55.65 (34.35)	45.02 (23.72)
Noise Variance Changed at N/4	5		60.45 (45.98)	45.94 (31.46)
	10		75.67 (-0.07)	75.79 (0.04)
	15		81.19 (7.05)	84.82 (10.69)
	20		72.92 (24.77)	64.84 (16.69)
	25		60.03 (38.74)	48.34 (27.04)
Noise Variance Changed at N/8	5			42.84 (28.37)
	10			75.35 (-0.40)
	15			85.36 (11.23)
	20			64.56 (16.41)
	25			47.03 (25.73)

Table 14

MSE x 10 of Transformed Coherences When the noise Variance was Changed Halfway in the Segments

	0.5 s Segments			1.0 s Segments			2.0 s Segments		
freq	FFT	AR	MEM	FFT	AR	MEM	FFT	AR	MEM
1		2.957	4.055		2.172	1.834		1.076	0.660
2		3.070	4.285		2.081	1.778		1.037	0.624
3		3.267	4.837		1.948	1.754		0.966	0.586
4		3.550	5.673		1.782	1.743		0.852	0.552
5	12.494	3.913	5.714	4.428	1.600	1.647	2.043	0.701	0.527
6		4.333	5.456		1.411	1.451		0.538	0.516
7		4.745	5.901		1.309	1.453		0.445	0.545
8		5.025	6.668		1.406	1.869		0.506	0.671
9		4.594	7.340		1.692	2.543		0.961	1.052
10	3.352	3.971	6.410	2.838	2.510	3.247	2.608	1.934	2.233
11		5.151	8.971		3.369	4.194		1.785	1.976
12		18.369	14.347		12.018	9.622		7.437	5.646
13		3.981	6.384		2.205	2.451		1.086	0.919
14		4.362	6.641		2.088	1.992		0.977	0.754
15	3.833	4.047	5.253	2.097	1.851	1.695	3.157	0.961	0.681
16		3.495	4.534		1.609	1.537		0.948	0.647
17		2.973	3.815		1.451	1.463		0.906	0.626
18		2.533	3.501		1.356	1.444		0.854	0.593
19		2.185	3.575		1.272	1.348		0.799	0.564
20	9.257	1.959	3.777	5.256	1.219	1.202	1.670	0.748	0.531
21		1.830	3.968		1.209	1.086		0.714	0.522
22		1.790	4.120		1.211	1.044		0.704	0.522
23		1.810	4.315		1.223	1.094		0.715	0.521
24		1.861	4.673		1.334	1.346		0.758	0.576
25	8.289	2.055	5.716	3.628	1.519	1.759	1.798	0.813	0.669

mates had a MSE of 0.779 compared with the nonstationary estimate's MSE of 1.249, but in the 20 Hz band the nonstationary transformed estimate had a smaller MSE (0.926) than the stationary one (1.305). As the record length was increased, the MSEs of the nonstationary FFT estimates in the noise regions became very similar to those obtained for stationary estimates.

Compared to the MSE of the stationary estimates, the nonstationary transformed coherence estimates of both AR and MEM methods had consistently greater MSEs in all interval length conditions. The MSEs of the AR and MEM transformed nonstationary estimates were at least twice as large than they were in the stationary conditions, except at the 10 and 12 Hz frequencies where the MSEs of the nonstationary estimates were only slightly larger.

The tabled MSEs of the AR 12 Hz estimates of 1.837,1.202, and 0.744 from the 0.5, 1.0, and 2.0 second intervals, respectively, correspond to actual MSEs of 0.951, 0.834, and 0.652. For the corresponding MEM estimates, the actual MSEs are 0.893, 0.745, and 0.511.

Although the MSE of the FFT transformed estimates generally decreased with interval length, this decrease was much more gradual in the 10 Hz frequency band than in the other frequency bands. In the 0.5 second condition, the MSEs in the 10 and 15 Hz bands were the smallest than in all the other bands, while in the 1.0 second conditions these MSEs were within the range of the others, and in the 2.0 second condition they were larger than all those in the other frequency bands.

In the noise regions of the coherence function obtained from intervals of all tested lengths, the MSEs of the FFT nonstationary transformed estimates were larger than the MSEs of the MEM estimates, while the MEM estimates generally had greater MSEs than the AR estimates. In the 10 Hz range, the MSE of the FFT coherences from the shortest segments was the smallest when compared to the AR and MEM estimates. With longer intervals the MSEs of the FFT 10 Hz transformed estimates decreased more gradually and became close to the MSEs of the AR and MEM estimates. In the 15 Hz range, the same was true in the 0.5 and 1.0 second conditions, however, the MSE of the 15 Hz estimate from 2.0 second segments was considerably larger than the AR and MEM MSEs in this range.

Comparing the MSEs of the AR and MEM transformed estimates, in the 0.5 second condition the MEM estimates had larger MSEs than the AR estimates at all frequencies except at 12 Hz where the MSE of the MEM estimate was smaller than that of the AR estimate. In the longer interval conditions, the MSEs of the AR and MEM estimates were more similar to each other and generally smaller than the MSEs of the FFT estimates. In the 1.0 second condition, the MSEs of the AR and MEM estimates were almost identical. The MSEs of the

MEM estimates in the 2.0 second condition were everywhere smaller than those of the AR estimates except in the 7 to 11 Hz range.

Figures 14 and 15 present the AR and MEM coherence estimates, respectively, obtained in each different interval length condition, and with the variance of the input noise changed for different proportions of the data segment; that is, always the last 32 data points, regardless of interval length, were generated with $S=\begin{bmatrix} 9 & 0 \\ 0 & 9 \end{bmatrix}$. Both methods produced estimates that were more biased across the entire frequency range than those when the variance was changed consistently halfway for all interval lengths. Comparison of the diagonal entries in Table 13 indicates that the bias of the FFT estimates again increased with increasing interval length in the 15 Hz frequency band where the FFT estimates were progressively more overestimated. At 10 Hz, the bias of the FFT estimates remained very low regardless of the amount of nonstationary data, while in all other frequency bands the bias decreased with increasing interval length and the decreasing relative amount of nonstationary data.

These nonstationary estimates may also be compared for the effects of changing the proportion of nonstationary data for a fixed segment length. For the 2.0 second segments, there are three conditions where the variance of the input noise was changed at different times in the segment; (a) halfway for N/2 (128) data points, (b) for N/4 (64) data

Figure 14. Coherence estimates of the AR method obtained from data with the noise variance changed for the last 32 data points in the 0.5 second (▲), 1.0 second (■), and 2.0 second (●) intervals. (In the 0.5 second interval, the change was made for half of the segment; in the 1.0 second interval for a quarter; and in the 2.0 second interval for the last eighth of the segment.)

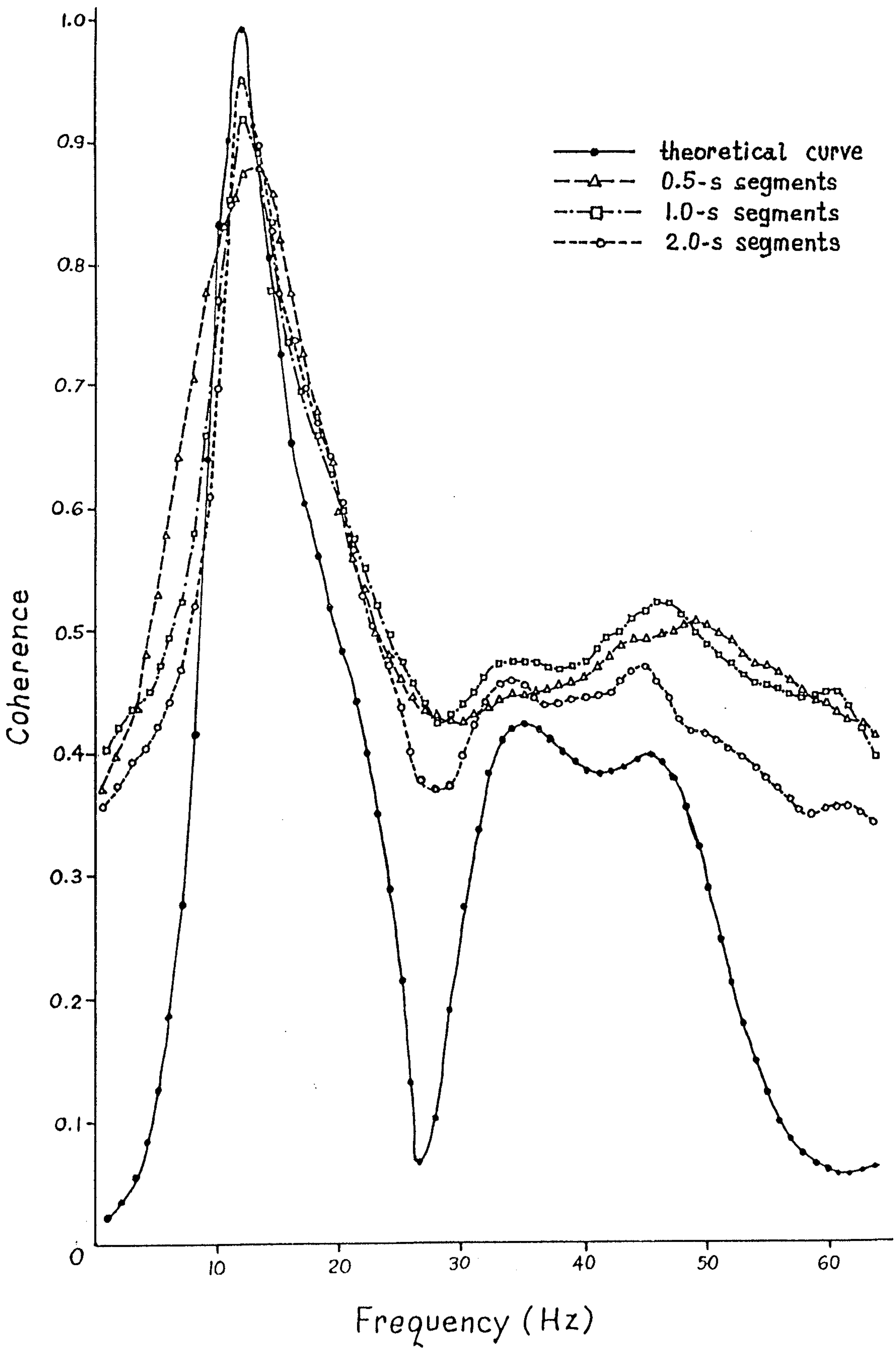

theoretical curve
0.5-s segments
1.0-s segments
2.0-s segments
Coherence
Frequency (Hz)
1.0
0.9
0.8
0.7
0.6
0.5
0.4
0.3
0.2
0.1
0
10
20
30
40
50
60

Figure 15. Coherence estimates of the MEM method obtained from data with the noise variance changed for the last 32 data points in the 0.5 second (▲), 1.0 second (◘), and 2.0 second (●) intervals. (In the 0.5 second interval, the change was made for half of the segment; in the 1.0 second interval, for a quarter; and in the 2.0 second interval for the last eighth of the segment.)

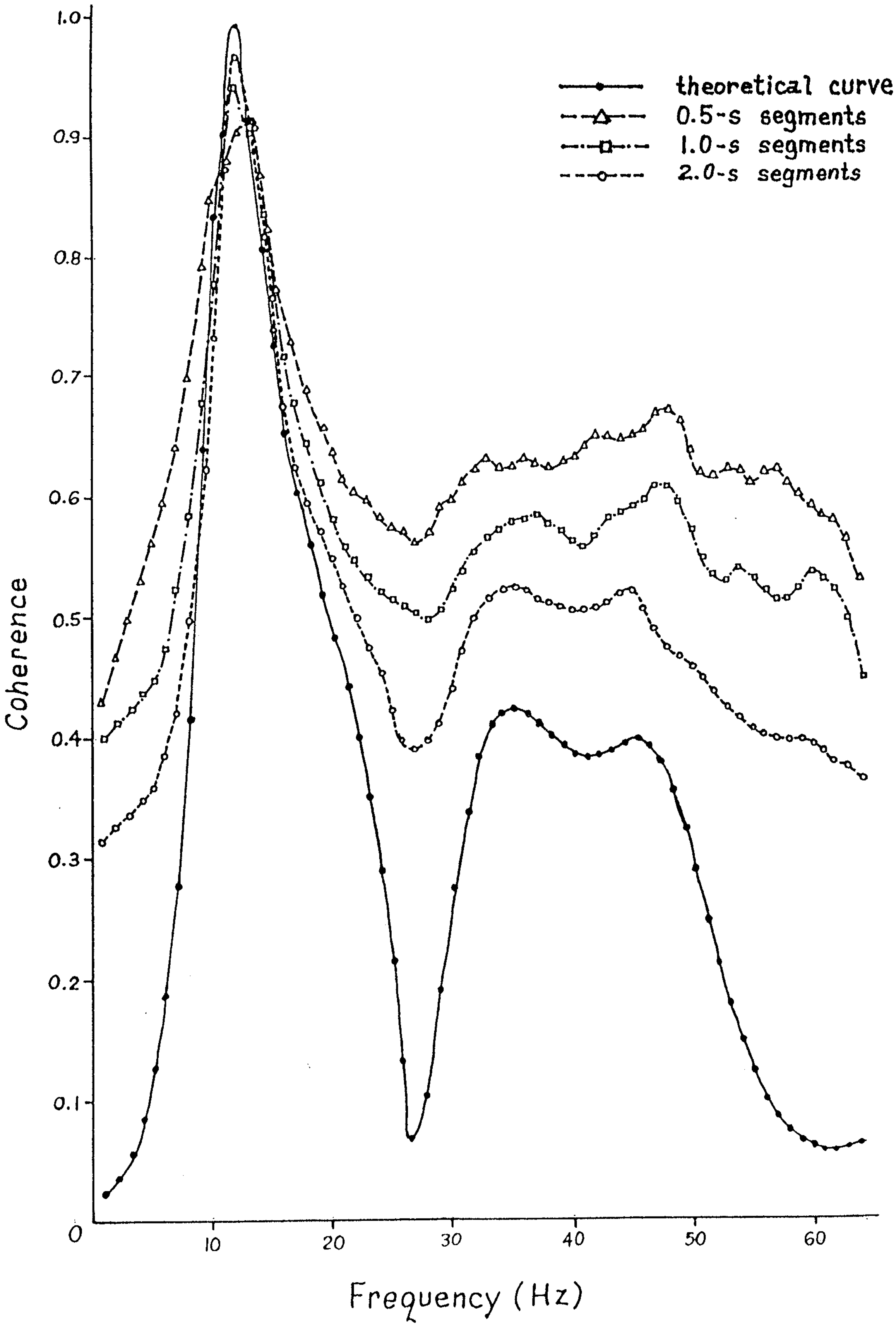

theoretical curve
0.5-s segments
1.0-s segments
2.0-s segments
1.0
0.9
0.8
0.7
0.6
0.5
0.4
0.3
0.2
0.1
0
10
20
30
40
50
60
Coherence
Frequency (Hz)

points, and (c) for N/8 (32) data points. In Table 13, the 2.0 second column compares the FFT estimates and their bias over these three conditions. These estimates are very similar compared over the nonstationary conditions, and also very similar to FFT coherence estimates of completely stationary series (compare with Table 10). Figure 16 compares the AR and MEM estimates obtained from 2.0 second intervals in which the variance was changed for half and for the last eighth of the series. The coherence peak was estimated almost identically regardless of the amount of data that was changed, when the same method of estimation was used. The tails of the coherence function were estimated with less bias by both AR and MEM methods when the variance was changed for an entire half of the segment, rather than for the smaller amounts. Overall, the MEM estimates were generally marginally less biased than the AR estimates in the peak region of the coherence function under these conditions.

The MSEs of the transformed coherence estimates of the three kinds of 2.0 second nonstationary segments are given in Table 15. As the number of data points that were nonstationary decreased (from a half to a quarter to an eighth of the segment), the MSEs of the FFT transformed estimates remained relatively constant within each frequency band and also very similar to the respective FFT estimates obtained in the 2.0 second stationary condition (see Table 12). The

<u>Figure 16</u>. Coherence estimates from 2.0 second segments obtained by the AR method (triangles) and the MEM method (squares) where the noise variance was changed for half of the segment (open symbols) or for an eighth of the segment (solid symbols).

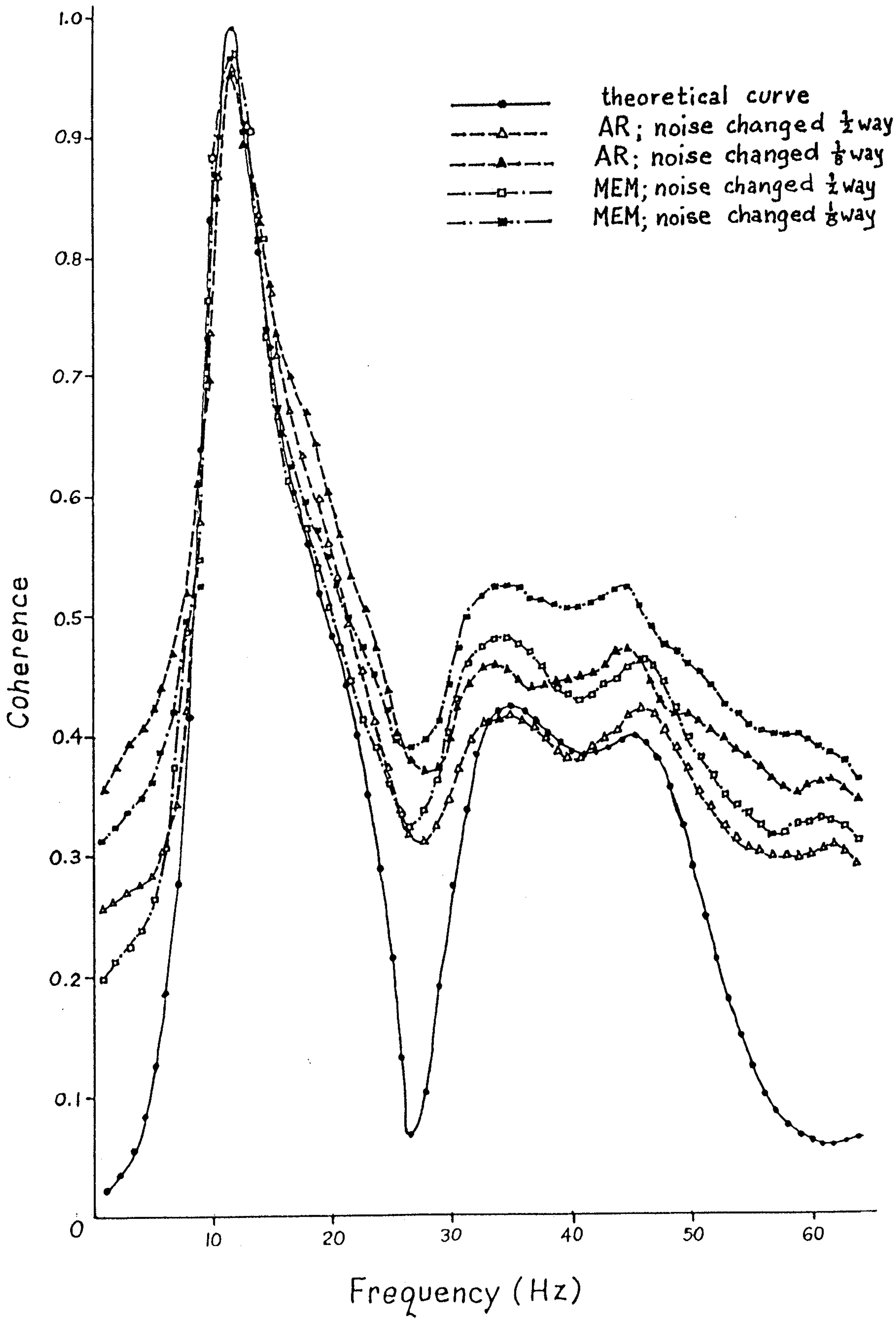

theoretical curve
AR; noise changed ½ way
AR; noise changed ⅛ way
MEM; noise changed ½ way
MEM; noise changed ⅛ way
Coherence
Frequency (Hz)
1.0
0.9
0.8
0.7
0.6
0.5
0.4
0.3
0.2
0.1
0
10
20
30
40
50
60

Table 15

MSE x 10 of Transformed Coherences from 2.0-sec Segments with Noise Variance Changed at Different Locations

	Change at N/2			Change at N/4			Change at N/8		
freq	FFT	AR	MEM	FFT	AR	MEM	FFT	AR	MEM
1		1.076	0.660		2.012	1.375		2.386	1.555
2		1.037	0.624		1.941	1.307		2.297	1.434
3		0.966	0.586		1.849	1.255		2.211	1.374
4		0.852	0.552		1.712	1.195		2.100	1.329
5	2.043	0.701	0.527	2.060	1.509	1.120	1.769	1.924	1.234
6		0.538	0.516		1.252	1.043		1.672	1.113
7		0.445	0.545		1.009	0.033		1.385	1.071
8		0.506	0.671		0.997	1.203		1.176	1.193
9		0.961	1.052		1.302	1.636		1.208	1.552
10	2.608	1.934	2.233	2.261	2.036	2.122	2.093	2.023	1.909
11		1.785	1.976		2.159	2.766		1.405	1.529
12		7.437	5.646		7.914	6.117		8.506	5.801
13		1.086	0.919		1.484	1.499		1.353	1.379
14		0.977	0.754		1.332	1.155		1.390	1.306
15	3.157	0.961	0.681	2.392	1.281	1.064	2.974	1.400	1.104
16		0.948	0.647		1.211	1.043		1.434	1.013
17		0.906	0.626		1.181	1.031		1.480	1.027
18		0.854	0.593		1.199	1.009		1.477	1.020
19		0.799	0.564		1.182	0.949		1.403	0.978
20	1.670	0.748	0.531	2.186	1.162	0.911	2.007	1.310	0.940
21		0.714	0.522		1.185	0.977		1.255	0.910
22		0.704	0.522		1.242	1.118		1.227	0.923
23		0.715	0.521		1.342	1.200		1.235	0.968
24		0.758	0.576		1.456	1.258		1.304	1.030
25	1.798	0.813	0.669	2.163	1.530	1.319	1.781	1.382	1.188

MSEs of the AR transformed estimates were also quite similar in the three conditions, but did increase very slightly as the number of nonstationary data decreased at some frequencies; at the other frequencies, the MSEs increased from the N/2 to N/4 conditions but decreased as the number of nonstationary data was further decreased to N/8. In the noise regions, all the MSEs of the AR transformed estimates in all three nonstationary conditions were about four times higher than MSEs of AR transformed estimates of stationary 2.0 second segments. Results for the MEM estimates were similar to those of the AR estimates. The MSEs of the nonstationary MEM transformed estimates were consistently larger than MSEs of stationary data; however, as in the 2.0 second stationary condition, the MSE of the MEM estimates in these nonstationary conditions were generally smaller than those of the AR estimates.

Changing the variance only in one series, that is changing the noise variance-covariance matrix from $\begin{bmatrix} 1 & 0 \\ 0 & 1 \end{bmatrix}$ to $\begin{bmatrix} 9 & 0 \\ 0 & 1 \end{bmatrix}$ in generating the bivariate AR series, will change the noise variance in both series, since in simulating a bivariate series, each univariate series is a combined function of its own past, as well as the past of the second series. However, a condition was run for a 1.0 second interval where the noise variance was changed only in series 1 halfway through the interval. Figure 17 shows that the AR and MEM coherence estimates were less biased in the 12 Hz peak region when the noise was changed only in series 1 than when both series were changed. Generally, however, in all the other frequency ranges, the estimates of both AR and MEM methods were more biased when the variance was changed only in series 1 than when both series were changed. Overall, the MEM estimates were generally more biased than the AR estimates, except again at the 12 Hz frequency where the MEM estimates were closer to the theoretical peak than the AR estimates in their respective conditions.

As in the stationary condition, in all the change of variance nonstationary conditions, the squared bias accounted for less than one percent of the MSE of the AR and MEM estimates in the 11 to 14 Hz frequencies and the 10 Hz FFT estimates. In all other frequency estimates, the percentage ranged from zero to about 60 percent.

Addition of a transient sine wave. When a transient sine wave was added to series 1, the mean coherence estimates of the AR method, shown in Figure 18, were very similar to the estimates obtained for stationary series (compare with Figure 10). There were very small peaks around the 3 Hz frequency, particularly in the 2.0 second interval conditions, and the 12 Hz peak was estimated less accurately in the shortest intervals than in the stationary condition. As Figure 19 demonstrates, the MEM estimates were more sensitive to the transient nonstationarity in one series than the AR estimates. The peaks around the 3 Hz frequency were much

Figure 17. Coherence estimates obtained by the AR method (triangles) and the MEM method (squares) from 1.0 second intervals where the noise variance was changed halfway in series 1 only (open symbols) or in both series (solid symbols).

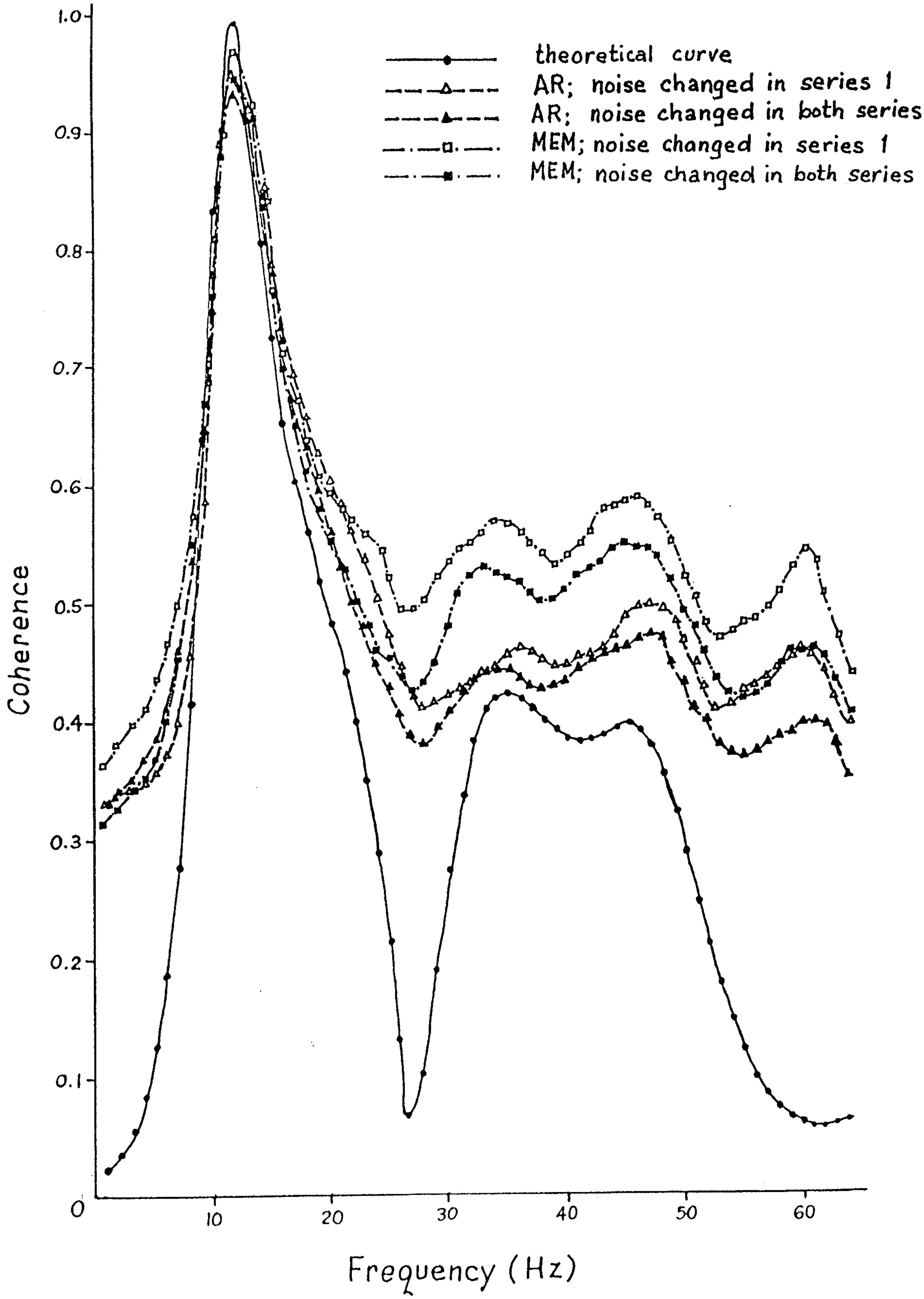
theoretical curve
AR; noise changed in series 1
AR; noise changed in both series
MEM; noise changed in series 1
MEM; noise changed in both series
Coherence
1.0
0.9
0.8
0.7
0.6
0.5
0.4
0.3
0.2
0.1
0
10
20
30
40
50
60
Frequency (Hz)

Figure 18. Coherence estimates obtained with the AR method in 0.5 second (▲), 1.0 second (◘), and 2.0 second (○) conditions where a transient sine wave was added to series 1.

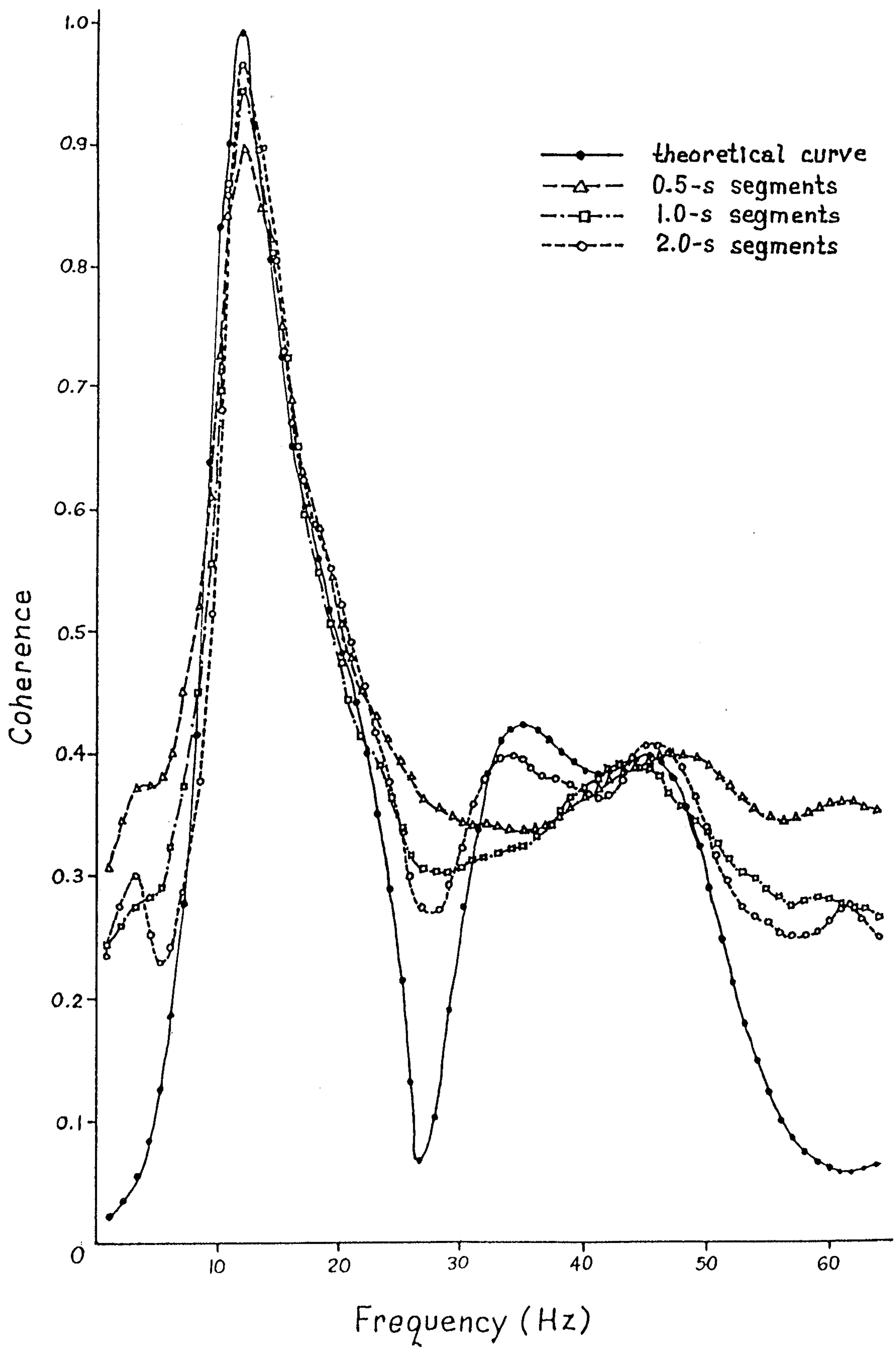

theoretical curve
0.5-s segments
1.0-s segments
2.0-s segments
Coherence
Frequency (Hz)
0
0.1
0.2
0.3
0.4
0.5
0.6
0.7
0.8
0.9
1.0
10
20
30
40
50
60

Figure 19. Coherence estimates obtained with the MEM method in 0.5 second (▲), 1.0 second (■), and 2.0 second (●) conditions where a transient sine wave was added to series 1.

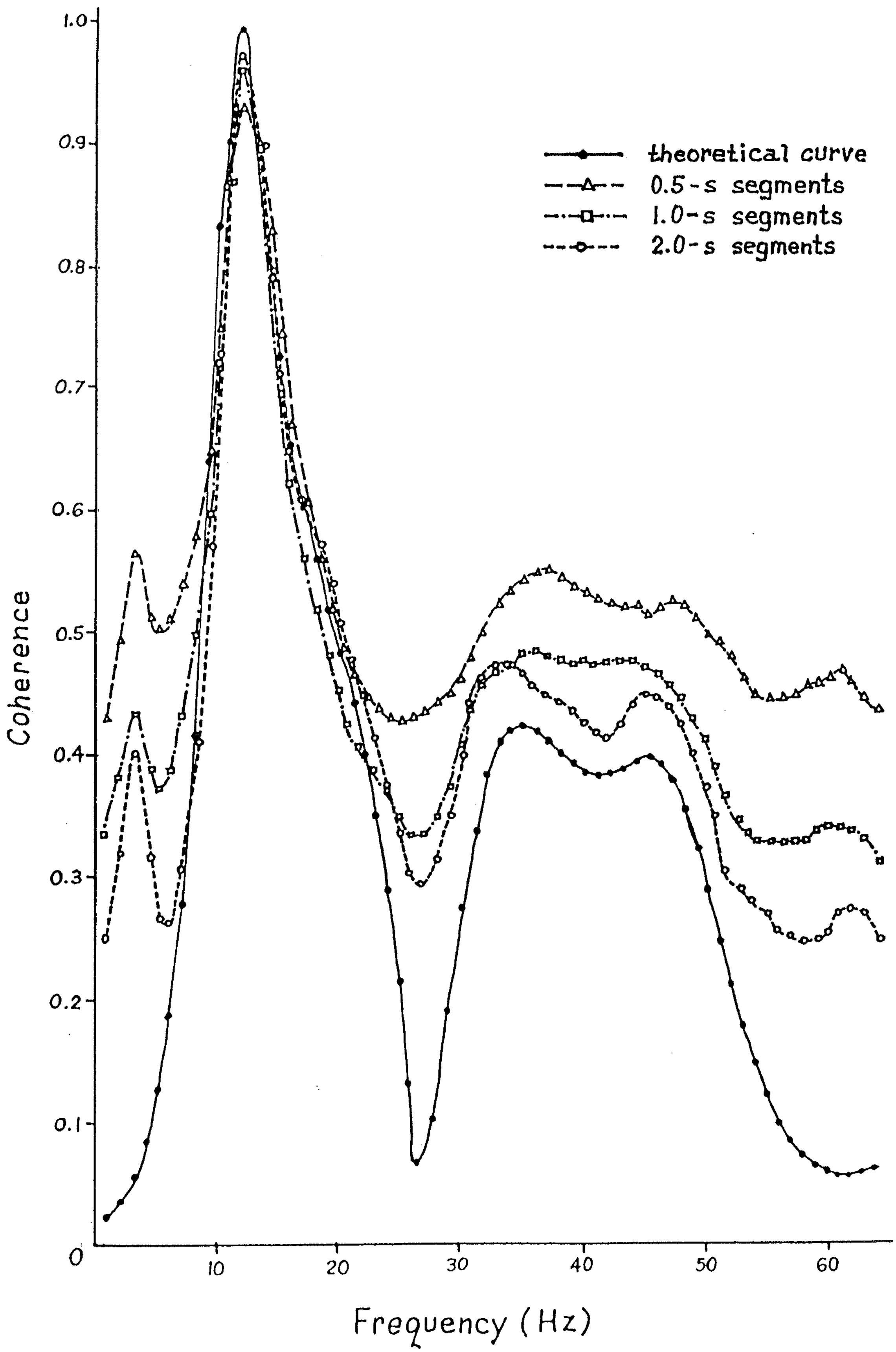

theoretical curve
0.5-s segments
1.0-s segments
2.0-s segments
Coherence
Frequency (Hz)
1.0
0.9
0.8
0.7
0.6
0.5
0.4
0.3
0.2
0.1
0
10
20
30
40
50
60

more prominent in all three interval length conditions. Otherwise the mean MEM estimates were almost identical to the stationary estimates (compare with Figure 11).

Table 16 gives the MSEs of the transformed coherence estimates that were obtained from data with a transient sine wave added to series 1. The MSEs of the AR and MEM transformed estimates were generally very similar to the MSEs of stationary estimates. The exception was in the 1 to about 6 Hz frequency region where the MSEs were greater in the nonstationary condition, with a peak at 3 Hz. At the 12 Hz frequency the MSEs were also slightly greater than the MSEs of the stationary estimates, although generally in the major coherence peak region, the MSEs of the nonstationary estimates were even very slightly smaller. Comparing the AR and MEM methods in the nonstationary condition, except at the 12 Hz frequency, the MSEs of the AR coherences were smaller than the MSEs of the MEM estimates. In the low frequencies around 3 Hz, the MSEs of the MEM transformed estimates were relatively much larger than of the AR estimates, especially in the shorter segments. For example, in the 0.5 second condition at 3 Hz, the MSE of the transformed AR estimate was 0.1963 (actual MSE=0.1938 for the original coherence) and of the MEM transformed estimate was 0.9418 (actual MSE=0.7360), but this difference was greatly reduced as the intervals were lengthened to 2.0 seconds where the MSE of the AR estimate was 0.1218 (actual MSE=0.1212) and the MSE of the MEM estimate was 0.2169 (actual MSE=0.2136).

Table 16

MSE x 10 of Transformed Coherences Obtained from Data with a Transient Sine Wave Added to Series 1

	0.5 s Segments			1.0 s Segments			2.0 s Segments		
freq	FFT	AR	MEM	FFT	AR	MEM	FFT	AR	MEM
1		1.475	4.462		0.908	1.764		0.705	0.836
2		1.648	5.871		0.978	2.165		0.889	1.232
3		1.963	9.418		1.129	3.322		1.218	2.169
4		1.656	5.681		0.841	1.992		0.602	0.970
5	6.837	1.348	4.353	2.923	0.645	1.308	0.467	0.310	0.452
6		1.190	3.584		0.545	1.039		0.212	0.283
7		1.056	2.866		0.483	0.860		0.216	0.247
8		0.920	2.147		0.462	0.740		0.315	0.297
9		0.919	2.055		0.707	0.904		0.759	0.692
10	2.848	1.973	2.684	2.606	1.662	1.017	2.406	1.790	1.693
11		2.740	4.328		1.289	1.704		1.133	1.186
12		16.777	11.725		9.788	7.298		6.369	4.698
13		2.506	2.634		1.030	1.000		0.552	0.610
14		1.562	1.883		0.653	0.768		0.472	0.516
15	2.279	1.168	1.421	1.577	0.542	0.726	2.738	0.476	0.496
16		0.966	1.075		0.486	0.679		0.473	0.484
17		0.853	1.074		0.453	0.642		0.464	0.466
18		0.793	1.162		0.439	0.666		0.454	0.448
19		0.756	1.056		0.437	0.710		0.450	0.447
20	4.064	0.740	0.889	2.424	0.437	0.719	1.540	0.452	0.465
21		0.737	0.934		0.437	0.719		0.460	0.485
22		0.744	1.110		0.444	0.718		0.470	0.499
23		0.776	1.296		0.449	0.723		0.452	0.498
24		0.858	1.536		0.462	0.735		0.434	0.466
25	6.635	1.028	1.919	2.231	0.526	0.794	1.383	0.468	0.479

The mean coherence estimates obtained by the FFT method when a transient sine wave was added to either one or both series are given in Table 17. When the transient was added to only one series, the FFT estimates in the noise frequencies were generally less biased than when the series was stationary. In the 10 and 15 Hz bands the biases of the nonstationary coherence estimates were comparable to, although slightly larger than, the biases of the stationary estimates. The MSEs of these transformed nonstationary FFT coherence estimates, given in Table 16, were smaller in all frequency bands than the MSEs of the respective stationary estimates. In the 5 Hz band, which contains the transient in one spectrum, as the segment length was increased the MSE of the nonstationary estimates decreased more rapidly, from 0.684 (actual MSE=0.594) in the 0.5 second interval to 0.047 (actual MSE=0.0467) in 2.0 second interval than the corresponding MSEs of the stationary transformed estimates, which decreased from 0.779 (actual MSE=0.652) to 0.209 (actual MSE=0.206).

The transient in only one series also failed to affect to any great extent the percentage of MSE accounted for by squared bias. In the low frequencies, the percentage of MSE accounted for by squared bias remained fairly high, as in the stationary conditions, ranging from 32 to about 67 percent over the estimates of all three methods in all interval length conditions. In the coherence peak frequencies the

Table 17

Mean FFT Coherence Estimates x 10 (and Bias x 10)

in the Presence of Transient Sine Waves

Condition	freq band	Segment Length 0.5 s	1.0 s	2.0 s
Sine Wave Added to Series 1	5	6.357 (4.909)	5.224 (3.777)	2.781 (1.333)
	10	7.876 (0.301)	7.549 (-0.026)	7.501 (-0.074)
	15	6.291 (-1.122)	7.681 (0.267)	8.526 (1.112)
	20	6.658 (1.842)	6.617 (1.801)	6.027 (1.211)
	25	6.524 (4.395)	4.967 (2.838)	4.413 (2.283)
Sine Wave Added to Both Series	5	9.600 (8.153)	9.440 (7.993)	9.370 (7.922)
	10	7.919 (0.345)	7.199 (-0.376)	7.354 (-0.221)
	15	5.849 (-1.565)	6.626 (-0.787)	8.282 (0.868)
	20	6.976 (2.161)	5.430 (0.614)	5.394 (0.578)
	25	7.777 (5.647)	4.708 (2.578)	4.082 (1.953)

percentages were again low, less than one percent for the MEM estimates in the 11 to 15 Hz, AR estimates in the 12 to 14 Hz frequencies and the 10 Hz FFT estimates of all segment lengths. In the immediately surrounding frequencies, however, the percentages of squared bias in the MSE were slightly larger, by about one to eight percent, for all three methods than the corresponding percentages obtained in the stationary cases, with the AR method showing the largest increase of the three methods.

The mean FFT estimates and their bias for nonstationary data where the transient sine wave was added to both series are given in the lower half of Table 17. The most obvious feature of these estimates is the large means, and correspondingly the large biases of these estimates, in the 5 Hz frequency band in all segment length conditions. As the segments were lengthened the biases decreased, but even in the longest intervals where the transient affected only approximately 16 percent of the data, i.e., 40 of the 256 data points of each series, the bias of the coherence estimates remained very high at 0.7922.

The AR and MEM methods produced mean coherence estimates that were also extremely biased in the 1 to 8 Hz frequency region when a transient sine wave was added to both series, regardless of interval length. Figure 20 shows the coherence curve estimates obtained by the AR method, and Figure 21 shows these estimates obtained by the MEM method. Even

Figure 20. Coherence estimates obtained with the AR method in 0.5 second (▲), 1.0 second (■), and 2.0 second (●) conditions where a transient sine wave was added to both series.

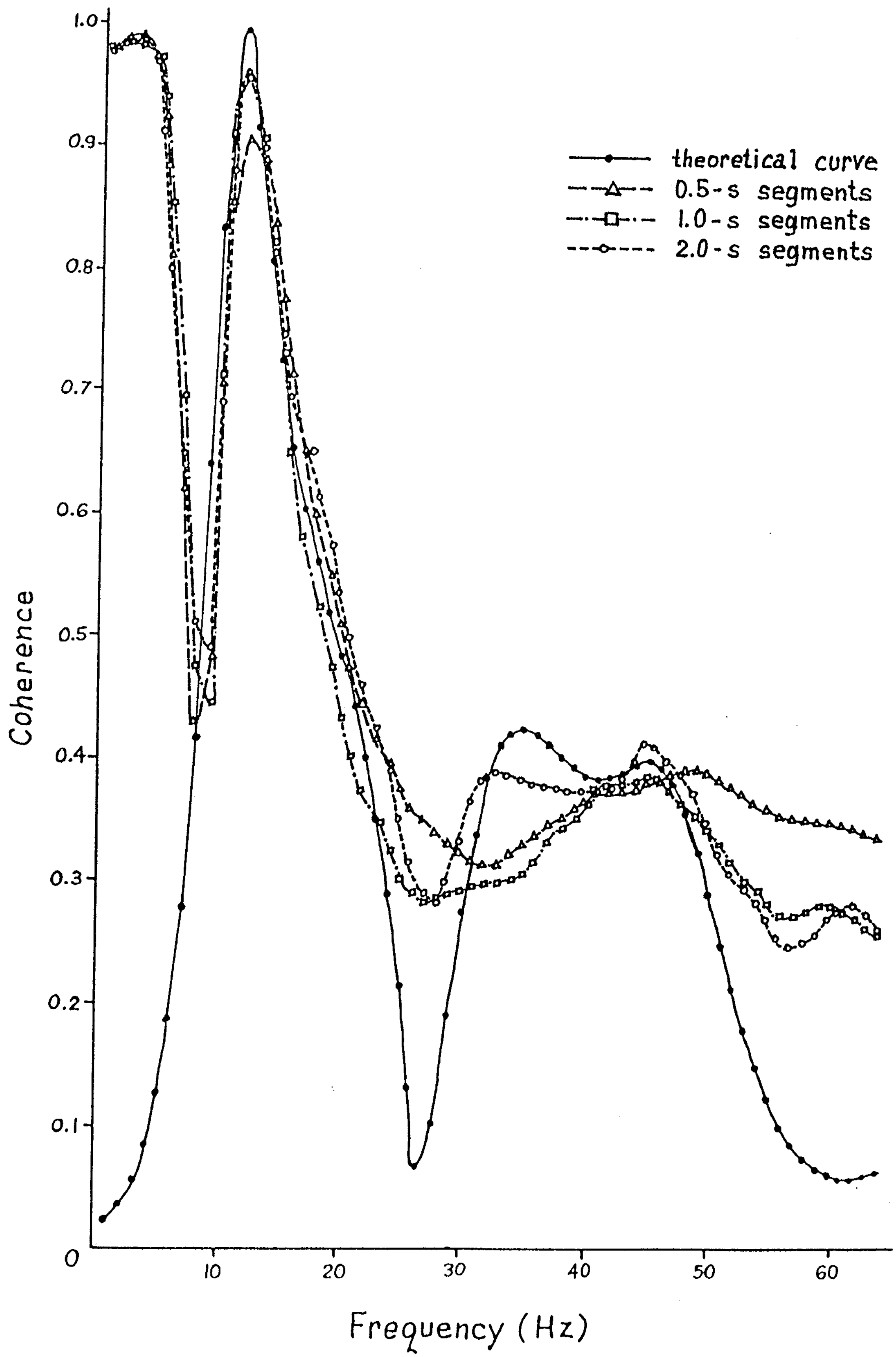
theoretical curve
0.5-s segments
1.0-s segments
2.0-s segments
Coherence
1.0
0.9
0.8
0.7
0.6
0.5
0.4
0.3
0.2
0.1
0
10
20
30
40
50
60
Frequency (Hz)

Figure 21. Coherence estimates obtained with the MEM method in 0.5 second (▲), 1.0 second (◘), and 2.0 second (○) conditions where a transient sine wave was added to both series.

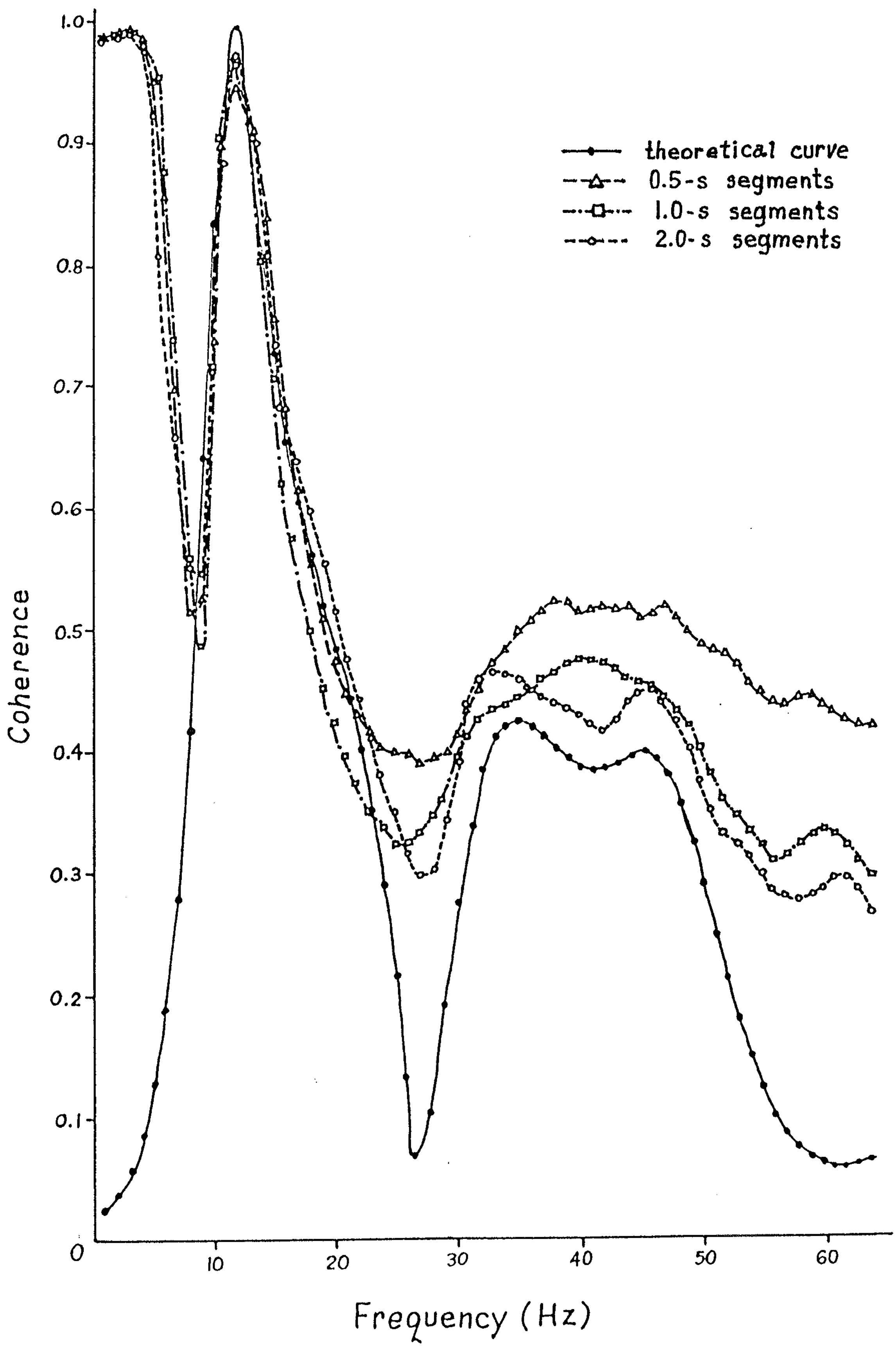

theoretical curve
0.5-s segments
1.0-s segments
2.0-s segments
Coherence
1.0
0.9
0.8
0.7
0.6
0.5
0.4
0.3
0.2
0.1
0
10
20
30
40
50
60
Frequency (Hz)

though the low frequency estimates were so biased, the estimates of both methods in the other frequencies, and especially the peak region, remained relatively unaffected in this condition.

The MSEs of the transformed estimates obtained by all three estimation methods are shown in Table 18. For the transformed estimates of all three methods, the MSEs in the 1 to 8 Hz region were 4 to 20 times larger than the MSEs for the 12 Hz estimates, which always had the largest MSEs in all the otstationary and nonstationary conditions. In the 0.5 second segments, the highest MSE was obtained for the 3 Hz MEM estimate (11.314, corresponding to an actual MSE of 1.0 for the original estimate), followed by the MSE of the AR 3 Hz estimate (7.813, which also corresponds to an actual MSE of about 1.0) while the 5 Hz FFT estimate from the 0.5 second condition had an MSE of 4.042 (actual MSE=0.9994). With longer intervals, the MSEs of the low frequency estimates tended to drop slightly but slowly. In the 2.0 second conditions, the MSEs of the transformed coherences from all three methods were still at least 10 times larger in the low frequencies than at the 12 Hz peak values, and the actual MSEs remained close to 1.0. The MSEs in the other frequencies were affected relatively little; the MSEs of the transformed FFT estimates were slightly smaller than their MSEs of stationary series in each segment length condition, and the MSEs of the nonstationary transformed AR and MEM esti-

Table 18

MSE x 10 of Transformed Coherences Obtained from Data with a Transient Sine Wave Added to Both Series

	0.5 s Segments			1.0 s Segments			2.0 s Segments		
freq	FFT	AR	MEM	FFT	AR	MEM	FFT	AR	MEM
1		63.143	83.789		63.148	75.577		57.754	64.324
2		72.420	97.181		67.667	84.381		68.734	78.982
3		78.127	113.145		68.030	89.810		74.548	89.585
4		50.252	71.720		48.943	61.479		43.313	50.040
5	40.419	25.744	36.667	32.002	28.575	34.574	26.368	22.203	24.167
6		10.841	16.150		13.821	16.701		10.175	10.577
7		2.939	5.398		4.596	6.165		3.590	3.842
8		0.577	1.524		0.759	1.297		0.711	0.959
9		1.284	1.791		1.237	1.308		0.916	0.758
10	2.034	2.002	2.162	2.849	1.319	1.768	2.572	1.698	1.616
11		2.702	3.743		1.546	1.697		1.265	1.255
12		16.507	10.728		8.291	6.374		6.819	5.024
13		2.199	2.670		1.002	1.051		0.659	0.669
14		1.638	2.060		0.710	0.785		0.543	0.562
15	2.280	1.317	1.513	1.369	0.577	0.687	2.106	0.607	0.568
16		1.070	1.296		0.536	0.685		0.682	0.585
17		0.898	1.276		0.544	0.743		0.730	0.593
18		0.785	1.308		0.565	0.829		0.746	0.595
19		0.712	1.298		0.577	0.922		0.741	0.588
20	4.046	0.665	1.196	1.190	0.575	0.952	1.044	0.728	0.575
21		0.638	1.039		0.560	0.885		0.705	0.538
22		0.623	1.044		0.519	0.828		0.661	0.518
23		0.650	1.107		0.459	0.720		0.587	0.508
24		0.723	1.233		0.417	0.597		0.546	0.481
25	11.857	0.873	1.520	1.863	0.434	0.622	1.037	0.558	0.532

mates were smaller than the stationary ones in the 0.5 second intervals but were larger than the stationary one in the 2.0 second intervals.

In contrast to conditions where only one series was affected by the transient, when both series contained the transient sine wave, the percentage of MSE due to squared bias increased to over 60 percent for all three methods, and often to over 90 percent for the AR and MEM methods, in the low, 1 to 5 Hz, frequencies for all three methods. In the other frequencies, the percentages remained unaffected by the addition of a transient to both series.

In summary, only estimates around the transient's own frequency were affected but only when both series contained the transient. When the low frequency transient was added to either one or both series, the estimates in the higher frequencies were relatively unaffected. Figure 22 compares the mean AR and MEM estimates of 2.0 second intervals with the theoretical coherence curve when a transient sine wave was added only to series 1 and when each series contained the transient. Note again that the coherence estimates obtained by the MEM method were higher than the AR estimates at all frequencies.

<u>Exponentially distributed error</u>. Changing the distribution of the noise from normal to exponential with a mean of 2.0 halfway in the series of one or both series had practi-

Figure 22. Comparison of coherence estimates obtained with the AR method (triangles) and the MEM method (squares) from 2.0 second intervals with a transient sine wave added to one (open symbols) or both (solid symbols) series.

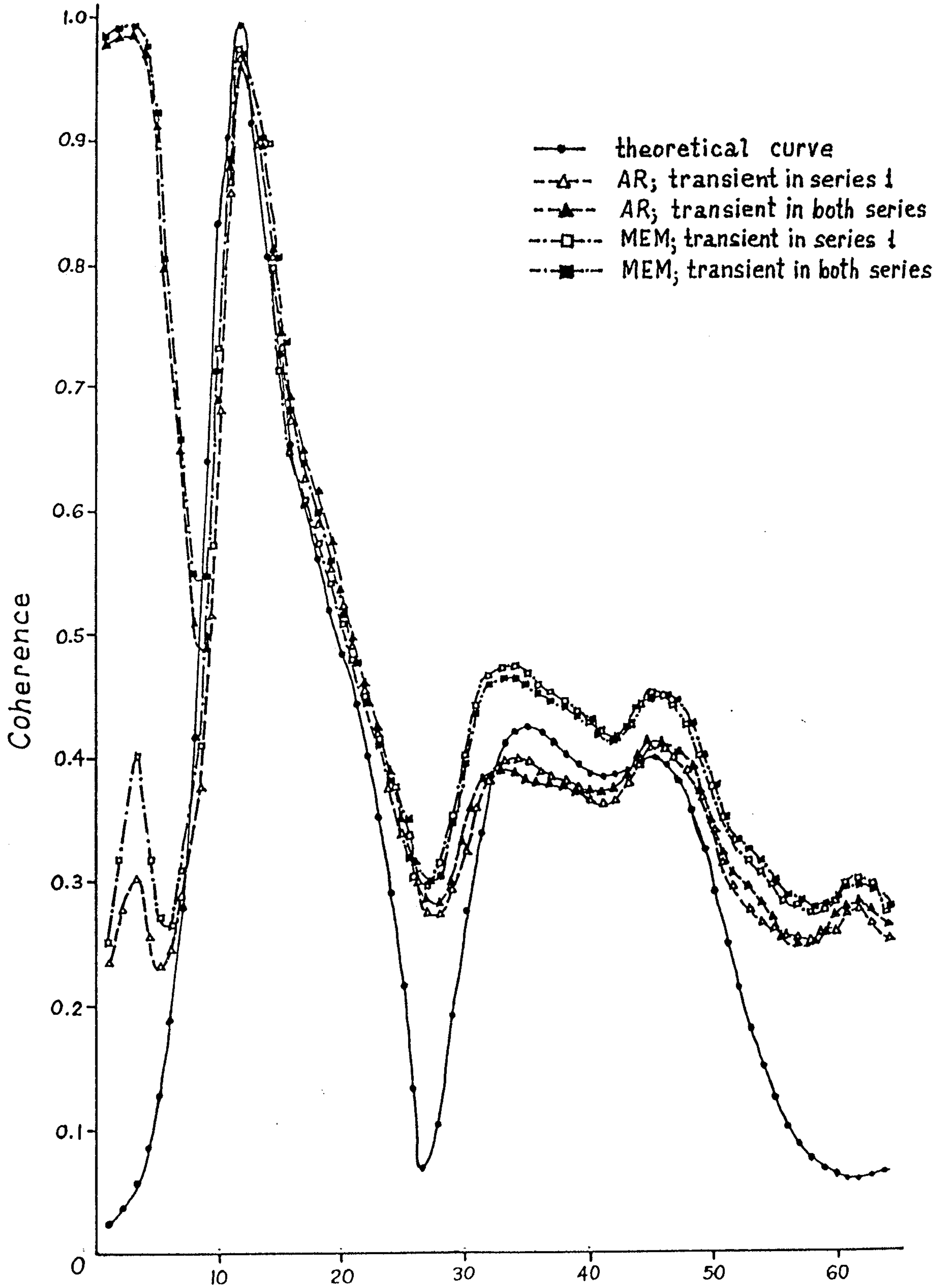
theoretical curve
AR; transient in series 1
AR; transient in both series
MEM; transient in series 1
MEM; transient in both series
Coherence
Frequency (Hz)
1.0
0.9
0.8
0.7
0.6
0.5
0.4
0.3
0.2
0.1
0
10
20
30
40
50
60

Table 19

Mean FFT Coherence Estimates x 10 (and Bias x 10)

from Series with Exponentially Distributed Noise

Condition	freq band	Segment Length 0.5 s	1.0 s	2.0 s
Noise changed to exp(mean=2.0) at N/2 in series 1	5	6.707 (5.260)	6.137 (4.690)	4.391 (2.943)
	10	7.188 (-0.387)	7.315 (-0.260)	6.944 (-0.631)
	15	7.521 (0.107)	7.823 (0.409)	8.471 (1.057)
	20	8.199 (3.384)	7.303 (2.487)	6.117 (1.302)
	25	6.842 (4.712)	5.581 (3.451)	4.667 (2.538)
Noise changed to exp(mean=2.0) at N/2 in both series	5	6.711 (5.263)	4.867 (3.420)	4.442 (2.994)
	10	7.012 (-0.563)	7.281 (-0.294)	7.540 (-0.035)
	15	7.605 (0.192)	7.823 (0.409)	8.769 (1.355)
	20	8.132 (3.317)	7.044 (2.228)	6.571 (1.755)
	25	6.579 (4.449)	5.458 (3.328)	4.624 (2.494)

cally no effect on the mean FFT coherences (Table 19). These estimates were almost identical to those obtained by FFT where the noise was entirely normally distributed (compare with Table 10). The similarity was especially noticeable when the distribution of the noise was changed halfway through both 2.0 second series.

The mean AR coherence estimates from all segment lengths are shown in Figure 23 for the conditions where the noise distribution was change to exponential halfway in series 1, and in Figure 24 for the conditions where both series contained this nonstationarity. Generally the AR estimates were less biased when the error distribution was changed only in one series, particularly in the low frequencies, for each corresponding interval length; however, the very peak of the coherence function was estimated more accurately when both series were the same, that is when both were nonstationary. The same was also true for the MEM coherence estimates, which are shown in Figure 25 for series 1 nonstationary and in Figure 26 when both series were nonstationary. In both kinds of nonstationary conditions for each segment length, the AR estimates were less biased than the MEM estimates except at the 12 Hz frequency where the MEM method estimated the peak value more accurately. The increase in interval length resulted in more biased estimates at low frequencies in both methods, but the AR estimates were less affected than the MEM estimates. Figure 27 shows that the

Figure 23. Coherence estimates obtained with the AR method from data with exponentially (mean=2.0) distributed noise in half of series 1. (▲ are 0.5 second intervals, ■ are 1.0 second intervals, and ● are 2.0 second intervals.)

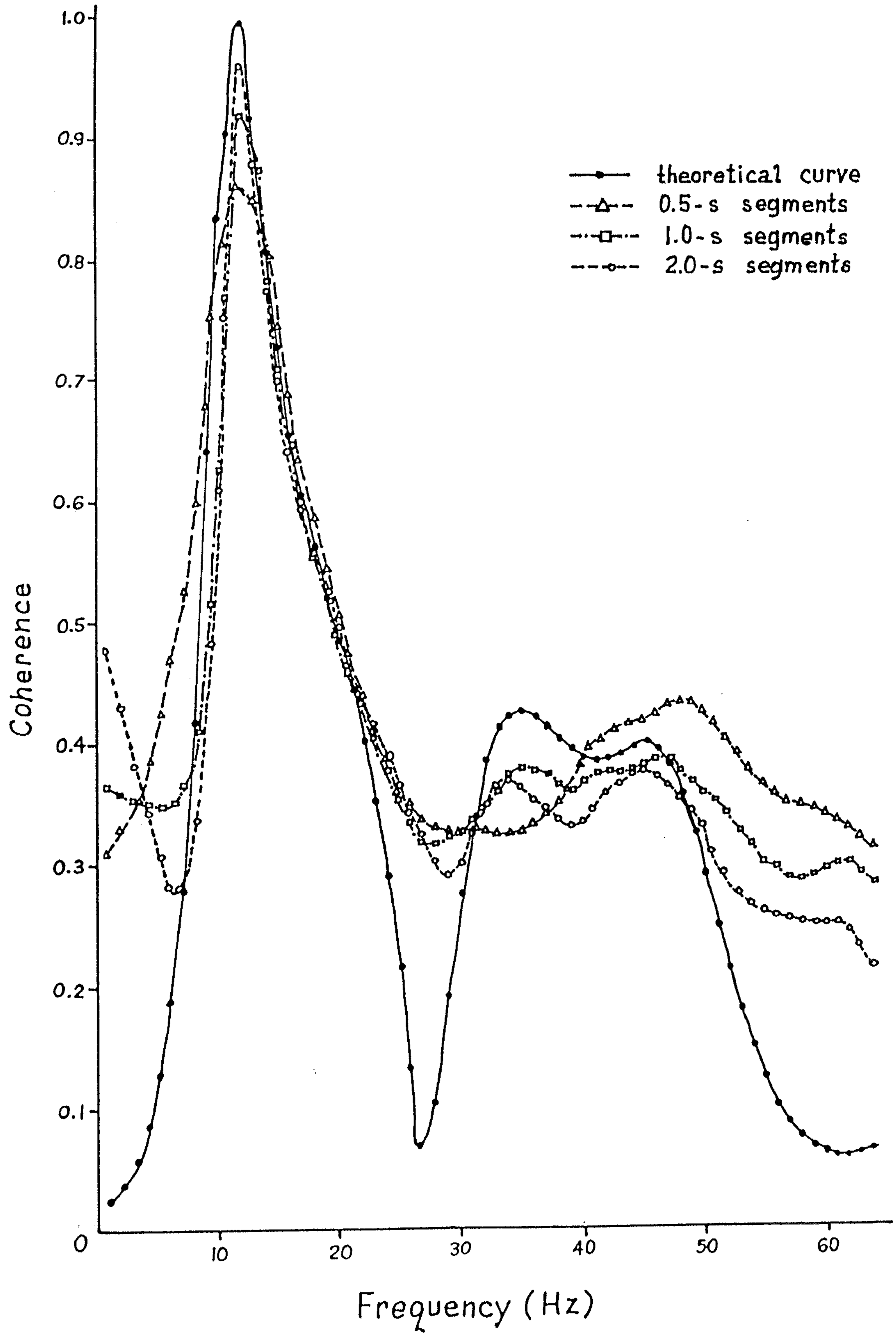

theoretical curve
0.5-s segments
1.0-s segments
2.0-s segments
Coherence
1.0
0.9
0.8
0.7
0.6
0.5
0.4
0.3
0.2
0.1
0
10
20
30
40
50
60
Frequency (Hz)

Figure 24. Coherence estimates obtained with the AR method from data with exponentially (mean=2.0) distributed noise in half of both series. (▲ are 0.5 second intervals, ◘ are 1.0 second intervals, and ○ are 2.0 second intervals.)

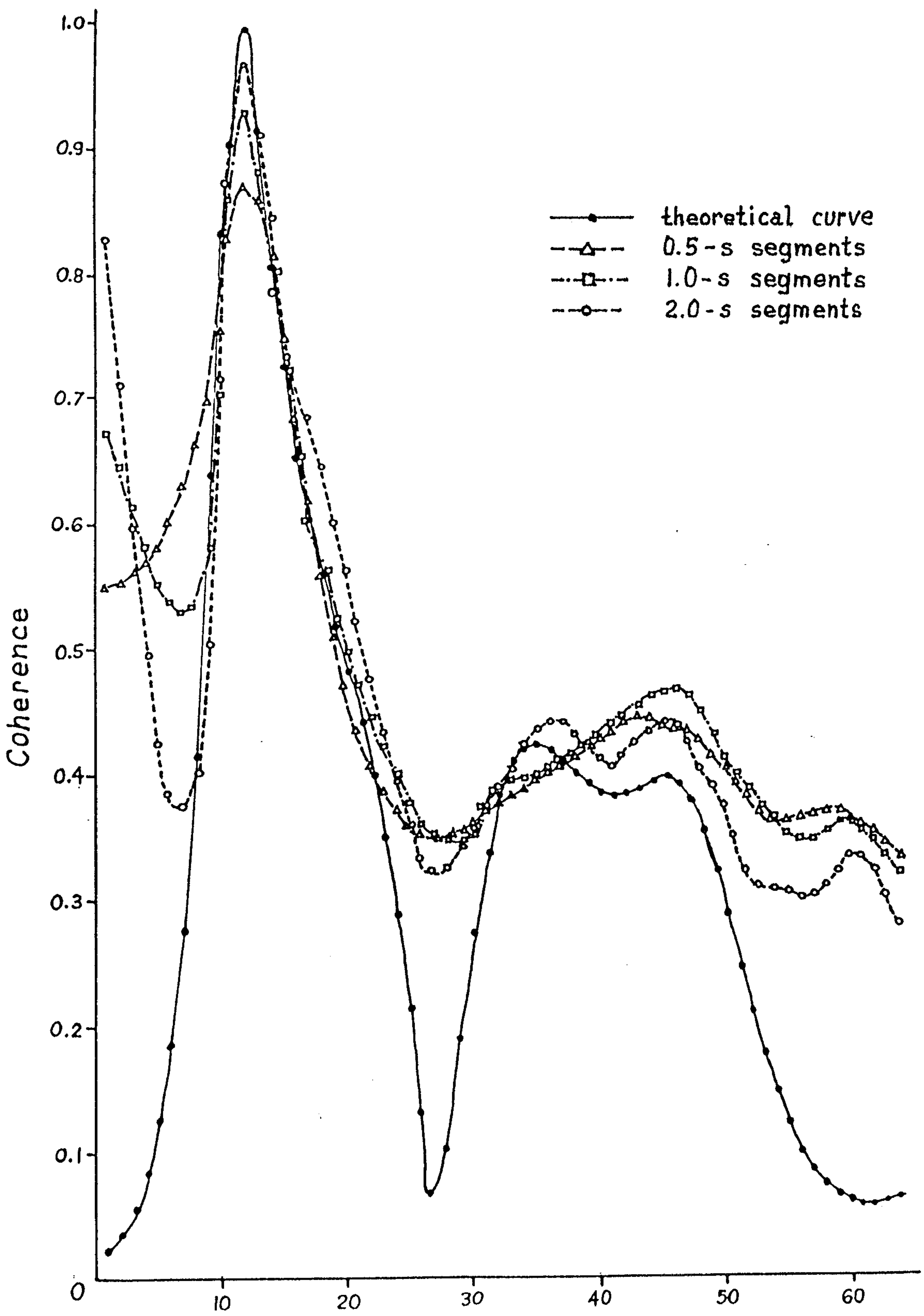

theoretical curve
0.5-s segments
1.0-s segments
2.0-s segments
Coherence
Frequency (Hz)
1.0
0.9
0.8
0.7
0.6
0.5
0.4
0.3
0.2
0.1
0
10
20
30
40
50
60

Figure 25. Coherence estimates obtained by the MEM method from data with exponentially (mean=2.0) distributed noise in half of series 1. (▲ are 0.5 second intervals, ◘ are 1.0 second intervals, and ○ are 2.0 second intervals.)

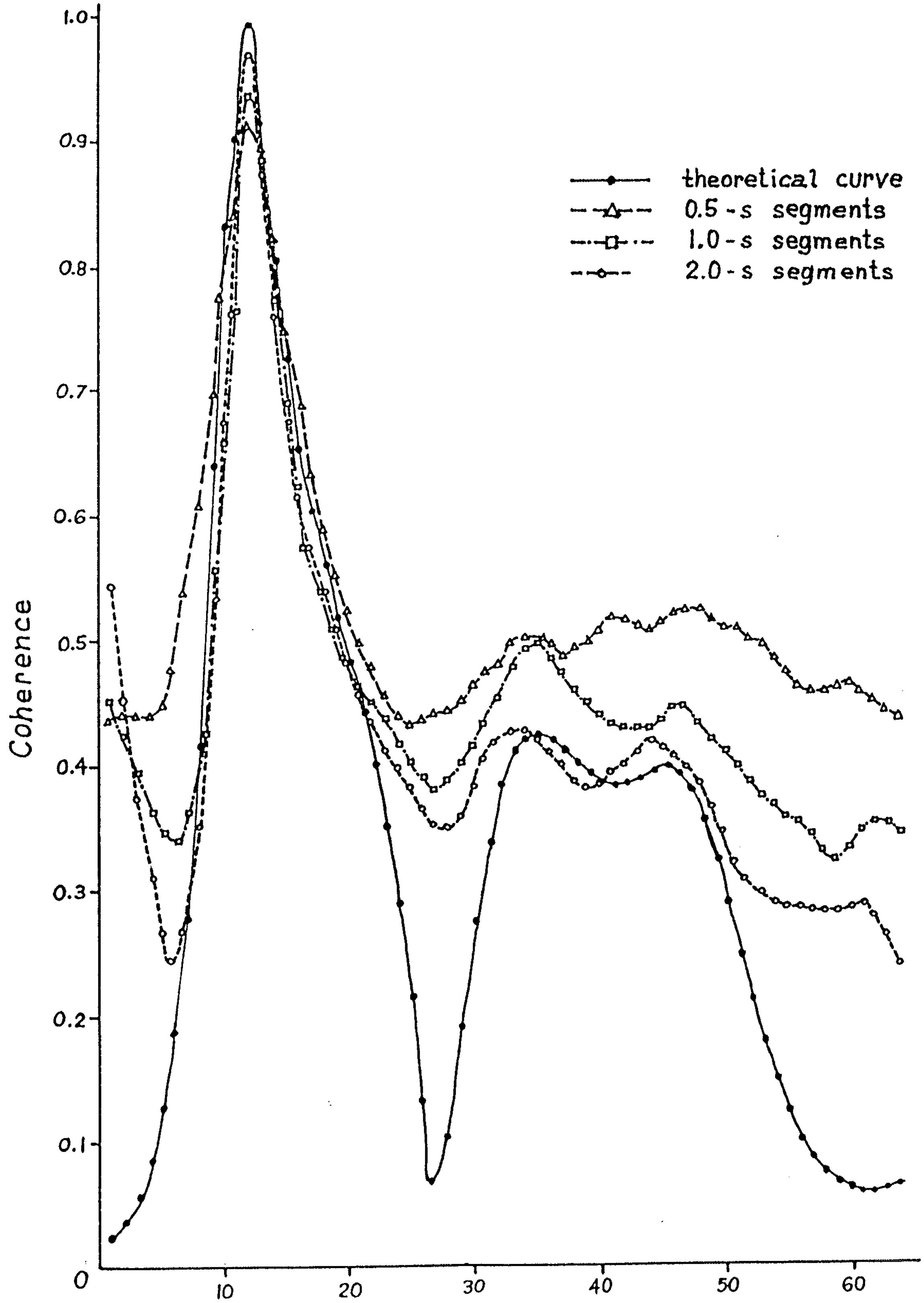

1.0
0.9
0.8
0.7
0.6
0.5
0.4
0.3
0.2
0.1
0
Coherence
10
20
30
40
50
60
Frequency (Hz)
theoretical curve
0.5-s segments
1.0-s segments
2.0-s segments

Figure 26. Coherence estimates obtained by the MEM method from data with exponentially (mean=2.0) distributed noise in half of both series. (▲ are 0.5 second intervals, ■ are 1.0 second intervals, and ● are 2.0 second intervals.)

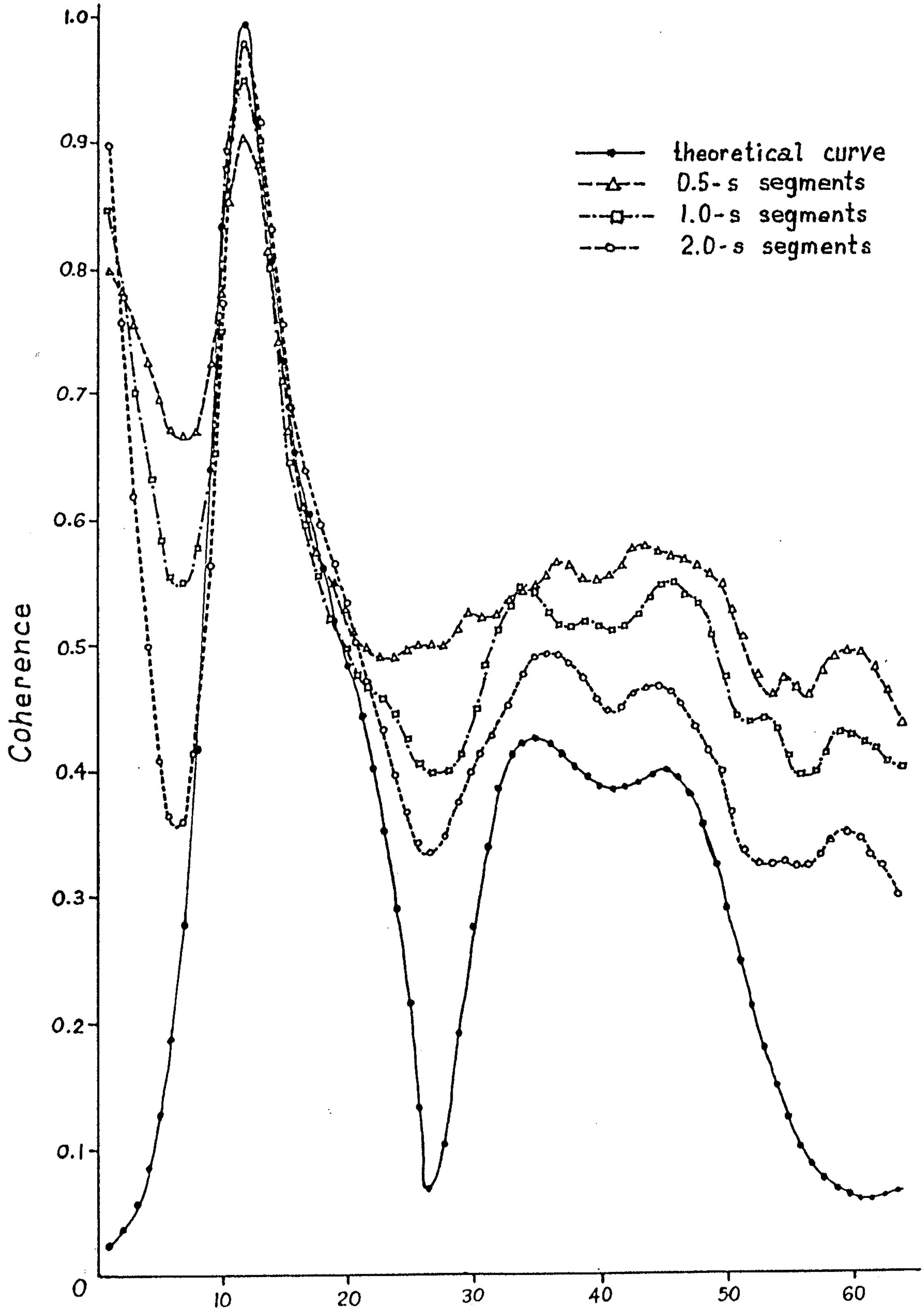
1.0
0.9
0.8
0.7
0.6
0.5
0.4
0.3
0.2
0.1
0
10
20
30
40
50
60
Coherence
Frequency (Hz)
theoretical curve
0.5-s segments
1.0-s segments
2.0-s segments

mean coherence estimates of the AR and MEM methods obtained in the 2.0 second condition were very similar for each nonstationary condition, although as was also noted in previous conditions, the estimates of the MEM method were higher than the AR estimates at each frequency.

The MSEs of the transformed coherence estimates of all three methods in the three interval length conditions are presented in Table 20 for the nonstationary condition with the noise distribution changed only in series 1. As the intervals lengthened, the MSEs of the AR estimates decreased at all frequencies except at 1,2, and 10 Hz where the MSEs increased with increasing interval length. The MSEs of the MEM estimates decreased with each increase in interval length at each frequency. For both AR and MEM estimates, the nonstationary MSEs were larger than the MSEs of the respective stationary estimates, particularly in the lowest frequencies where the effect of this nonstationarity was most notable. Within each interval length condition, the largest MSE of the AR and MEM still occurred at 12 Hz, with the AR estimates having the larger MSE than the MEM estimate at this frequency. The MSEs of the FFT transformed estimates were more similar to their stationary counterparts than were the MSEs of the AR and MEM estimates. Even in the 5 Hz band where the AR and MEM estimates were most affected, the FFT estimates resembled the stationary estimates, particularly as the segments were lengthened.

Figure 27. Coherence estimates obtained with the AR method (triangles) and the MEM method (squares) from 2.0 second intervals where the noise was exponentially (mean=2.0) distributed in half of series 1 (open symbols) or in half of both series (solid symbols).

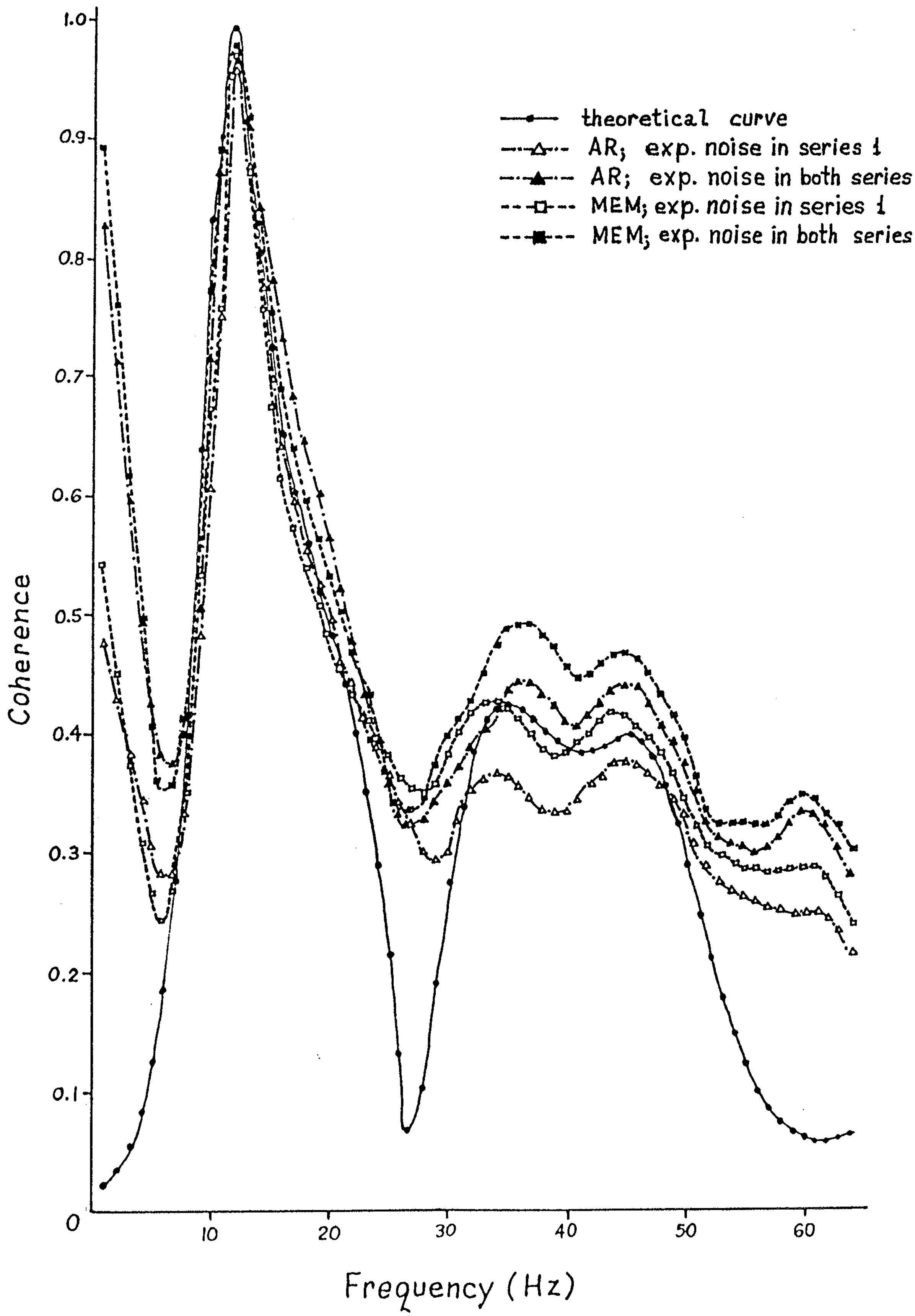

theoretical curve
AR; exp. noise in series 1
AR; exp. noise in both series
MEM; exp. noise in series 1
MEM; exp. noise in both series
Coherence
1.0
0.9
0.8
0.7
0.6
0.5
0.4
0.3
0.2
0.1
0
10
20
30
40
50
60
Frequency (Hz)

Table 20

MSE x 10 of Transformed Coherences Obtained from Data with Exponential Noise in Half of Series 1

freq	0.5 s Segments			1.0 s Segments			2.0 s Segments		
	FFT	AR	MEM	FFT	AR	MEM	FFT	AR	MEM
1		1.732	5.583		2.402	4.348		3.590	4.791
2		1.758	4.734		2.083	3.050		2.494	2.767
3		1.820	4.028		1.756	2.146		1.701	1.594
4		1.921	3.305		1.417	1.497		1.099	0.878
5	9.477	2.063	2.844	5.114	1.073	1.030	1.826	0.637	0.447
6		2.247	2.662		0.757	0.718		0.316	0.234
7		2.445	2.858		0.534	0.552		0.188	0.202
8		2.560	3.002		0.534	0.607		0.346	0.368
9		2.259	2.865		1.047	1.115		0.998	0.912
10	3.792	2.474	3.018	3.015	2.773	2.721	3.308	2.987	2.302
11		3.780	4.718		3.099	3.463		2.998	2.856
12		20.628	14.562		14.355	11.526		7.809	5.625
13		3.218	3.641		1.290	1.294		0.676	0.780
14		2.435	3.098		0.828	0.774		0.391	0.493
15	2.543	1.944	2.326	1.976	0.702	0.665	2.559	0.343	0.397
16		1.606	2.129		0.632	0.633		0.351	0.361
17		1.363	2.365		0.587	0.636		0.368	0.348
18		1.179	2.149		0.556	0.652		0.358	0.335
19		1.030	2.036		0.530	0.667		0.339	0.337
20	9.859	0.903	1.896	4.658	0.503	0.638	1.610	0.336	0.364
21		0.799	1.705		0.490	0.614		0.331	0.387
22		0.720	1.625		0.485	0.636		0.347	0.421
23		0.670	1.610		0.485	0.744		0.405	0.501
24		0.674	1.670		0.516	0.862		0.509	0.632
25	7.968	0.768	2.022	3.213	0.607	1.012	1.573	0.664	0.819

The percentage of MSE of the FFT estimates accounted for by squared bias also remained unaffected by having exponentially distributed error in one series. The MSEs of the AR and MEM nonstationary estimates in the coherence peak region, however, consisted of higher percentage of squared bias than did the stationary estimates. In the 11 to 14 Hz frequencies, the squared bias now accounted to up to 7 percent of the MSEs of the AR and MEM nonstationary estimates. In the other frequencies the percentages remained relatively unaffected.

Table 21 shows the MSEs of transformed coherence estimates with the nonstationarity in both series. In this condition, the MSEs of the FFT transformed estimates were also very similar to those of the stationary estimates. When both series were nonstationary, the MSE of the 5 Hz FFT estimates in the longer intervals had a smaller MSE than these stationary estimates; the MSE of the 0.5 second interval estimate was larger than of the stationary one.

The MSEs of the AR and MEM transformed estimates in the lowest frequencies were about four times greater in this condition than the MSEs of these estimates when only series 1 was nonstationary. At the 12 Hz frequency, however, the MSEs of both AR and MEM estimates were smaller when both series were nonstationary than when only series 1 was nonstationary in each segment length condition, but they were not as small as the MSEs of the stationary estimates. In the 1

Table 21

MSE x 10 of Transformed Coherences Obtained from Data with Exponential Noise in Half of Both Series

	0.5 s Segments			1.0 s Segments			2.0 s Segments		
freq	FFT	AR	MEM	FFT	AR	MEM	FFT	AR	MEM
1		6.137	20.745		10.766	20.446		16.807	22.302
2		5.647	16.977		8.138	12.983		9.283	11.175
3		5.168	13.379		6.180	8.728		5.231	5.841
4		4.780	10.409		4.725	6.092		3.017	3.100
5	10.280	4.502	8.305	2.709	3.612	4.350	1.808	1.772	1.655
6		4.298	6.795		2.730	3.148		1.052	0.898
7		4.085	5.706		2.009	2.344		0.628	0.547
8		3.714	5.173		1.446	1.953		0.516	0.523
9		3.079	4.254		1.217	2.105		1.008	1.059
10	4.223	3.459	5.193	2.732	2.235	2.940	2.059	2.015	2.556
11		4.492	6.862		2.715	3.720		1.450	1.684
12		19.602	15.105		12.461	9.003		6.110	3.989
13		2.857	4.226		1.691	2.203		1.115	1.135
14		2.358	3.290		1.467	1.682		1.114	0.928
15	2.870	1.943	2.435	1.867	1.475	1.471	3.300	1.092	0.796
16		1.576	2.074		1.471	1.289		1.051	0.691
17		1.306	2.157		1.418	1.178		1.002	0.636
18		1.126	2.189		1.338	1.075		0.924	0.616
19		0.992	2.357		1.273	1.054		0.837	0.598
20	11.276	0.874	2.088	4.054	1.214	1.071	1.756	0.756	0.584
21		0.768	2.028		1.146	1.051		0.704	0.600
22		0.691	1.828		1.076	1.066		0.674	0.642
23		0.661	2.154		1.014	1.158		0.649	0.688
24		0.702	2.632		1.011	1.238		0.629	0.688
25	7.605	0.855	2.954	3.148	1.092	1.360	1.612	0.656	0.713

to 4 Hz region, the MSEs, particularly of the MEM transformed estimates, were also much larger than the MSEs of the estimates in the other frequencies, the actual MSEs of these estimates were close to 1.0. The MSEs of these estimates did not seem to decrease much with segment length as did the MSEs of the estimates in the other frequecies. The MSEs of these low frequency MEM transformed estimates from 0.5 second intervals were about three times larger than those of the AR estimates; for example, at 1 Hz the MSE of the MEM transformed estimates was 2.07 while that of the AR transformed estimate was 0.61 (actual MSEs were 0.969 and 0.544, respectively). With increasing segment length, however, the MSEs of the AR estimates in these frequencies tended to increase while those of the MEM estimates generally decreased slightly, and thus the MSEs of the two methods approached similar values; for example, for the 2.0 second interval transformed estimates at 3 Hz, the MSE of AR was 0.523 (actual MSE=0.480) the MSE of the MEM was 0.584 (actual MSE=0.526). In the 0.5 second intervals, the AR estimates also had smaller MSEs than the MEM estimates in all other frequency regions, except at the 12 Hz frequency, but as intervals lengthened the MSEs of the AR and MEM estimates became more similar, and in the coherence peak region the MEM estimates had slightly smaller MSEs at about half of the frequencies.

The percentages of MSEs of these nonstationary estimates consisting of squared bias were almost unchanged from the percentages obtained with stationary estimates. In the coherence peak region, the percentage of MSE due to squared bias remained below one percent for all three estimation methods. At the 1 and 2 Hz frequencies, the percentages were by about 10 percent higher than those of the stationary estimates to the AR and MEM methods, while the percentages remained the same as in the stationary conditions for the FFT estimates.

Two other 1.0 second interval conditions were run using exponentially distributed error in generating the series, to determine how the estimation methods performed in more extreme circumstances. In one condition both series consisted entirely of exponentially distributed error with a mean of 2.0; thus in this condition, the bivariate series was stationary but non-Gaussian. In the second condition, the normal error in series 1 was changed at halfway to an exponentially distributed error but with a larger mean of 5.0, while the second series remained normal throughout. The mean estimates obtained in these conditions are compared to 1.0 second segments of the two nonstationary conditions described above in Table 22 for the FFT estimates, and in Figures 28 and 29 for the AR and MEM estimates, respectively.

The FFT coherence estimates in the non-Gaussian condition, shown in the third column of Table 22, compared very

Table 22

Mean FFT Coherence Estimates x 10 (and Bias x 10) from Various 1.0-sec Segments with Exponentially Distributed Noise

freq band	Exp(mean=2.0) for N/2 in series 1	Exp(mean=2.0) for N/2 in both series	Exp(mean=2.0) for all N in both series	Exp(mean=5.0) for N/2 in series 1
5	6.137 (4.690)	4.867 (3.420)	5.953 (4.505)	6.316 (4.868)
10	7.315 (-0.260)	7.281 (-0.295)	7.672 (0.097)	6.281 (-1.294)
15	7.823 (0.409)	7.823 (0.409)	8.222 (0.809)	7.556 (0.142)
20	7.303 (2.487)	7.044 (2.228)	7.302 (2.486)	7.064 (2.249)
25	5.581 (3.451)	5.458 (3.328)	5.484 (3.354)	6.772 (4.642)

<u>Figure 28</u>. Coherence estimates obtained with the AR method from the various 1.0 second data sets containing exponential noise. (Exponential, mean=2.0, noise was in half of series 1 (▵) or in half of both series (▴); exponential, mean=5.0, noise was in half of series 1 (○); and both series consisted entirely of exponential, mean=2.0, noise (■).)

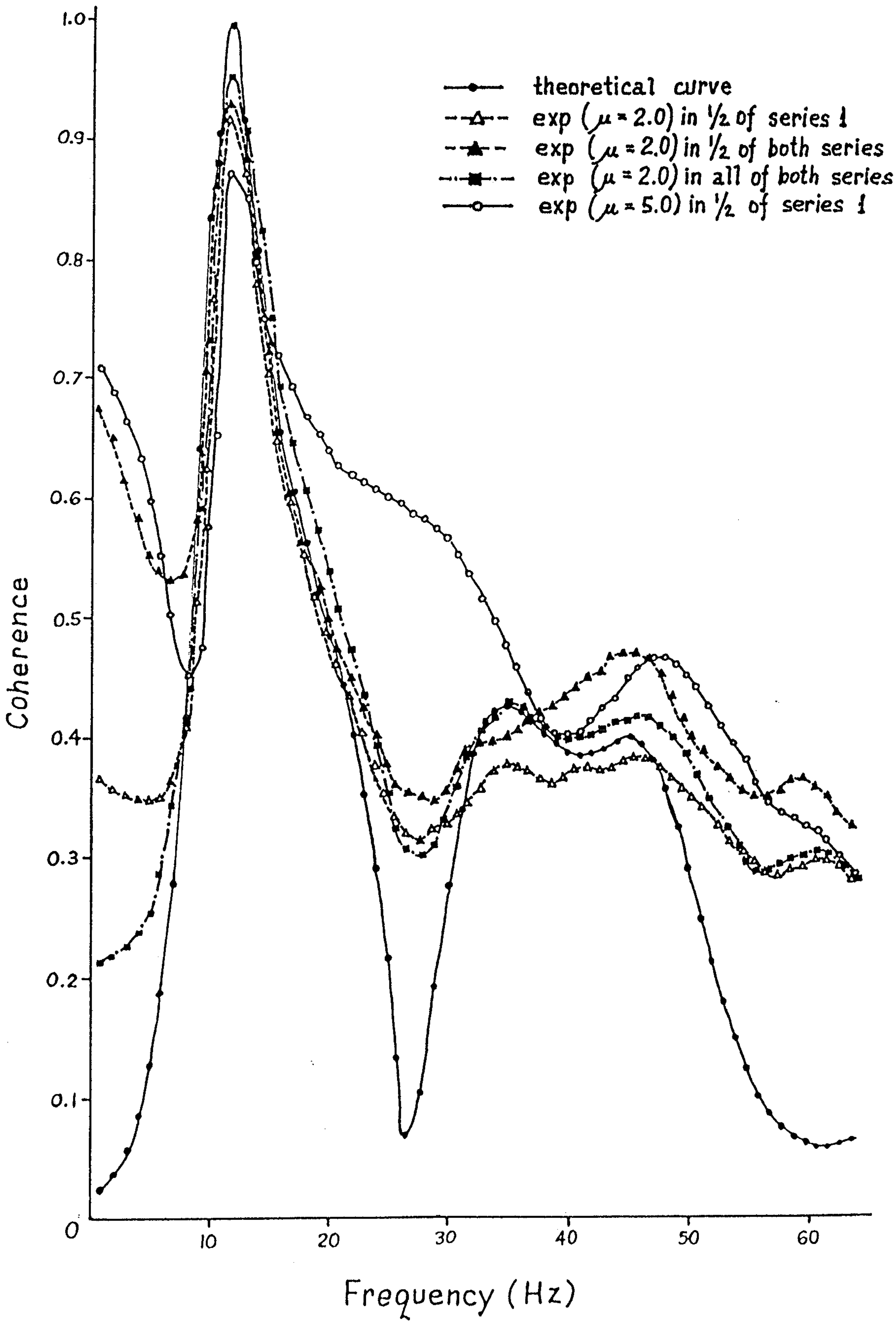
theoretical curve
exp (μ = 2.0) in ½ of series 1
exp (μ = 2.0) in ½ of both series
exp (μ = 2.0) in all of both series
exp (μ = 5.0) in ½ of series 1
Coherence
1.0
0.9
0.8
0.7
0.6
0.5
0.4
0.3
0.2
0.1
0
10
20
30
40
50
60
Frequency (Hz)

Figure 29. Coherence estimates obtained with the MEM method from the various 1.0 second data sets containing exponential noise. (Exponential, mean=2.0, noise was in half of series 1 (△) or in half of both series (▲); exponential, mean=5.0, noise was in half of series 1 (○); and both series consisted entirely of exponential, mean=2.0, noise (■).)

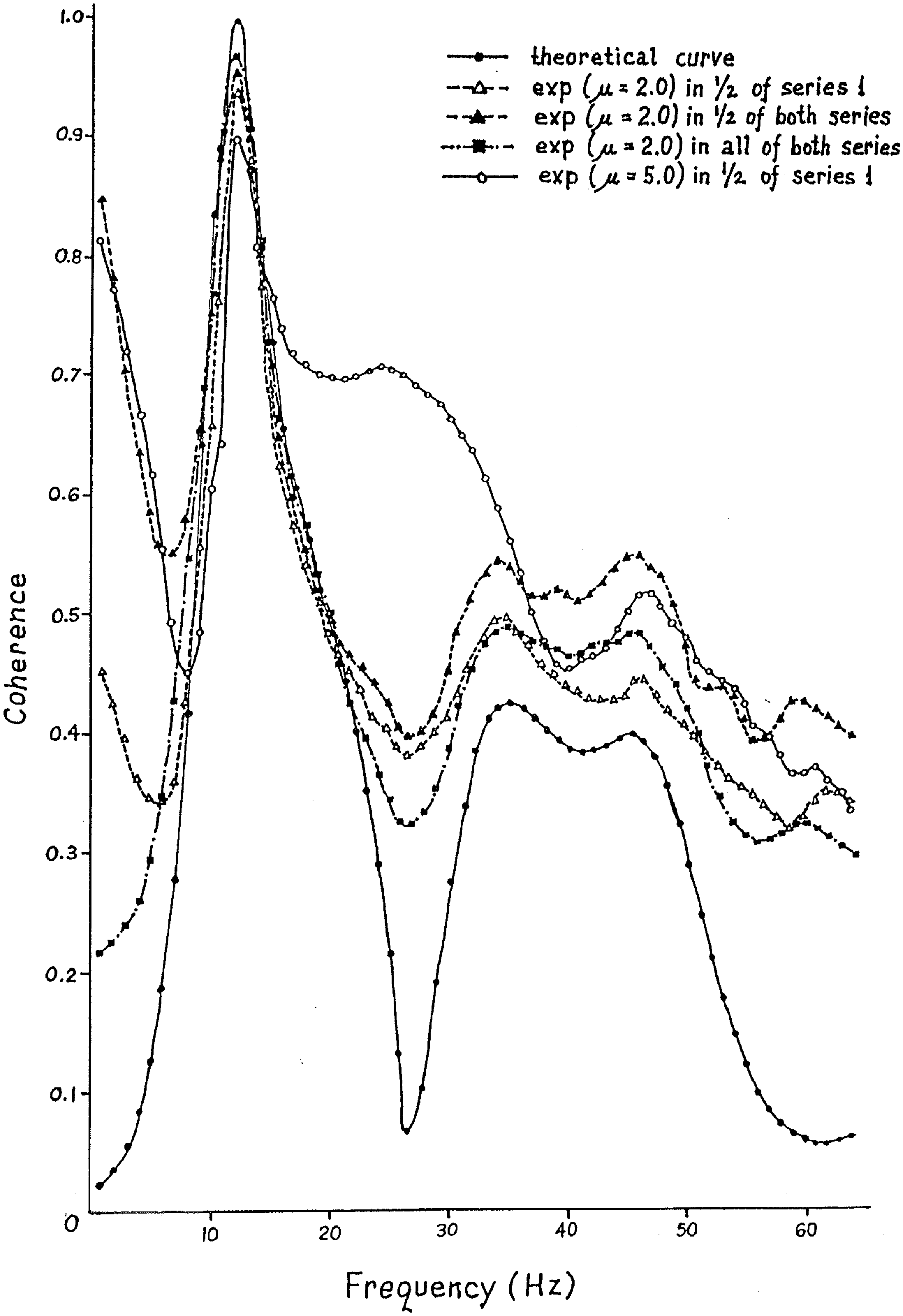

theoretical curve
exp (μ = 2.0) in ½ of series 1
exp (μ = 2.0) in ½ of both series
exp (μ = 2.0) in all of both series
exp (μ = 5.0) in ½ of series 1
Coherence
Frequency (Hz)
0
0.1
0.2
0.3
0.4
0.5
0.6
0.7
0.8
0.9
1.0
10
20
30
40
50
60

favourably with the Gaussian stationary estimates. The non-Gaussian estimates in the 10 and 15 Hz frequency bands were slightly more biased than the stationary estimates, but in each of the other frequency bands the bias tended to be marginally smaller in the non-Gaussian than the Gaussian stationary estimates from 1.0 second intervals. The most biased estimates were obtained in the condition where the error distribution was changed halfway in the segment to exponential with a mean of 5.0, shown in the last column of Table 22. In this condition, the 10 Hz FFT estimate was the most biased of the nonstationary conditions with exponential errors, and was about three times as biased as the stationary estimate.

For both the AR and MEM methods, the most biased estimates were also obtained in the conditions where the distribution of the error was changed in the middle of the segment to exponential with a mean of 5.0. In all these nonstationary conditions, both methods estimated the peak of the coherence function more or less accurately with the MEM method again producing less biased 12 Hz estimates while the AR method's estimates were less biased in the more extreme regions of the function. Of all these conditions, the estimates of the non-Gaussian series, where both series had entirely exponentially distributed noise, were the least biased. In fact, the non-Gaussian estimates of both methods were practically identical to the stationary estimates, and for the AR estimates from the non-Gaussian series, these were less biased than the AR stationary estimates at all frequencies.

DISCUSSION

The simulated data in this study appear to provide an adequate representation of EEG. The frequency components of the simulated data fall into the alpha band in both series which would represent the EEG of normal, resting, awake adults. With alpha activity present in the EEG, beta, delta, and theta activities would most likely be suppressed, thus in this respect the simulated data seems to provide a model of EEG that is commonly observed in practice. The order of the bivariate model for the simulation was chosen to be seven, since Jones (1974) reported a bivariate autoregression of order six to model the EEG of a sleeping human infant, and Gersch and Yonemoto (1977) found univariate AR models of order ten to represent adult awake EEG. Considering the difficulties of simulating a stable bivariate AR model of order seven, the overall simulation appears satisfactory.

A number of studies in the past have compared various methods of spectral estimation using real EEG. Some of these were discussed in the introduction. In another study by Pigeau, Hoffman, and Moffitt (1981), it was found that the FFT spectra of real EEG contain the same information as estimates of period analysis which are simpler and thus faster to calculate than the FFT spectra and may thus be advantageous in some applications. Jansen et al. (1981) found that univariate AR spectra were approximately the same as FFT spectral estimates of short, one second, N=64, EEG segments, although the AR and Burg's univariate MEM methods were slightly more accurate in estimating the peaks of the spectra. Their study used discriminant analysis to evaluate the estimates. The present study replicated the results of Jansen et al. for spectral estimates with simulated EEG data, and also found that the same results extend to coherence estimates obtained from the three methods.

A recent study by Chan and Miskowicz (1984) has compared the statistical bias and variability of squared coherence estimates obtained by ARMA models and the FFT method. In their study, three different test signals of N=1024 were generated to produce three different squared coherence functions. For the first signal, which was white noise with a signal to noise ratio (SNR) of 3 dB, and the second signal, a nonwhite noise with SNR of 3 dB, the ARMA squared coherence estimates were found to be less biased and less variable than the FFT estimates. The third test signal was the same nonwhite noise as the second signal with an added sinusoid. In this condition the FFT estimates were found to be superior, although neither method obtained the correct squared coherence value at the frequency of the sinusoid. In this third condition, the estimated orders of the ARMA models were found to be about twice as large as the orders of the nonwhite noise alone signals, to which the authors attributed the poorer performance of the ARMA models. This is in contrast to the findings of the present study, where even models of overestimated orders of both the AR and MEM methods produced coherence estimates that were as accurate as the estimates from models with the correct order.

The results of the present study extend those of the above studies in evaluating the statistical properties of coherence estimates of three different methods. In the present study the FFT methods was compared with the AR and MEM methods for much shorter segments and for different signals, some of which violated the stationarity and Gaussian assumptions underlying the estimation procedures. In most tested conditions, the spectral and coherence estimates obtained by the three estimation methods were very similar to each other in terms of the statistical criteria considered, their bias and MSE. The exceptions were the spectral estimates of the adaptive method of the Kalman type, which in comparison with the other methods were much worse in all respects, except perhaps for peak identification.

The similarity of the AR and MEM methods emerged because they are both based on the same underlying method of fitting a bivariate autoregression to the series. The difference between the two methods is that the MEM method uses the original series only to estimate the first order model; in each subsequent p-th step, for p=2, 3, ... , however, the residual errors remaining in the series after the p-1 order model was fit are used in place of the original series for estimating the p-th order MEM model (Jones, 1978).

Like the AR and MEM methods, the adaptive method of the Kalman type also needs to have the order of the model specified or estimated. Estimation of the order at each, or at least some, time points of the series is usually avoided due to the amount of computation required. The orders may also change as modeling of the series progresses, resulting in added complexity. Rather, either past experience may suggest what orders to use, or a univariate autoregression may be fit using some criterion such as Akaike's FPE, and the same order then used for the adaptive method (e.g., Jansen et al., 1981). In the present study it was known that the bivariate model had an order of seven, thus this value was also used for the adaptive method. The univariate model fit to each single series that was simulated by a bivariate model, however, may not have a comparable order to the bivariate model. Perhaps higher orders are required to model each univariate series.

In addition, the estimated coefficients used in calculating the adaptive method's spectra were those obtained after the last update, under the assumption that they will have stabilized at this point (Clarke, 1980). But the coefficients may not be stable in very short data segments, or may become destabilized in longer intervals. As a result of how the parameters are estimated, the adaptive method is very sensitive to small changes and thus if spectra are obtained only at the last time point they could inaccurately represent estimates of the entire interval. Users of the adaptive method of the Kalman type should examine the stability of the coefficient estimates prior to calculating one spectrum that is to represent the estimate of the entire interval.[2]

A more appropriate application of the adaptive Kalman method may be in actually tracking changes in a spectrum within an epoch of nonstationary series (e.g., Bohlin, 1977), rather than using it to obtain one spectrum to represent the estimate of the entire epoch for which other, more suitable estimation methods exist.

In the present study, the estimates of the single spectra of the adaptive method, even of stationary series, were very biased for these reasons. Since the adaptive method produced similar results in all other conditions, they will not be discussed further.

Order Selection

Although the final prediction error (FPE) criterion was developed for the AR estimation method (Akaike, 1969a), the FPE estimated orders of the stationary MEM models were less biased and more consistent than those ofthe AR models within each different interval length condition. In the 0.5 second intervals, the average order selected by the FPE for the AR method was two orders smaller than the theoretical order of seven. These smaller orders produced somewhat smoother looking spectra for series 1, failing to detect the minor spectral peak at 10 Hz. The AR spectra computed from models of the known order of seven, however, were not notably improved, although slightly larger spectral values were detected in the 9 and 10 Hz frequencies. Gersch and Yonemoto (1977) and Jones (1974) have reported that estimates of models with smaller orders resulted in smoother looking graphs of EEG spectra than when larger orders were used. In the present study this order effect was present in both spectra and coherence functions but was relatively negligible.

In the nonstationary conditions, it is interesting to note that even though the estimated orders were often larger than the theoretical order of seven, particularly of MEM models, he coherence estimates were very close to the theoretical values. Thus it would seem that regardless of the actual order used in the estimation, the coherence estimates remain relatively unharmed, particularly if the order is overestimated. From the present study, however, it is unclear whether this resulted because the model coefficients of the higher lags were very small thus contributing negligibly to the spectral estimates.

Stationary Estimates

Since the AR and MEM spectral estimates are obtained from estimates of the model coefficients and the estimate of the prediction error matrix, the spectral estimates, and thus also the coherence estimates, can only be as accurate as are the estimates of these underlying parameters. In the present study, as intervals became longer (i.e., as sample size increased) the coefficients of both methods became much less biased and less variable with smaller MSEs, and the bias of each individual element of the predicion error matrices also decreased. Correspondingly, the spectra of both methods became less biased as intervals lengthened. For all segment lengths, the estimates of the coefficients and the prediction error matrix obtained by the MEM method were less biased than the AR estimates, and thus the MEM spectral estimates were less biased than the AR estimates. The MSEs of the MEM spectra, however, were slightly larger than those of the AR spectra. Since the MSEs of the MEM coefficients were similar to the MSEs of the AR coefficients, on the average, it was probably the MSEs of the prediction error estimates of the MEM method that were larger than the MSEs of the AR method resulting in the larger observed MSEs of the MEM spectra.

The stationary FFT spectral estimates were less biased than the AR and MEM spectral estimates in the 10 and 15 Hz frequencies. The FFT estimates, however, are not directly comparable to the AR and MEM estimates, since the bias and MSE of each FFT estimate was calculated using the averaged, i.e., smoothed, theoretical value for the parameter. This was done so the FFT estimate would be more comparable to the actual spectral value of the entire band, rather than comparing the estimate to the spectral value only in one, or in each, of the contributing frequencies. Since the AR and MEM estimates were most biased in the 10 to 12 Hz frequency range and the biases of the estimates in the surrounding frequencies were much smaller, if these were averaged into the same frequency bands as were the FFT estimates, the resulting values would be very similar. Thus, although the estimates of the three methods appear very comparable from this viewpoint, the FFT estimates clearly suffer from lack of resolution.

Unsmoothed FFT estimates are biased, but as the degree of smoothing or averaging is increased to reduce this bias, the variability of the estimates also increases (e.g., Brillinger, 1981, pp. 136; Otnes & Enochson, 1972, pp. 215). Table 23 is a rearrangement of some previously presented FFT results, and shows that in the frequency bands where both spectra had larger values, primarily at 10 Hz, this theoretical result is empirically supported in this study for the spectra of both series, but not the coherence estimates. In the 0.5 second intervals, spectral estimates of both series were obtained by smoothing over three values; these estimates in the 10 Hz band had the largest biases but were the least variable. Upon increasing the intervals to 1.0 second, the estimates were smoothed over five values, and the resulting estimates were less biased but more variable than those obtained from 0.5 second intervals. Similarly, in the 2.0 second intervals, smoothing was over ten values and the bias of the 10 Hz estimates was reduced further while they became even more variable. Note that, however, this trend was not true where the spectra had low values; there both bias and variability decreased as smoothing increased.

For the 10 Hz FFT coherence estimate, both variability and bias decreased with more smoothing, although the variability of the 10 Hz spectral estimates increased with more smoothing in both series. This implies that investigators using coherence estimates obtained by the FFT method need be less concerned with their estimates becoming more variable as they increase the degree of smoothing.

In addition to the increased variability of the spectral estimates, the requirement to smooth the FFT estimates also has the disadvantage of lowering the resolution of the estimates, unless longer intervals or higher sampling rates can

Table 23

Bias and Variability (σ^2) of Stationary FFT Estimates as a Function of Smoothing

freq	Interval Length	Series 1		Series 2		Coherence	
		σ^2 x 100	Bias x 100	σ^2 x 100	Bias x 100	σ^2 x 100	Bias x 100
5	0.5*	0.26	6.22	0.06	2.80	4.94	50.06
	1.0**	0.04	1.64	0.02	0.94	3.83	46.90
	2.0***	0.01	0.62	0.00	0.22	3.58	30.68
10	0.5	2.19	-121.99	1.64	-80.42	3.94	-1.10
	1.0	23.57	-84.54	15.48	-55.50	2.79	0.44
	2.0	31.14	-66.47	21.56	-46.99	2.46	-0.64
15	0.5	0.05	-1.41	0.05	-2.69	2.43	5.81
	1.0	0.21	1.63	0.10	-0.95	2.22	6.09
	2.0	0.51	5.54	0.34	2.67	0.83	12.66
20	0.5	0.06	2.31	0.05	1.81	2.67	36.08
	1.0	0.03	1.26	0.01	1.02	2.95	28.73
	2.0	0.00	0.39	0.00	0.27	3.06	16.37

* Three (3) frequency estimates were smoothed to obtain the estimate for each frequency band.

** Five (5) frequency estimates were smoothed.

*** Ten (10) frequency estimates were smoothed.

be used for estimation. Increasing the interval length, however, increases the probability that the EEG record will be nonstationary (McEwen & Anderson, 1975), while care must be taken in increasing the sampling rate so that the assumption of statistical independence remains satisfied. It is unclear at what sampling rates the EEG data will become dependent. By far the majority of applied research has used sampling rates between 100 and 128 samples per second, although a few studies have used rates as high as 200 samples per second (e.g., Bromm & Scharein, 1982; Elul, 1969). In practice, the resolution versus smoothing issue must be settled according to the individual requirements and interests of the specific investigations, whether one requires high resolution or unbiased estimates.

The quality of the coherence estimates obtained by the AR and MEM methods depends only on the sample size and does not suffer from the lack of resolution as do the FFT estimates. As sample size increases, or as the intervals were lengthened using the same sampling rate as in this study, the estimates improve in all respects; they become less biased, less variable and have smaller MSEs. For stationary estimates, the MEM method preserved the shape of the coherence function better than the AR method in all interval lengths, although the MEM estimates were more biased in the tail regions of the coherence function.

Violations of the Stationarity Assumption

With some exceptions to be discussed below, the coherence estimates obtained in the nonstationary conditions differed very little from estimates of stationary series. It is possible that the simulated nonstationarities were not as severe as encountered in practice, although visually the original series did appear nonstationary. Figures of some of the simulated nonstationary original series are contained in the Appendix. The types of simulated nonstationarities were chosen to represent actual nonstationary activity observed in real EEG data. The transient sine wave added to the series may represent an EEG artifact such as an eyeblink that would be superimposed on actual ongoing EEG activity. Similarly, it may represent an event-related potential. The changes in the variance and distribution of the innovation errors may represent changes in cognitive activity, where the strength of the signal may change relative to the noise. The distribution of the innovation process can also change as cognitive activity changes. Anninos, Zenone, and Elul (1983) have shown in a simulated neural network that as the number of 'neurons' become more interconnected, the collective output becomes less Gaussian in distribution, but not when the distribution of individual neurons is changed.

The coherence peak was estimated accurately by all three estimation methods in all nonstationary conditions. As expected, and as in the stationary conditions, the estimates from the shortest segments were always relatively worse, and generally the longest segments' estimates were the best in all respects. Usually estimates in the tails of the coherence function were affected most by the nonstationarities. Although some of these tail effects will be discussed for the purposes of more general estimates, it is unclear whether the effects of some of the nonstationarities in the more extreme frequencies would be similar had there been spectral peaks in these frequencies. This may imply that coherences may only be useful or meaningful when at least one of the individual spectra contains some power (e.g., Gotman, 1983). In the present study, this power was contained only in the 8 to 14 Hz frequencies, and the more extreme frequencies contained no power.

The frequency of the added sine wave was about 3 Hz, since the wave lasted over forty of the data points at the sampling rate of 128 per second. When it was added only to one series, it was accurately detected in the spectra of that series, but the AR and MEM estimates of the coherence function showed only a relatively negligible peak around the 3 Hz frequency. When the sine wave was added to both series, however, all three methods estimated a coherence peak in the 3 Hz frequency region which was larger than the the true peak at 12 Hz. Although the biases and MSEs of these low frequency estimates were very large, their variabilities were much smaller than those of the stationary estimates at

3 Hz since the added sine waves themselves lacked the presence of noise.

Whether the sine wave was added to only one series or both, the MEM coherences in the low, 1 to 5 Hz, frequency region were more sensitive to these nonstationarities - the estimates were more biased, more variable and with much larger MSEs than the low frequency AR estimates. The MSEs of the FFT estimates were similar to those of the MEM estimates; however, when the sine wave was added to one series only, the effect on the bias of the FFT coherence estimates was negligible.

These results seem to indicate that the coherence estimates are relatively unaffected by transients when these occur in one of the series, or perhaps even if each series contains a transient but of different frequencies. If both series, however, contain a transient of the same or similar frequency, the coherence estimate at that frequency may be very inaccurate. Thus, for example, if low frequency eyeblinks occurred in the EEG of frontal derivations, the estimate of the coherence function between the frontal and the occipital derivations would remain relatively accurate, while the estimate of the coherences between the two frontal derivations may be adversely affected at the low frequencies but the coherence estimates of the shared alpha or beta activities between each derivation may remain unaffected. This implies that practitioners need not be overly concerned about low frequency artifacts affecting coherence estimates in the frequency bands of psychological interest.

Since the sine wave contributed only a 3 Hz frequency component to the series, the estimates in the 12 Hz peak region were not affected. Had the sine wave been of a higher frequency such as 10 Hz, however, or the true spectra contained peaks in the low frequencies, for example, delta activity occurring in a pathological case, the added sine wave would have significantly handicapped those spectral and coherence estimates, especially if both series contained interference in the same frequencies. The coherence estimates may not be significantly affected by these types of nonstationarities if their frequency components differ in both series and occur where the spectra contain little power, since in this case even though one spectrum may have large values, the cross spectrum would be small and thus the coherence estimate would also remain small. If the transient added power to one spectrum at frequencies where some power existed in the signal, it is unclear how adversely the coherence estimates would be affected. The effects would probably depend on the amplitude of the added nonstationarity and would be less damaging in one series than if both series were thus affected. Further studies would be required to test these conditions.

Increasing the variance of the normally distributed error of the series from $S=\begin{bmatrix}1 & 0\\ 0 & 1\end{bmatrix}$ to $S=\begin{bmatrix}9 & 0\\ 0 & 9\end{bmatrix}$ at the halfway point in each of the different interval lengths also increased the bias and MSE of the AR and MEM estimates in all frequencies, as compared to their stationary estimates from segments of the same length. At the extremes of the coherence function, the MEM nonstationary estimates had larger MSEs and were more biased than the AR estimates, while in the peak region the MSEs and biases of the MEM estimates were smaller than those of the AR estimates. Varying the segment length and the proportion of nonstationary data increased the bias of the AR and MEM estimates further; for example, in the 1.0 second intervals, eventhough only one quarter of each interval was simulated with $S=\begin{bmatrix} 9 & 0 \\ 0 & 9 \end{bmatrix}$, the bias of the resulting estimates was greater in all frequencies than when half of the interval contained such data. Also, in the 2.0 second segments, as the proportions of the nonstationary data decreased from one half to one eighth, the MSE and variability of the AR and MEM estimates did not decrease as may have been expected. In fact, although the differences in estimates from these conditions were quite small, the least biased estimates and smallest MSEs were obtained when one half of the data was nonstationary.

One explanation for these differences may be sampling variability, since in each nonstationary condition the estimates in the peak region, and for the most part in the other frequencies as well, were within one standard error of the parameter values. But the standard errors of the coherence estimates were also larger when less of the interval was nonstationary. It seem that a smaller amount of nonstationary contamination may have more of an adverse effect than when the system has a longer time to adjust to the new activity. It would be expected that as more of the original series was replaced, the new activity would dominate and the original series would become the contamination. Under these conditions, when the innovation variance is changed, the most stable estimates would be obtained when exactly each half of the series consisted of one 'type' of data. The results of the present study support this interpretation. Further studies, however, would be required to determine what would happen if the variance of the innovation process was changed more than once in the interval, or was of a continuously evolving nature. These latter conditions may be more characteristic of EEG. As a first indication, however, the results of the present study suggest that the AR and MEM methods are slightly more sensitive to the presence of smaller amounts of contaminating activity than when half of the entire interval contains 'different' data.

In contrast to the AR and MEM estimates, the FFT coherence estimates were affected very little by changing the variance at any point in the interval. Regardless of the amount of nonstationary data, these estimates were very similar to each other as well as to the estimates from stationary series. This nonstationarity seemed to affect primarily the 5 Hz FFT estimate of the shortest interval length; the remaining estimates remained relatively unaffected. It is possible that the change in the variance of the innovation process halfway in the interval may have very roughly resembled a 1 Hz frequency activity, which the FFT method would average into the 5 Hz estimate of the 0.5 second interval but not into the estimates of the 1.0 and 2.0 second intervals.

The FFT coherence estimates were also quite robust to changes in the distribution of the error from Gaussian to exponential halfway through one or both series. But particularly when both series were nonstationary, these estimates were almost identical to the stationary estimates. From the AR and MEM estimates it was observed that it was the low frequencies, one to about five Hz, that were affected most by this type of nonstationarity. The largest mean estimates, and also the ones with the largest bias and MSEs, were obtained at the 1 Hz frequency and decreased to a local minimum at around 6 Hz. The 5 Hz bands of the FFT estimates were not affected as much as the AR and MEM estimates since in smoothing the FFT estimates, the low frequencies corresponding to 1 and 2 Hz were not averaged into the band estimate of the longer intervals.

In the 12 Hz coherence peak region, both the AR and MEM estimates containing some exponentially distributed error were more biased than the stationary estimates, but interestingly these estimates of the peak were less biased when both series were nonstationary than when only one series was changed. As in the stationary segments, in both these nonstationary conditions the MEM peak estimates were less biased than the AR peak estimates. In the extreme frequencies, the reverse was true; the AR estimates were less biased than the MEM estimates, and also both AR and MEM estimates in these frequencies were more biased when both series were nonstationary than when only one series was affected. In the extremes, the spectra estimate only noise. When the noise is not distributed normally with zero mean and the identity variance-covariance matrix, as was used in calculating the theoretical spectra, but also contains some exponentially distributed errors which are all positive values, higher spectral values are then detected in both series. Consequently, the estimated coherences are greater than the parameters resulting in greater positive bias. As intervals were lengthened, the AR and MEM estimates in the extremes became more biased, particularly at 1 Hz, as more exponentially distributed error was present. It is interesting to note that some EEG spectra reported in past studies (e.g., Bohlin, 1977) had a similar shape, with very large values at 1 Hz and decreasing rapidly for the next frequencies, which may indicate that EEG in some cases contains exponentially distributed activity.

The FFT method was notably robust to exponentially distributed error. Even when the distribution of the innovation process was changed to exponential with a mean of five halfway in the interval such that the AR and MEM estimates were quite biased in most frequencies, the FFT coherence estimates were similar to estimates obtained from Gaussian and stationary data.

In developing robust methods for parametric time series analysis, Martin (1981; Kleiner et al., 1979) considers two models of outliers that may be encountered. One is the additive outlier model, the second involves innovation outliers. To define these models, consider the general AR univariate model

$$y(t)=\{\sum_{k=1}^{p} a(k)\ y(t-k)+e(t)\}+v(t).$$

If the innovation process, $e(t)$, is Gaussian and $v(t)\neq 0$ for some proportion of the interval, $v(t)$ is defined as the additive outlier, while if $v(t)=0$ for all t and $e(t)$ is not normally distributed, an innovation outlier model results. In the present study, the addition of a transient sine wave to the simulated EEG corresponds to an additive outlier model, while conditions that changed the variance or the distribution of $e(t)$ represent innovation outlier models.

Although Martin considers outliers that are somewhat structurally simpler than the ones used in this study, he does illustrate how differently the additive versus innovation outliers affect the least square estimates of the model parameters, a(k), k=1,...,p (Martin, 1981). The additive outlier has much more severe effects on the least squares estimates than the innovation outlier. The innovation outlier has to be large compared to the scale of the innovation process in order to have serious effects on the spectral estimates (Kleiner et al., 1979).

In the present study, when the variance of the Gaussian innovation process was increased in the interval or when its distribution was changed from normal to exponential, the innovations were not so extreme as to greatly affect the estimates. The transient sine wave added to the series had larger effects on the spectra than the other nonstationarities introduced, but the effect on coherence estimates when the sine wave additive outliers were present was much smaller than on the spectral estimates if the transient was present only in one series. It would be of interest to compare the effects of a transient sine wave added to the series as in this study with the effects of the transient occurring in the innovation process, and to see if the results of Kleiner et al. (1979) generalize from spectral estimates to coherence estimates. From the results of this study, the coherence estimates seem more robust to the additive-type outliers than the spectral estimates.

Violations of the Normality Assumption

From the one condition in which both series were simulated from only exponentially distributed innovations in both series, it appears that all three methods of estimation may be more robust to violations of normality, than to violations of nonstationarity, at least as far as coherence estimates are concerned. All three estimation methods produced estimates that were practically identical to those obtained where the innovations were entirely Gaussian and stationary.

Recommendations for Coherence Estimation in Practice

The results of the present study seem to indicate that, in general, coherence estimates are relatively robust when data do not satisfy underlying assumptions of stationarity and normally distributed error.

For stationary data, Jones' (1978) MEM method appears slightly better than the classical AR model fitting, both in preserving the overall shape of the coherence function and in obtaining accurate estimates of coherence values in the regions where spectra have larger values. It also has computational advantages since it employs triangular decomposition rather than matrix inversion as in the usual methods of AR estimation. For bivariate series matrix inversion is a minor disadvantage, but for a larger number of series which are often encountered in practice, this may prove to be a significant disadvantage. The AR procedure might be made more efficient by incorporating the same numerical methods as were used by the MEM method, for example, by using the Cholesky decomposition of positive definite matrices, to avoid matrix inversion.

The FFT method appears very adequate for estimating coherences, even in relatively short intervals of 1.0 second, if high resolution is not required. For non-Gaussian data, it appears to be the method of choice. If finer resolution is desirable, or if interval lengths are very short, of sample size of less than, say, 100, then the AR and MEM methods are preferrable, unless ensemble averaging is possible for the FFT estimates.

In terms of the nonstationarities tested, all three methods perform well. The MEM method is slightly more sensitive to all three types of nonstationarities tested than is the AR method over the entire curve, but again the MEM method is marginally better in estimating the coherences in the peak region of the coherence function. Thus if coherence estimates of the entire curve are required, the AR method will give overall slightly less biased estimates for data types similar to those examined in this study. If more precise estimates in the high power region are important, then the MEM method may be preferrable. But the differences in the estimates of the two methods are small, and the two methods do perform almost identically under the same conditions.

The FFT coherence estimates are practically unaffected by the nonstationarities tested in this study. Only when the transient sine wave was added to both series are these estimates significantly worsened. Thus probably in the majority of cases, investigators can feel relatively secure in using the FFT method even when the series are nonstationary. But, as with the stationary estimates, the FFT method performs less well than the AR and MEM methods on data from very short, less than about 100 data points, intervals.

REFERENCES

Akaike, H. (1969a). Fitting autoregressive models for prediction. _Annals of the Institute of Statistical Mathematics_, _21_, 243-247.

Akaike, H. (1969b). Power specrum estimation through autoregressive model fitting. _Annals of the Institute of Statistical Mathematics_, _21_, 407-419.

Akaike, H. (1971). Autoregressive model fitting for control. _Annals of the Institute of Statistical Mathematics_, _23_, 163-180.

Akaike, H. (1973). Maximum likelihood identification of Gaussian autoregressive moving average model. _Biometrika_, _60_, 255-265.

Andersen, N. (1974). On the calculation of filter coefficients for maximum entropy spectral analysis. _Geophysics_, _39_, 69-72.

Anninos, P., Zenone, S., & Elul, R. (1983). Artificial neural nets: Dependence of the EEG amplitude's probability distribution on statistical parameters. _Journal of Theoretical Biology_, _103_, 339-348.

Athans, M. (1974). The importance of Kalman filtering methods for economic systems. _Annals of Economic and Social Measurement_, _3_, 49-64.

Barlow, J. S. (1979). Computerized clinical electroencephalography in perspective. _IEEE Transactions on Biomedical Engineering_, _BME-26_, 377-391.

Bendat, J. S., & Piersol, A.G. (1971). _Random data: Analysis and measurement procedures_. New York: John Wiley & Sons.

Bernstein, A.S., Taylor, K.W., Starkey,P., Lubowsky,J. Juni, S. & Paley, H. (1983). The effects of prolonged stimulus repetition on autonomic response and EEG activity in normal subjects, schizophrenic, and nonschizophrenic patients. _Psychophysiology_, _20_, 332-342.

Bierman, G. J. (1977). _Factorization methods for discrete sequential estimation_. New York: Academic Press.

Blackman, R. B., & Tukey, J. W. (1958). The measurement of power spectra from the point of view of communications engineering. New York: Dover.

Bloomfield, P. (1976). Fourier analysis of time series analysis: An introduction. New York: Wiley.

Bohdanecky, Z., Lansky, P., & Radil, T. (1982). An integral measure of the coherence function between pairs of EEG recordings. Electroencephalography and Clinical Neurophysiology, 54, 587-590.

Bohlin, T. (1977). Analysis of EEG signals with changing spectra using a short-word Kalman estimator. Mathematical Biosciences, 35, 221-259.

Boddy, J. (1981). Evoked potentials and the dynamics of language processing. Biological Psychology, 13, 125-140.

Bowling, P.S., & Bourne, J.R. (1978). Discriminant analysis of electroencephalograms recorded form renal patients. IEEE Transactions on Biomedical Engineering, BME-25, 12-17.

Box, G. E. P., & Jenkins, G. M. (1976). Time series analysis: Forecasting and control. Rev. Ed. San Francisco: Holden-Day.

Brillinger, D.R. (1981). Time series: Data analysis and theory. San Francisco: Holden-Day.

Bromm, B., & Scharein, E. (1982). Principal component analysis of pain-related cerebral potentials to mechanical and electrical stimulation in man. Electroencephalography and Clinical Neurophysiology, 53, 94-103.

Brown, R.L., Durbin, J., & Evans, J.M. (1975). Techniques for testing the constancy of regression relationships over time, with comments. Journal of the Royal Statistical Society, Series B, 37, 149-192.

Burg, J.P. (1967). Maximum entropy spectral analysis. In Proceedings of the 37th Meeting of the Society of Exploration Geophysicists.

Busk, J., & Galbraith, G. C. (1975). EEG correlates of visual-motor practice in man. Electrencephalography and Clinical Neurophysiology, 38, 415-422.

Chan, Y. T., & Miskowicz, R. K. (1984). Estimation of coherence and time delay with ARMA models. IEEE Transactions on Acoustics, Speech, and Signal Processing, ASSP-32, 295-303.

Clarke, D. W. (1980). Some implementation considerations of self-tuning controllers. In F. Archetti & M. Cugiani (Eds.), Numerical techniques for stochastic systems (pp.81-110). North-Holland.

Cooley, J.W., & Tukey, J.W. (1965). An algorithm for the machine calculation of complex Fourier series. Mathematics of Computation, 19, 297-301.

Dafny, N. (1983). Interferon modifies EEG and EEG-like activity recorded from sensory, motor and limbic system structures in freely behaving rats. Neurotoxicology, 4, 235-240.

Devlin, S. J., Gnanadesikan, R., & Kettenring, J.R. (1981). Robust estimation of dispersion matrices and principal components. Journal of the Americal Statistical Association, 76, 354-362.

Douglas, R. R., & Rogers, L. J. (1983). Comparative factor analysis models for an empirical study of EEG data. International Journal of Neuroscience, 18, 211-226.

Duncan, D. B., & Horn, S. D. (1972). Linear dynamic recursive estimation from the viewpoint of regression analysis. Journal of the Americal Statistical Association, 67, 815-821.

Durbin, J. (1960). The fitting of time series models. Rev. Int. Inst. Stat., 28, 233-244.

Elul, R. (1969). Gaussian behavior of the electroencephalogram: Changes during performance of mental tasks. Science, 164, 328-331.

Garbade, K. (1977). Two methods for examining the stability of regression coefficients. Journal of the American Statistical Association, 72, 54-63.

Gasser, T., Bacher, P., & Mocks, J. (1982). Transformations towards the normal distribution of broad band spectral parameters of the EEG. Electroencephalography and Clinical Neurophysiology, 53, 119-124.

Gersch, W. (1970). Spectral analysis of EEGs by autoregressive decomposition of time series. Mathematical Biosciences, 7, 205-222.

Gersch, W., & Sharpe, D. R. (1973). Estimation of power spectra with finite-order autoregressive models. IEEE Transactions on Automatic Control, AC-18, 367-369.

Gersch, W., & Yonemoto, J. (1977). Parametric time series models for multivariate EEG analysis. Computers and Biomedical Research, 10, 113-125.

Gevins, A. S. (1983). Brain potential evidence for lateralization of higher cognitive functions. In J. B. Hellige (Ed.), Cerebral hemisphere asymmetry: Method, theory and application (pp.). New York: Praeger.

Gevins, A.S., Doyle, J.C., Schaffer, R.E., Callaway, E., & Yeager,C. (1980). Lateralized cognitive processes and the electroencephalogram. Science, 207, 1006-1007.

Gevins, A.S., Yeager, C.L., Diamond, S.L., Spire, J.P., Zeitlin, G.M., & Gevins, A.H. (1975). Automated analysis of the electrical activity of the human brain (EEG): A progress report. Proceedings of the IEEE, 1382-1399.

Gevins, A.S., Yeager, C.L., Zeitlin, G.M., Ancoli, S., & Dedon, M.F. (1977). On-line computer rejection of EEG artifact. Electroencephalography and Clinical Neurophysiology, 42, 267-274.

Gevins, A.S., Zeitlin, G.M., Ancoli, S., & Yeager, C.L. (1977). Computer rejection of EEG artifact. II. Contamination by drowsiness. Electroencephalography and Clinial Neurophysiology, 42, 31-42.

Gevins, A.S., Zeitlin, G.M., Doyle, J.C., Yingling, C.D., Schaffer, R.E., Callaway, E., & Yeager, C.L. (1979). Electroencephalogram correlates of higher cortical functions. Science, 203, 665-668.

Gevins, A.S., Zeitlin, G.M., Doyle, J.C., Schaffer, R.E., & Callaway, E. (1979). EEG patterns during 'cognitive' tasks. II. Analysis of controlled tasks. Electroencephalography and Clinical Neurophysiology, 47, 704-710.

Gevins, A.S., Zeitlin, G.M., Yingling, C.D., Doyle, J.C., Dedon, M.F., Schaffer,, R.E., Roumasset, J.T., & Yeager, C.L. (1979). EEG patterns during 'cognitive' tasks. I. Methodology and analysis of complex behaviors. Electroencephalography and Clinical Neurophysiology, 47, 693-703.

Gliner, J.A., Mihevic, P.M., & Horvath, S.M. (1983). Spectral analysis of electroencephalogram during perceptual-motor learning. Biological Psychology, 16, 1-13.

Gotman, J. (1981). Interhemispheric relations during bilateral spike-and-wave activity. Epilepsia, 22, 453-465.

Gotman, J. (1983). Measurement of small time differences between EEG channels: Method and application to epileptic seisure propagation. Electroencephalography and Clinical Neurophysiology, 56, 501-514.

Guyton, A. C. (1981). Textbook of medical physiology (6th ed.) (pp. 675-680). Philadelphia: W.B. Saunders.

Harrison, P. J., & Stevens, C. F. (1976). Bayesian forcasting. Journal of the Royal Statistical Society, Series B, 38, 205-247.

Herning, R. I., Jones, R. T., & Bachman, J. (1983). EEG changes during tobacco withdrawal. Psychophysiology, 20, 507-512.

Isaksson, A., & Wennberg, A. (1976). Spectral properties of nonstationary EEG signals, evaluated by means of Kalman filtering: Application examples from a vigilance test. In P. Kellaway & I. Petersen (Eds.), Quantitative analytic studies in epilepsy (pp.389-402). New York: Raven Press.

Jansen, B.H., Bourne, J.R., & Ward, J.W. (1981). Autoregressive estimation of short spectra for computerized EEG analysis. IEEE Transactions on Biomedical Engineering, BME-28, 630-638.

John, E.R., Karmel, B.Z., Corning, W.C., Easton, P., Brown, D., Ahn, H., John, M., Harmony, T., Prichep, L., Toro, A., Gerson, I., Bartlett, F., Thatcher, R., Kaye, H., Valdes, P., & Schwartz, E. (1977). Neurometrics: Numerical taxonomy identifies different profiles of brain functions within groups of behaviorally similar people. Science, 196, 1393-1410.

Johnson, T.L., Wright, S.C., & Segall, A. (1979). Filtering of muscle artifact from the electroencephalogram. IEEE Transactions of Biomedical Engineering, BME-26, 556-563.

Jones, R.H. (1974). Identification and autoregressive spectrum estimation. IEEE Transactions on Automatic Control, AC-19, 894-897.

Jones, R. H. (1978). Multivariate autoregression estimation using residuals. In D. F. Findley (Ed.), Applied time series analysis (pp.139-162). New York: Academic Press.

Kalman, R. E. (1960). A new approach to linear filtering and prediction problems. Journal of Basic Engineering, 82, 34-45.

Kalman, R. E., & Bucy, R. S. (1961). New results in linear filtering and prediction theory. Journal of Basic Engineering, 83, 95-108.

Keene, D.L., Metrakos, K., Belmonte, M., Watters, G.V., & Singer, S. (1983). EEG abnormalities and convulsions in juvenile diabetes mellitus. Canadian Journal of Neurological Sciences, 10, 198-199.

Kleiner, B., Martin, R.D., & Thomson, D.J. (1979). Robust estimation of power spectra. Journal of the Royal Statistical Society, Series B, 41, 313-351. Levinson, H., & Wiener, N. (1949). Extrapolation, interpolation and prediction of stationary time series. New York: Wiley.

Martin, R. D. (1981). Robust methods for time series. In D. F. Findley (Ed.), Applied time series analysis II (pp.683-759). New York: Academic Press.

McClellan, J. H. (1981). Multidimensional spectral estimation. In Proceedings of the first ASSP workshop on spectral estimation (pp. 3.1.1-3.1.10).

McEwen, J.A., & Anderson, G.B. (1975). Modeling the stationarity and Gaussianity of spontaneous electroencephalographic activity. IEEE Transactions on Biomedical Engineering, BME-22, 361-369.

Meinhold, R. J., & Singpurwalla, N. D. (1983). Understanding the Kalman filter. The American Statistician, 37, 123-127.

Morstyn, R., Duffy, F.H., & McCarley, R.W. (1983). Altered topography of EEG spectral content in schizophrenia. Electroencephalography and Clinical Neurophysiology, 56, 263-271.

Otnes, R.K., & Enochson, L. (1972). Digital time series analysis. New York: John Wiley & Sons.

Pfurtscheller, G., & Haring, G. (1972). The use of an EEG autoregressive model for the time-saving calculation of spectral power density distributions with a digital computer. Electroencephalography and Clinical Neurophysiology, 33, 113-115.

Pigeau, R. A., Hoffmann, R. F., & Moffitt, A. R. (1981). A multivariate comparison between two EEG analysis techniques: Period analysis and Fast Fourier transform. Electroencephalography and Clinical Neurophysiology, 52, 656-658.

Pollock, V.E., Volavka, J., Goodwin, D.W., Mednick, S.A., Gabrielli, W.F., Knop, J., & Schulsinger, F. (1983). The EEG after alcohol administration in men at risk for alcoholism. Archives of General Psychiatry, 40, 857-861.

Reilly, E. L. (1976). Neuropharmacology and the EEG. American Journal of EEG Technology, 16, 99-108.

Rosenberg, B. (1973). The analysis of a cross section of time series by stochastically convergent parameter regression. Annals of Economic and Social Measurement, 2, 399-428.

Sawaragi, Y., Soeda, T., & Nakamizo, T. (1981). 'Classical' methods and time series estimation. In P. Eykhoff (Ed.), Trends and progress in system identification (chapter 3). Oxford: Pergamon Press.

Schaffer, C. E., Davidson, R. J., & Saron, C. (1983). Frontal and parietal electroencephalogram asymmetry in depressed and nondepressed subjects. Biological Psychiatry, 18, 753-761.

Selin, C.L., & Gottschalk, L.A. (1983). Schizophrenia, conduct disorder and depressive disorder: Neuropsychological, speech sample and EEG results. Perceptual and Motor Skills, 57, 427-444.

Shaw, J.C., Colter, N., & Resek, G. (1983). EEG coherence, lateral preference and schizophrenia. Psychological Medicine, 13, 299-306.

Shepherd, R., & Gale, A. (1982). EEG correlates of hemisphere differences during a rapid calculation task. British Journal of Psychology, 73, 73-84.

Siegel, A., Grady, C. L., & Mirsky, A. F. (1982). Prediction of spike-wave bursts in Absence epilepsy by EEG power spectrum signals. Epilepsia, 23, 47-59.

Swenson, R.A., & Tucker, D.M. (1983). Multivariate analysis of EEG coherence: Stability of the metric, individual differences in patterning and response to arousal. Biological Psychology, 17, 59-75.

Ulrych, T., & Bishop, T.N. (1975). Maximum entropy spectral analysis and autoregressive decomposition. Review of Geophysics and Space Physics, 13, 183-200.

Walter, D.O. (1963). Spectral analysis of electroencephalograms: Mathematical determination of neurophysiological relationships from records of limited duration. Experimental Neurology, 8, 155-181.

Wennberg, A., & Isaksson, A. (1976). Simulation of nonstationary EEG signals as a means of objective clinical interpretation of EEG. In P. Kellaway & I. Petersen (Eds.), Quantitative analytic studies in epilepsy. (pp.493-508). New York: Raven Press.

Whittle, P. (1963). On the fitting of multivariate autoregressions and the approximate canonical factorization of a spectral density matrix. Biometrika, 50, 129-134.

Woestenburg, J.C., Verbaten, M.N., & Slangen, J.L. (1983). The removal of the eye-movement artifact from the EEG by regression analysis in the frequency domain. Biological Psychology, 16, 127-147.

Woods, J. W., & Radewan, C. H. (1977). Kalman filtering in two dimensions. IEEE Transactions on Information Theory, IT-23, 473-482.

FOOTNOTES

[1] This proceduree was suggested independently by Morf, Vierra, and Kailath (1976) -- unpublished manuscript. ILS Stanford University -- and by Robinson (1976) -- personal communication -- both of which were referenced as such in Jones (1978).

[2] One possible method of testing the significance of coefficient variation is that of variable parameter regression (Athans, 1974; Rosenberg, 1973). Garbade (1977) found this method more powerful in rejecting a false null hypothesis of coefficient stability than the tests proposed by Brown, Durbin, and Evans (1975).

APPENDIX

This appendix contains the graphs of the original series for selected nonstationary conditions. Note the change of scale on the vertical axes. The arrows indicate where the nonstationarity was present.

Figure 30. Raw data of series 1 simulated by the AR(7) model with noise variance changed from $\begin{bmatrix} 1 & 0 \\ 0 & 1 \end{bmatrix}$ to $\begin{bmatrix} 9 & 0 \\ 0 & 9 \end{bmatrix}$ at time t=64.

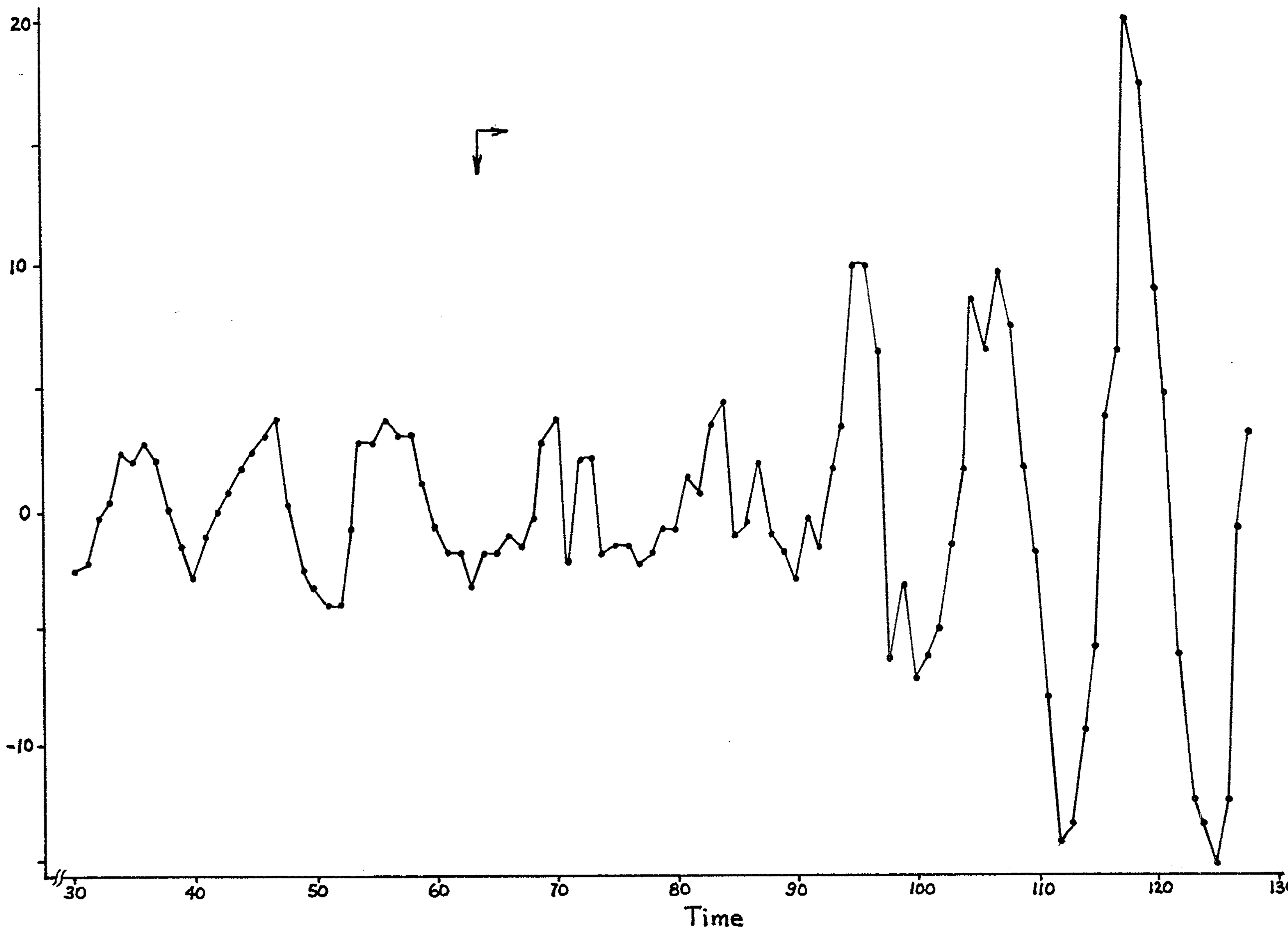

20
10
0
-10
30
40
50
60
70
80
90
100
110
120
130
Time

Figure 31. Raw data of series 2 simulated by the AR(7) model with noise variance changed from $\begin{bmatrix}1 & 0\\0 & 1\end{bmatrix}$ to $\begin{bmatrix}9 & 0\\0 & 9\end{bmatrix}$ at time t=64.

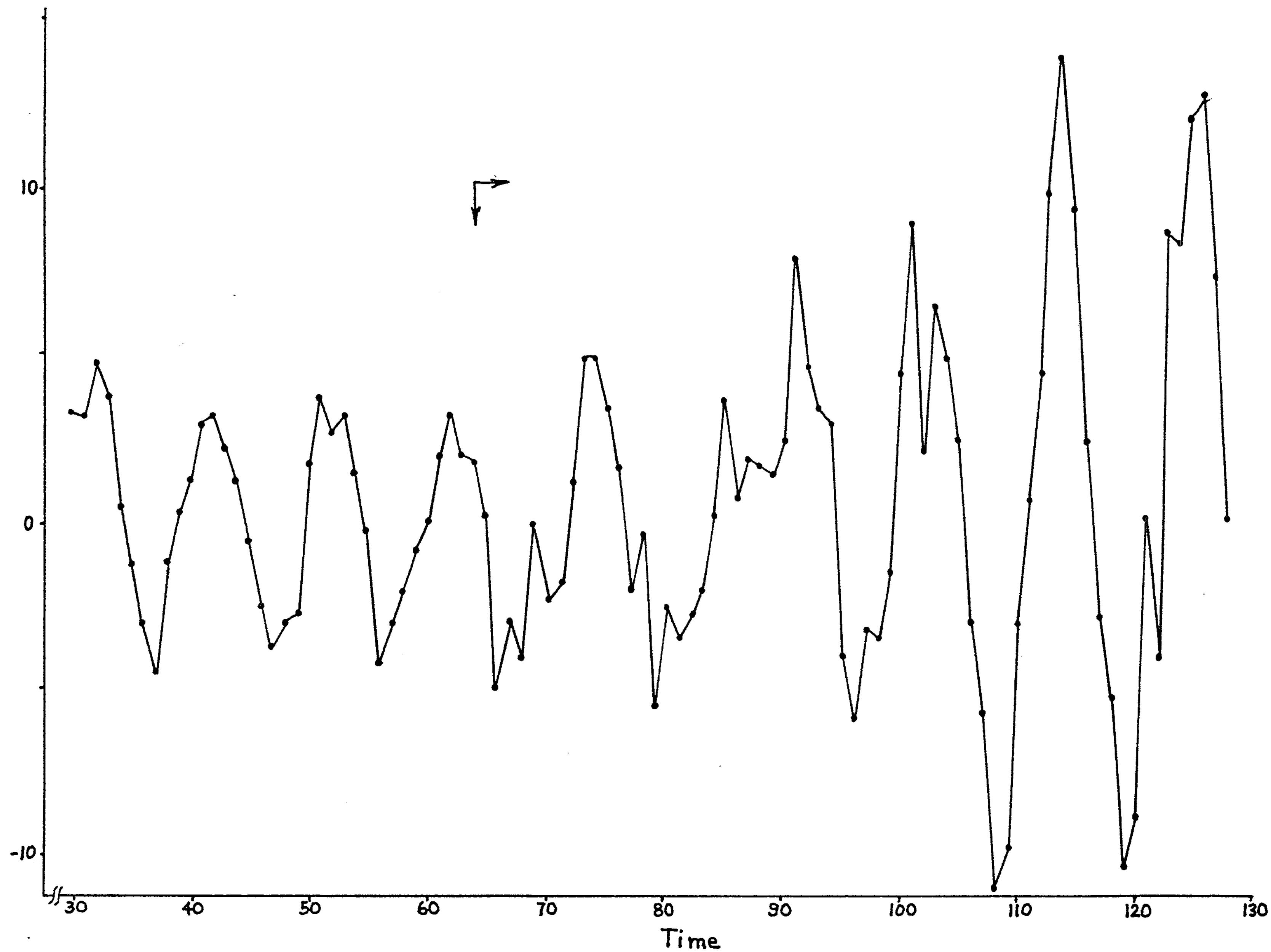
10
0
-10
30
40
50
60
70
80
90
100
110
120
130
Time

Figure 32. One series of raw data simulated by the AR(7) model to which a sine wave of amplitude 8 was added from time t=19 to t=59.

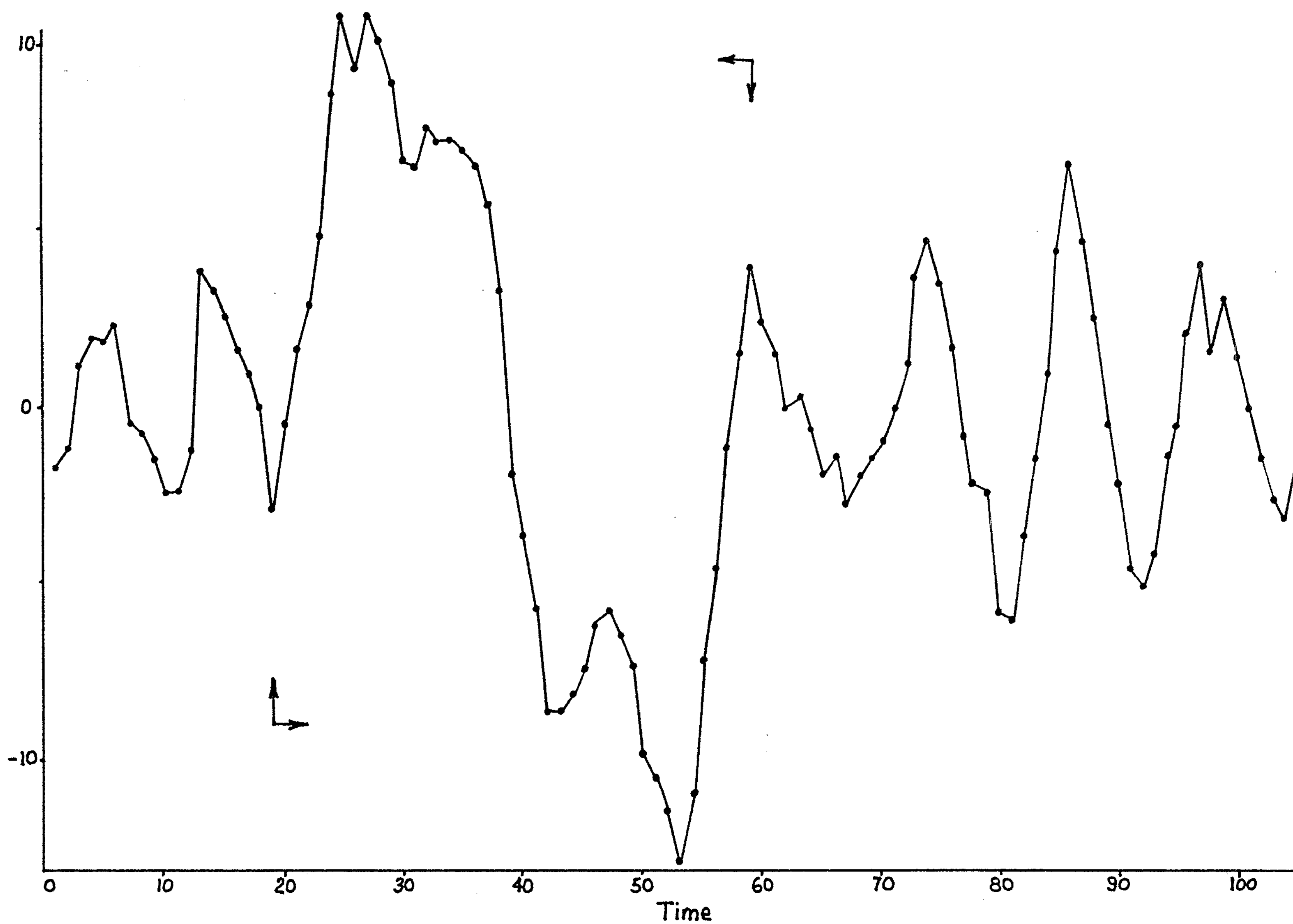

10
0
-10
0
10
20
30
40
50
60
70
80
90
100
Time

Figure 33. Raw data of series 1 simulated by the AR(7) model with the noise distributed N(0,I) for time t=1 to t=64, and distributed exponentially with mean=2.0 for time t=65 to t=128.

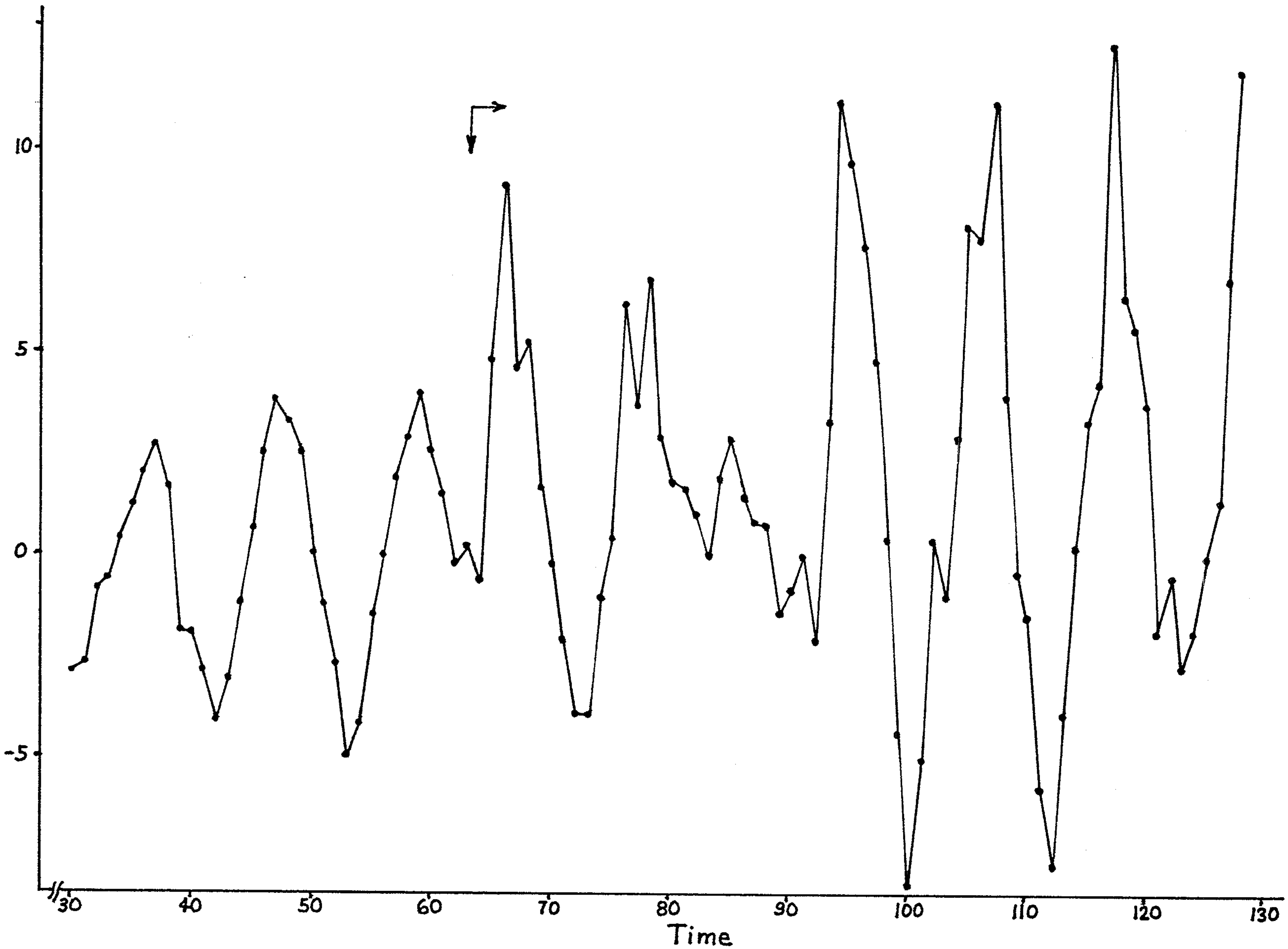

10
5
0
-5
30
40
50
60
70
80
90
100
110
120
130
Time

Figure 34. Raw data of series 2 simulated by the AR(7) model with the noise distributed N(0,I) for time t=1 to t=64, and distributed exponentially with mean=2.0 for time t=65 to t=128.

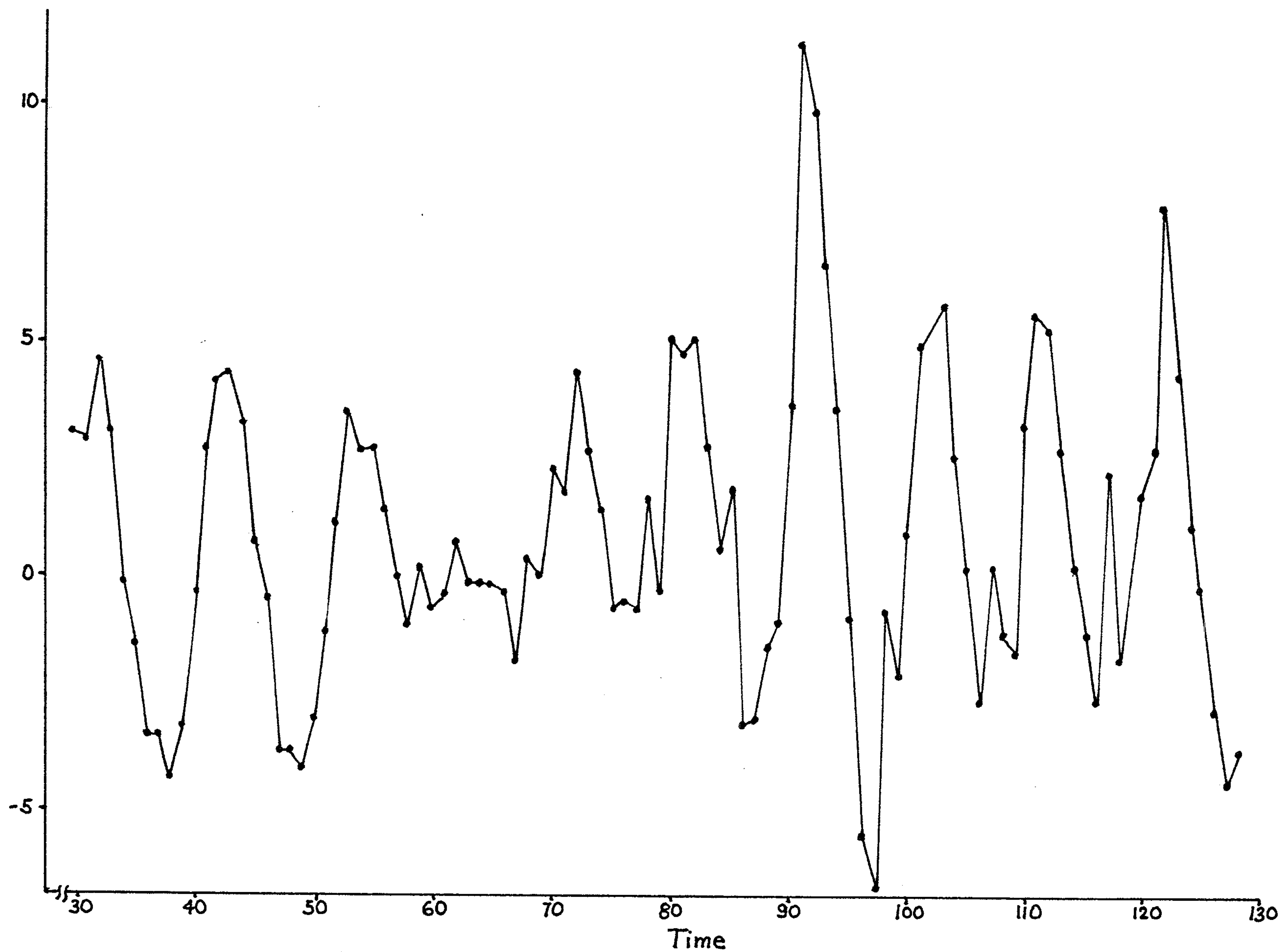
10
5
0
-5
30
40
50
60
70
80
90
100
110
120
130
Time

Figure 35. Raw data of series 1 simulated by the AR(7) model with exponentially distributed noise in both series for the entire duration of the series.

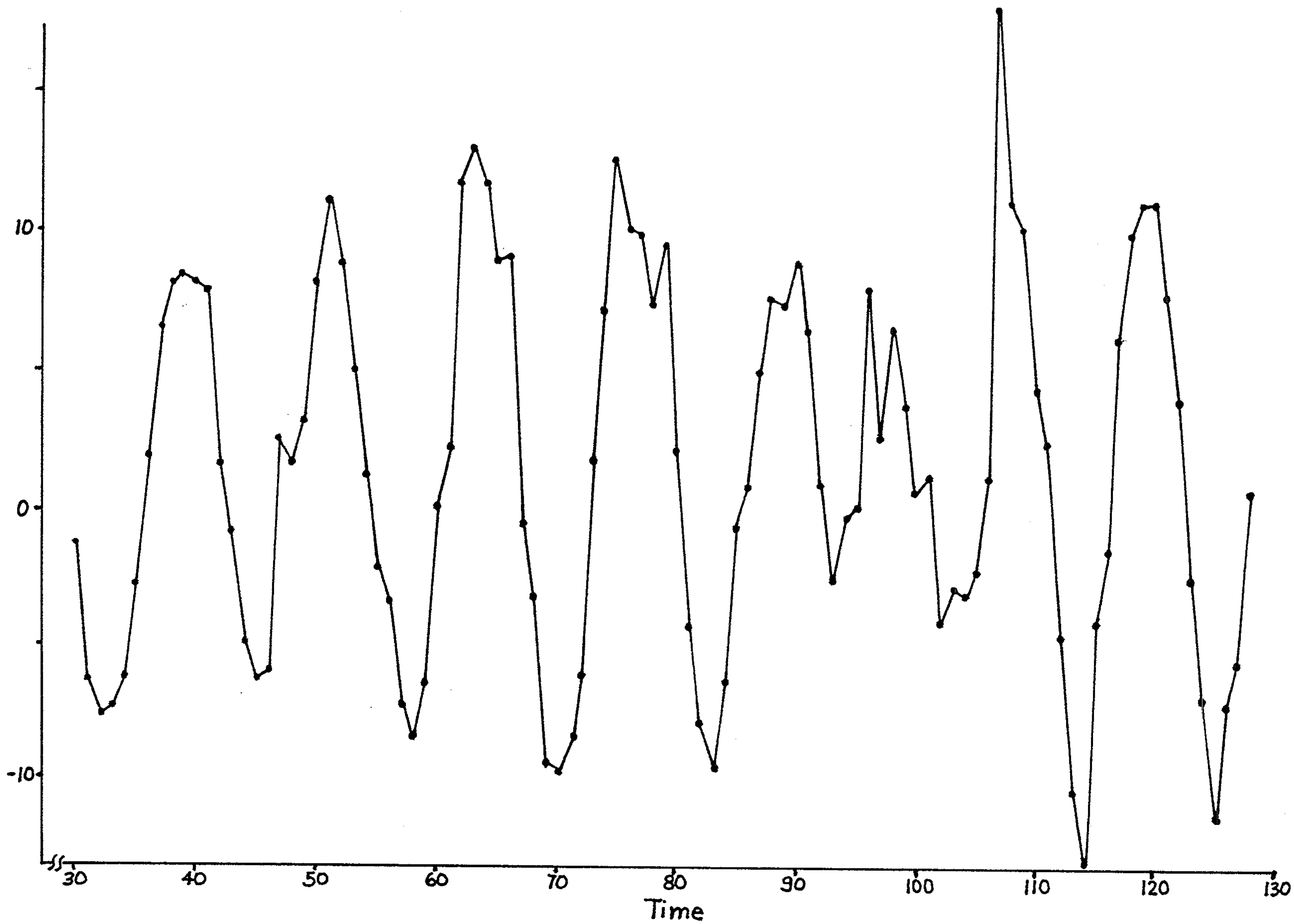

10
0
-10
30
40
50
60
70
80
90
100
110
120
130
Time

Figure 36. Raw data of series 2 simulated by the AR(7) model with exponentially distributed noise in both series for the entire duration of the series.

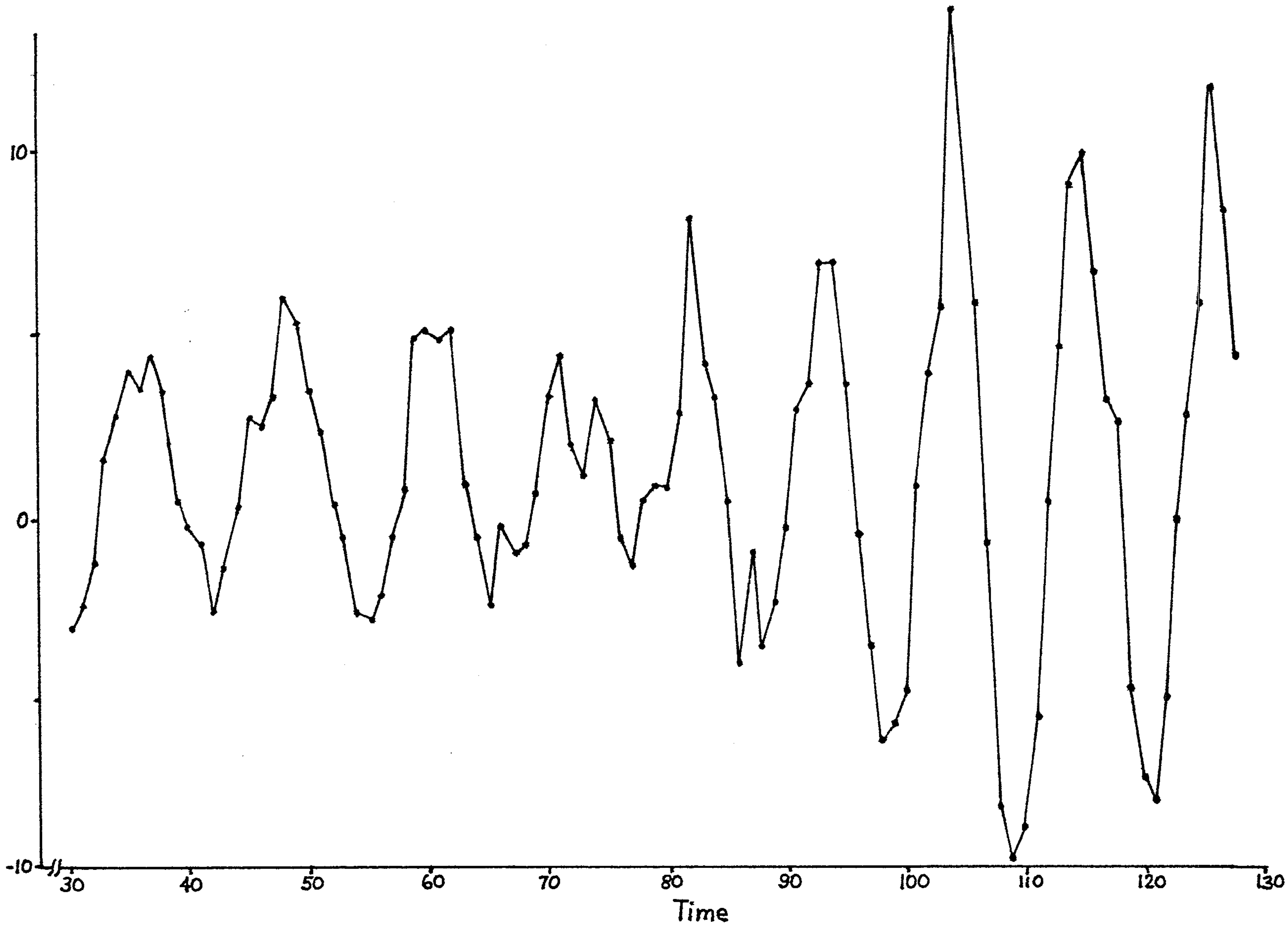

10
0
-10
30
40
50
60
70
80
90
100
110
120
130
Time

<u>Figure 37.</u> Raw data of series 1 with the noise distribution changed from normal to exponential with mean=5.0 at time t=65.

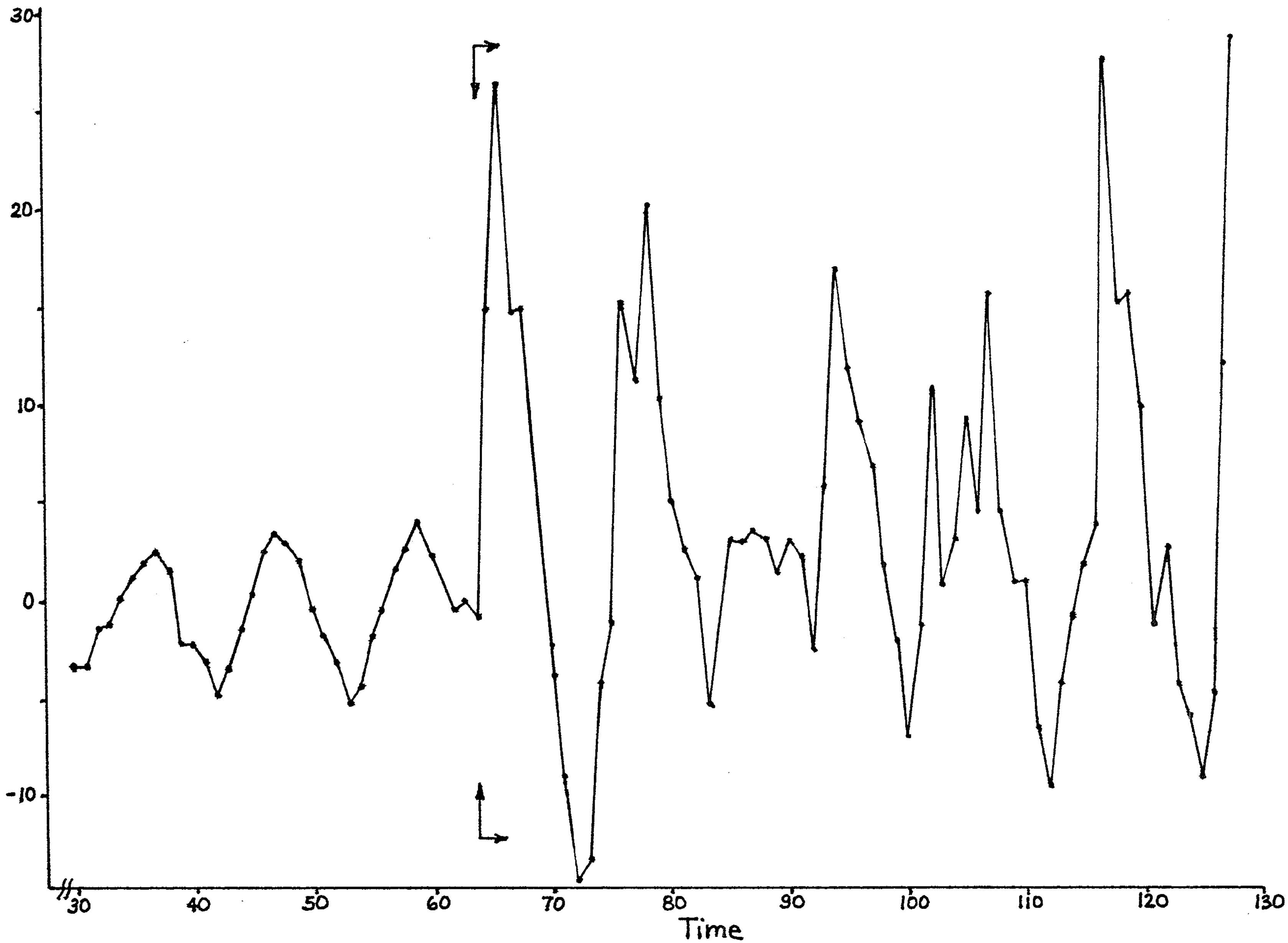
30
20
10
0
-10
30
40
50
60
70
80
90
100
110
120
130
Time